Evaluation of dispersive solid-phase microextraction using hydrogel microparticles for global metabolomics by liquid chromatography – mass spectrometry

Hanieh Peyman

A Thesis

in

the Department

of

Chemistry and Biochemistry

Presented in Partial Fulfillment of the Requirements

For the Degree of Master of Science (Chemistry) at
Concordia University

Montreal, Quebec, Canada

May 2016

CONCORDIA UNIVERSITY
School of Graduate Studies

This is to certify that the thesis prepared

By: Hanieh Peyman

Entitled: Evaluation of dispersive solid-phase microextraction using hydrogel microparticles for global metabolomics by liquid chromatography-mass spectrometry

and submitted in partial fulfillment of the requirements for the degree of

Master of Science (Chemistry)

---

complies with the regulations of the University and meets the accepted standards with respect to originality and quality.

Signed by the final examining committee:

Louis Cuccia_____Chair

Cameron Skinner_____Examiner

John Capobianco_____Examiner

Dajana Vuckovic_____Supervisor

Approved by _____ Chair
of Department or Graduate Program Director

_____
Dean of Faculty

Date 25 May, 2016

ABSTRACT

Evaluation of dispersive solid-phase microextraction using hydrogel microparticles for global metabolomics by liquid chromatography – mass spectrometry

Hanieh Peyman, M.Sc.

An ideal sample-preparation method for LC-MS metabolomic analysis should be as non-selective as possible for metabolites but still capable to remove the interferences such as salts and proteins. Microextraction methods have not been widely used in this application despite their potential to reduce ionization suppression and/or increase metabolite coverage. The main goal of this M.Sc. project was to develop a new dispersive solid phase microextraction (D-SPME) sample preparation method and investigate whether this approach can improve the coverage of the metabolome from human plasma. Different types of poly-N-isopropylacrylamide hydrogel extraction phases functionalized with vinyl acetate (VAC), acrylic acid (AAC) or N-3-aminopropyl methacrylamide hydrochloride (APMAH) were tested. Sample analysis was performed using three complementary liquid chromatography–high resolution mass spectrometry methods for high, intermediate and low polarity sub-metabolomes respectively. The extraction conditions were optimized in terms of desorption solvent, influence of pH, centrifugation time, extraction time, sorbent to sample ratio, increasing portion of functional monomer and evaluation of reproducibility. Finally, the performance of the optimized D-SPME method was compared against protein precipitation using methanol, which is currently the gold standard method for global metabolomics of human plasma, and commercial core-shell nanoparticles (CERES Nanotrap) functionalized with acrylic acid or Cibacron blue cores. The main criteria used for the comparison were ionization suppression, metabolite coverage and precision. Hydrogel microparticles performed as well as nanotraps in terms of extraction and performed better than nanotraps and methanol precipitation in terms of ion suppression. Hydrogel D-SPME had lower total coverage than methanol precipitation, as expected for a microextraction method, but successfully revealed more than 568 low abundance metabolites in positive ESI mode and 48 metabolites in negative mode that could not be observed using the methanol method. Therefore, hydrogel D-SPME appears to be a promising new method for global metabolomics.

Acknowledgements

My deepest gratitude to my supervisor, Professor Dajana Vuckovic, for her guidance, encouragement and support throughout my graduate career. The opportunities for growth and the excitement of working in our group are deeply appreciated; I am honored to have had the chance to be part of it. I would also like to thank my committee members, Professors Cameron Skinner and John Capobianco.

Many thanks to the Michael Serpe group from the University of Alberta and my colleagues Dmitri Sitnikov, Parsram Ramrup, Irina Slobodchikova, Cian Monnin, Mariana De Sá Tavares Russo and my friends who encouraged and helped me during this research program.

My deepest appreciation goes to my family for their sustained encouragement and support in all and every stage of my life; to my mother, Leila, for her endless love; to my father, Mohammad who inspired me to pursue my study; and to my sister, Sareh, a true friend.

Table of Contents:

List of Figures

List of Tables

List of Equations

List of Abbreviations

AAC. Acrylic acid

AC. Alternating current

ANOVA. Analysis of variance

APCI. Atmospheric pressure chemical ionization

APMAH. N-3-aminopropyl methacrylamide hydrochloride

BIS. Methylenebisacrylamide

C_0. Initial concentration in the sample

CID. Collision-induced dissociation

CSH. Charged Surface Hybrid

D-SPME. Dispersive solid-phase microextraction

D. Dipole moment

DC. Direct current

DES. Desorption

DG18:0-16:0. 1-octadecanoyl-2-hexadecanoyl-sn-glycerol

DNA. Deoxyribonucleic acid

ESI. Electrospray ionization

FA. Formic acid

FDA. Food and Drug Administration

FTIR. Fourier transform infrared spectroscopy

GC-MS. Gas chromatography–mass spectrometry

HESI. Heated electrospray ionization

HILIC. Hydrophilic interaction chromatography

HMDB. Human metabolome database

HPLC. High-performance liquid chromatography

K_{fs}. Distribution coefficient

LC-MS. Liquid chromatography–mass spectrometry

LCST. Lower critical solution temperature

Liver PI. L-α-phosphatidylinositol (Liver, Bovine)

LLE. Liquid-liquid extraction

LOQ. Limit of quantification

LTQ-Orbitrap. Linear trap quadrupole orbitrap

Lyso PC17:0. 1-heptadecanoyl-2-hydroxy-*sn*-glycero-3-phosphocholine

MCP. Microchannel plate

MeOH. Methanol

MG16:0. 1-hexadecanoyl-rac-glycerol

MS. Mass spectrometry

n. Number of moles of analyte

NA. Not applicable

NAD. Nicotinamide adenine dinucleotide

NIPAm. N-isopropyl acrylamide

NMR. Nuclear magnetic resonance

NPLC. Normal phase liquid chromatography

PA18:0. 1,2-distearoyl-*sn*-glycero-3-phosphate

PBS. Phosphate-buffered saline

PC19:0. 1, 2-dinonadecanoyl-*sn*-glycero-3-phosphocholine

PCA. Principal component analysis

PE17:0. 1, 2-diheptadecanoyl-sn-glycero-3-phosphoethanolamine

PFP. Pentafluorophenyl

PG18:0. 1, 2-dioctadecanoyl-sn-glycero-3-phospho-(1'-sn-glycerol)

pK_a. acid dissociation constant

PLS-DA. Partial least square-discriminant analysis

PMT. Photomultiplier tube

pNIPAm-co-AAC. Poly (N-isopropylacrylamide)-co-acrylic acid

PP1. Protein precipitation with evaporation and reconstitution

PP2. Protein precipitation with dilution

ppm. Parts per million

PPT. Protein precipitation

Q-TOF. Quadrupole time-of-flight

QC. Quality control

RAM. Restricted access materials

RF. Radio frequency

RNA. Ribonucleic acid

RPLC: Reversed phase liquid chromatography

rpm. Revolutions per minute

RSD. Relative standard deviation

RT. Retention time

SPE. Solid-phase extraction

SPME. Solid-phase microextraction

TG18:1-16:0-18:1. 1,3-di- (9Z-octadecenoyl)-2-hexadecanoyl-glycerol

TOF. Time-of-Flight

UHPLC. Ultra-high-performance liquid chromatography

v/v. Volume by volume

VAC. Vinyl acetate

V_f. Volume of the extraction phase

V_S. Volume of the aqueous sample

VSA. Vinyl sulfonic acid

YMDB. Yeast metabolome database

Chapter 1

Introduction

1.1 Metabolomics

Metabolomics is an emerging field that is complementary to the other 'omics' sciences of genomics and proteomics.[1] It is defined as the comprehensive analysis of metabolome. The metabolome is the full set of all low molecular weight metabolites with mass <1500 Da in a given biological system. The actual size of the metabolome is still subject to conjecture. Yeast cells are estimated to contain more than 2000 low molecular weight metabolites according to the Yeast Metabolome Database (YMDB)[2] while the Human Metabolome Database (HMDB)[3] contains 41,993 possible metabolites including both water soluble and lipid soluble metabolites. Among these, approximately 8000 have been observed in human samples to date. The remaining metabolites are expected metabolites which comprise of compounds for which biochemical pathways are known or compounds for which human intake is frequent but which have not yet been confidently detected in human biofluids or tissues tested. Metabolites present in HMDB include a wide variety of compound classes, such as amino acids, organic acids, amines, lipids, nucleotides and hormones. Metabolites are present at a wide range of concentrations (10^{-3} to 10^{-12} M) and differ extremely in their physical and chemical properties including polarity, charge, functional group and stability. Therefore, global metabolomics investigations are a challenging area for analytical chemistry and specifically mass spectrometry (MS). Over the past decade, MS instrumentation has evolved significantly, however, the analytical approaches that are used in global metabolomic studies need further research.[4] Biological fluids (e.g., blood, plasma, serum, urine) are very complex matrices, containing proteins, cells, salts, DNA, RNA and exogenous and endogenous metabolites. The selection of an appropriate sample preparation technique is critical to preserve or enrich metabolites while simultaneously removing other biomolecules in order to make the biofluid or biotissue sample compatible with subsequent MS analysis and achieve good metabolite coverage.

Although the term metabolomics was only recently defined[5], traditional Chinese medicine used metabolomics approaches to evaluate the urine of patients dating back to 2000-1500 B.C. to determine the presence of high glucose in urine for diagnosis of diabetes. In modern analysis, metabolomics was first explored by Horning[6] and Pauling *et al.*[7] in the early 1960's and 1970's respectively. They used gas chromatography (GC) to monitor the metabolites that exist in human urine and tissue extracts. Recent metabolomics efforts have taken advantage of improvements in analytical

instrumentation including mass spectrometry (MS) and nuclear magnetic resonance (NMR).[1]

The great advantages of NMR are minimal sample preparation, high sample throughput, excellent reproducibility, instrument robustness, and non-destructive nature of the technique. The major weakness of NMR spectroscopy is its poor detection limit (>μM), which is the major strength of MS. The low detection limit of MS makes it an important method for measuring metabolites in complex bio-samples. As a result, mass spectrometry-based metabolomics offers quantitative analyses with high selectivity and low detection limits to drastically improve the coverage of metabolites due to the detection of the low abundance species. In comparison to NMR, the combination of MS with a separation technique such as liquid chromatography (LC-MS) provides further advantages for complex biological samples by reducing the complexity of the mass spectra and increasing information space.[8-9] Therefore, LC-MS provides the most comprehensive metabolite coverage in a single analysis to date, whereby metabolite coverage is defined as the number of metabolites that can be detected using a given analytical method.

1.1.1 Metabolomics applications and approaches

Metabonomics is another term that was used by Nicholson *et al.*[10], which is used interchangeably with metabolomics and represents the quantitative measurement of changes in metabolite levels or concentrations in response to genetic modifications or pathophysiological stimuli.[11] These two terms rely on similar methodologies and their common purpose is to analyze the metabolome.[12] In this work, term metabolomics will be used throughout.

Metabolomic investigations have been applied in various research areas including plant metabolism[13,14], environmental science[15,16], functional genomics[17], biomarker discovery[18], systems biology[1], toxicology[19], food and nutrition[20,21], understanding mechanism of drug action, metabolisms or toxicity.[22]

Metabolic analysis can be categorized as either: targeted or untargeted (global) metabolomics. Targeted metabolomics focuses on quantitative analysis of a very limited number of metabolites in selected biochemical pathway(s) or a specific class of compounds. In this approach, metabolite identity and the chemical properties of compounds are known, therefore selective sample preparation and separation can be employed to provide better quantitation. The main disadvantage of this method is that it will provide limited coverage of the metabolome. Global metabolomics focuses on analyzing all classes of metabolites simultaneously and will attempt to measure all

molecules that ionize within a wide range of mass values. Therefore, it broadens the metabolite coverage but selecting an appropriate sample preparation is challenging.

1.2 Global metabolomics workflow

Global metabolomics has been performed in a wide variety of biological matrices, such as urine, plasma or serum, saliva, tissues or cells. Figure 1.1 illustrates a typical workflow of a metabolomic study using a LC-MS based platform. The first step of global LC–MS metabolomic study is the extraction of all small-molecule metabolites from the sample matrix. This is followed by the separation of metabolites using chromatography. All metabolites eluting from the chromatographic column are then introduced into an electrospray ionization source (ESI) for ionization, followed by their separation and detection according to their m/z values in mass spectrometer. High-resolution mass spectrometers are preferred for metabolite detection based on their ability to separate metabolites with the same nominal mass but different monoisotopic masses and different chemical formulas. After MS analysis, data is first processed to obtain a list of putative metabolites characterized by their accurate mass and retention time. Then, the features of interest are selected from the data using appropriate multivariate statistical approaches (for example, principal component analysis, PCA). Finally, follow-up studies to identify metabolites of interest are performed using database searches and MS/MS. Tentative metabolite identity is then confirmed by comparison to authentic standards.

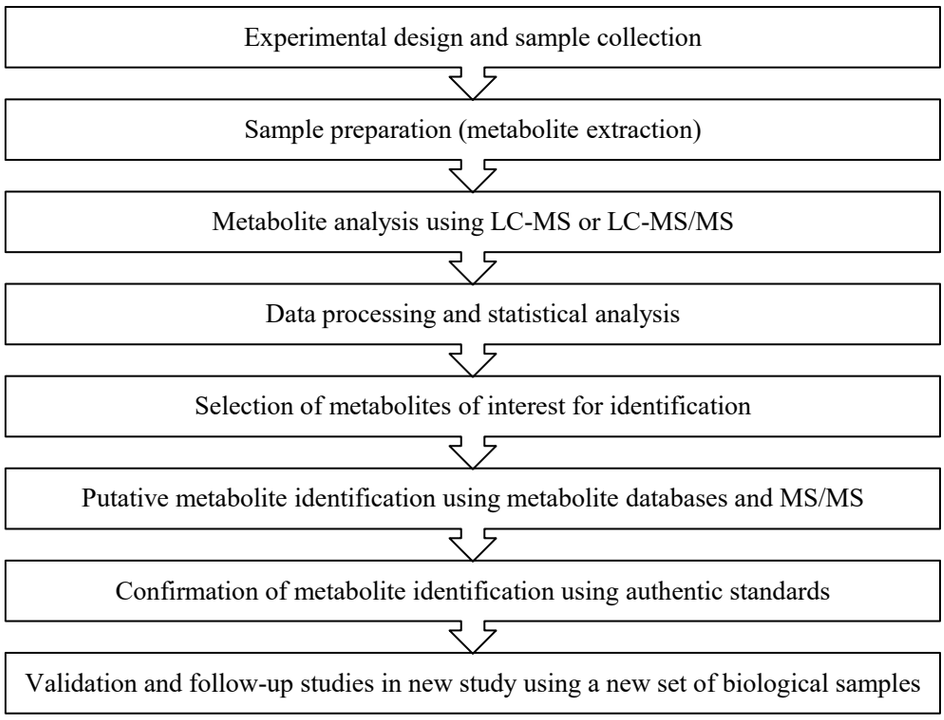

Figure 1.1 Main steps of LC-MS based untargeted (global) metabolomics workflow.

1.2.1 Experimental design and sample collection

Experimental design of a metabolomics study must consider (1) experimental type (time course study or comparative study); (2) experimental factors (e.g., time, dose, time, gender, age etc.)[23], and (3) sample size and type of biospecimen to examine. Sample collection and sample handling have critical influence on the composition of the metabolome the reproducibility and the quality of metabolomics data collected.[24] It is important that all study samples be collected using the same protocol without any changes in parameters so that experimental reproducibility is maximized. This avoids irreproducibility and the introduction of artifacts which include (i) m/z signals originating from contaminants introduced during sample preparation rather than present in the biological sample itself and (ii) changes in metabolite levels due to residual metabolism and/or degradation that can occur during sampling, sample storage and/or sample handling procedures. Thus, for biofluid samples, all factors of sample collection should be considered and strictly controlled including the type of syringe, vacuum system for blood collection, storage vessel, anticoagulant, temperature, velocity and duration of centrifugation.[25] Appropriate quality control samples must be run and quality control strategies will be discussed in more detail in Section 3.2.6.

1.2.2 Sample preparation methods

In metabolomics studies, the choice of sample preparation is essential, because it affects both the observed metabolite profile and biological interpretation of the data.[8,26] Sample preparation can easily be optimized for the extraction of target metabolites and matrix removal. However, in global metabolomics all small molecules are targets. Salts and macromolecules such as proteins or larger peptides are considered as matrix. Therefore, an ideal sample-preparation method for LC-MS metabolomics analysis should be as non-selective as possible for metabolites but still capable of removing these interferences. In other words, a sample of interest, such as plasma, should be converted to a format compatible with LC-MS analysis while preserving the original metabolite composition as much as possible. To achieve this goal, simple and short sample preparation procedures with a minimal number of steps are preferred in order to avoid losses, and degradation of metabolites during preparation.

In general, the choice of sample preparation depends on the sample type and objectives of the study. For instance, extraction of high-abundance metabolites can often be achieved with good recoveries using simple solvent extraction procedures, whereas extraction of low-abundance metabolites requires enrichment for better detection. The total protein concentration of blood serum or plasma is 6-8 g dL^{-1} so protein must be removed during sample preparation before LC-MS analysis.[26] If protein removal is not performed, this can reduce the lifetime of LC column, can cause column aging and high column back

pressure, can reduce number of metabolites detected and can lead to irreproducible analytical results in metabolomics studies. All of these effects are due to the accumulation of protein on the surface of the analytical column.[27,28]

For plasma, the methods employed to date include liquid-liquid extraction (LLE), solid-phase extraction (SPE), protein precipitation, and membrane methods (dialysis or ultrafiltration). The most common sample preparation method in global metabolomics of blood by LC-MS is protein precipitation with an organic solvent.[12] In this method, organic solvent is added to plasma sample, which results in precipitation of the proteins that can be removed by centrifugation. Among all the organic solvents tested, precipitation with methanol was found to be the most effective in terms of the number of detected metabolite features, method reproducibility and lowest protein interference.[26,29] The addition of organic solvent causes protein denaturation, which largely disrupts binding between the metabolites and proteins in the sample. Therefore, metabolite levels determined using this approach correspond to total metabolite concentration (sum of bound and unbound metabolite concentrations). The main disadvantages of solvent precipitation are ionization suppression and the losses of metabolites due to poor solubility of metabolite(s) in the chosen organic solvent and/or co-precipitation of metabolite(s) with the proteins. Ionization suppression can occur because of metabolite co-elution, during LC, which can cause changes in the signal intensity due to the charge competitive nature of the ESI technique. Therefore, it should be evaluated when developing any MS-based method.

Solid phase extraction can also be used for global LC–MS metabolomics[30] and it is an exhaustive extraction method which completely removes analytes from a liquid sample by retention on a solid sorbent. Based on the properties of analytes and the sorbent, analytes can be retained by van der Waals, dipole-dipole interactions, hydrogen bonding, or electrostatic forces. Numerous solid phase sorbents are available including silica-based, carbon-based and polymer-based sorbents functionalized with appropriate chemical functionalities such as alkyl chains, ion-exchange materials, and restricted access materials which remove macromolecules from sample. Recently, polymer materials have gained more attention for SPE especially in case of functionalized polymeric materials; they have better pH-stability and can improve retention and recovery of various types of analytes.[31] The main steps of SPE are: (i) loading the sample where the sample is passed through the sorbent to retain the compounds of interest and, potentially, some interfering compounds on the SPE sorbent; (ii) washing of SPE sorbent to remove as many concomitant species as possible; and (iii) elution of the retained analytes from the sorbent using an appropriate elution solvent. Wash solutions should be strong enough to remove non-analyte species such as salts, which are less strongly bound to the sorbent as compared to the compounds of interest. However, the wash solution has

to be weak enough to leave the compounds of interest behind. This method provides better sample clean-up than protein precipitation by increasing column lifetime, improving reproducibility and decreasing matrix effects in LC–MS metabolomics. For global metabolomics, the SPE sorbent is chosen to cover broad class of metabolites while removing salts from the sample. However, all SPE sorbents offer some degree of selectivity, which will in turn reduces metabolite coverage. It is also difficult to optimize SPE methods to achieve exhaustive extraction of all different classes of metabolites in a given sample. For this reason, SPE has been used extensively in targeted metabolomics, but rarely in untargeted metabolomics. For example, Michopoulos *et al*.[32] compared C18 SPE and solvent precipitation methods (with methanol or acetonitrile) for extraction of human plasma for global metabolomics. Solid phase extraction performed better in terms of repeatability than protein precipitation whereas solvent precipitation provided better overall coverage of metabolites. In another study, Rico *et al*.[89] used eight human plasma preparation protocols (organic solvent protein precipitation (PPT) with either methanol or acetonitrile in 2:1 and 3:1 (v/v) ratios with plasma; C18 or Hybrid SPE, combination of SPE C18 and PPT and microextraction by packed sorbent) to evaluate their suitability in metabolomic studies by ultra-high-performance liquid chromatography coupled with electrospray ionization time-of-flight mass spectrometry. Methanol precipitation provided the highest number of extracted features in comparison to SPE-based protocols.

1.2.3 LC-MS analysis

Most metabolomic studies use LC before mass spectrometry to reduce sample complexity and improve the chromatographic resolution of overlapping metabolites. Therefore, LC helps to increase metabolite coverage, decrease ion suppression caused by co-eluting compounds, reduce the background noise and improve the detection limits and MS data quality.

High performance liquid chromatography (HPLC) using different types of stationary phases can separate compounds with a wide range of polarity. It can be performed in different modes including reversed-phase (RP), which uses a polar (aqueous) mobile phase and hydrophobic stationary phase. As a result, hydrophobic metabolites can interact with the hydrophobic stationary phase and be retained and separated, while hydrophilic metabolites will remain in the mobile phase and elute in, or close to, the void volume. Reversed-phase chromatography is ideally suited for metabolites such as vitamins, steroid hormones, fatty acids and their derivatives, lipids, bile acids, etc. The majority of global metabolomics methods described in literature used a reversed-phase LC separation using C_{18} stationary phase with a simple linear gradient of acetonitrile or methanol/water with formic or acetic acid as volatile mobile phase additives to help the electrospray ionization process and improve chromatography via ion-pairing effect or via

reducing secondary interactions (minimize the ionization of the silanol groups). Few ion-pairing methods have been reported for global metabolomic studies but the use of ion-pairing in liquid chromatography is avoided because these additives are not volatile and can cause significant ionization suppression and adduct formation.[12] On the other hand, many metabolites are polar species, which are not sufficiently retained in reversed-phase methods. A promising method to increase metabolite coverage of such species is the use of hydrophilic interaction chromatography (HILIC) which has better retention of polar compounds such as sugars, amino sugars, amino acids, nucleotides, etc., than RP. It also has improved analytical sensitivity when using MS detection due to the use of mobile phases with high organic content. Hydrophilic interaction chromatography utilizes polar stationary phases such as silica or silica derivatized with amino, diol, amide, polysulfoethyl aspartamide, and polyhydroxyethyl aspartamide groups in combination with water-miscible solvents (e.g. acetonitrile) as a mobile phase. In this approach, polar compounds will partition between a largely organic mobile phase and a static water-rich layer at the surface of the stationary phase. Elution strength increases with increasing water in the mobile phase. The main drawbacks of this method are the need for long re-equilibration volumes, which decrease sample throughput.[34]

A mass spectrometer measures the mass-to-charge ratio (m/z) of gas-phase ions. A mass spectrometer is typically composed of three major parts: ion source, mass analyzer, and detector. The sample is first delivered to the mass spectrometer via a liquid chromatographic device where it is ionized and vaporized in the ion source. The ions are then sorted according to their m/z in the mass analyzer. The ions that pass through mass analyzer impact the detector surface and generate a cascade of electrons in electron multiplier, which results in detectable ion current. Finally, a mass spectrum is produced which is a plot of ion-abundance against m/z.[35] The ion source is the way to couple LC to MS. Electrospray ionization (ESI) is the most common ionization method used in global metabolomics and with LC-MS in general. It is also compatible with various separation techniques.[36] In this technique in general, high temperatures (200-500°C) and/or gas flows are used to nebulize LC effluent and an electric field (3000-5000 V) is applied between the LC outlet and the mass spectrometer to generate gas-phase ions.

The LC eluent passes through a syringe, the needle of which terminates at a capillary. The capillary and the instrument inlet are kept at some potential difference (typically in the range from 2.5 to 5 kV). This forces the spraying of charged droplets from the capillary with a surface charge of the same polarity. The solvent is evaporated via a heated capillary interface or using heated drying nitrogen gas and pumped away. As the solvent evaporation occurs, as it was shown in Figure 1.2 in ESI combination model, the droplet shrinks until it reaches the point that the surface tension can no longer keep the

charge (the Rayleigh limit) due to the repulsion of ions of the same charge at which point a "Columbic explosion" occurs and the droplet is ripped apart and produces smaller droplets.[103] This process continues with smaller and smaller droplets, until single ions are obtained.

Coupling of LC to MS puts restrictions in terms of mobile phase composition. Typically, simple mobile phases such as water/methanol or water/acetonitrile with a relatively small proportion additive (e.g., acetic acid, formic acid, ammonium acetate and ammonium formate) are used. It is critical that the additive should be volatile otherwise it will crystallize and block the ion source. Electrospray ionization is also called 'soft ionization' technique, since there is very little fragmentation. Therefore, it can be used to determine the molecular weight of intact (singly charged) molecules, and can provide multiply charged ions.[37]

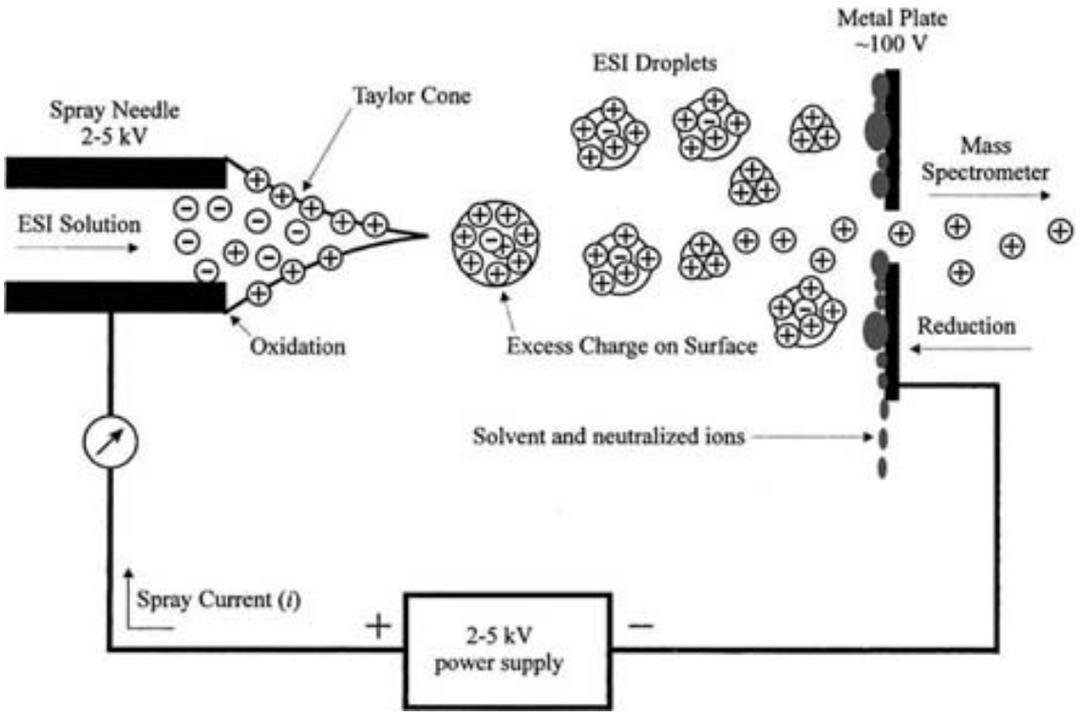

Figure 1.2 Schematic of an electrospray ionization interface. Figure from Reference 103, reprinted with permission from John Wiley and Sons publisher.

Electrospray ionization can operate in dual mode and according to the nature of the analyte of interest, positive or negative ion mode can be selected. In positive mode, the positive voltage is applied on the spray tip and negative voltage on the cone of mass spectrometer, thus providing positive ionization of molecules. Protonation is the dominant mechanism of ion formation in positive ESI and produces ions with the masses equal to sum of monoisotopic masses of analyte and proton which carries single positive charge $[M+H]^+$. In addition to protonated species, other commonly observed ions can form from the addition of single sodium $[M+Na]^+$, potassium $[M+K]^+$ or ammonium

$[M+NH_4]^+$ instead of hydrogen. Addition of more than one charged species may result in the formation of multiply charged ions. For example, the addition of 2 protons will result in formation of $[M+2H]^{2+}$ ion. Electrochemical reactions in ESI may also result in simultaneous loss of a part of molecule (such as neutral loss of carbon monoxide $[M+H-CO]^+$, water $[M+H-H_2O]^+$ and ammonia $[M+H-NH_4]^+$. In contrast to positive mode, a negative ESI predominantly causes de-protonation of molecules as $[M-H]^-$ or $[M-2H]^{2-}$ for the loss of one or two protons, respectively. Negative adducts may also occur in negative ESI and common negative ions are formed by adduction of formic acid $[M+CH_2O_2-H]^-$, acetic acid $[M+CH_3COO]^-$ or chloride $[M+Cl]^-$. Simultaneous loss of water and hydrogen may also occur forming ion $[M-H_2O-H]^-$.

Mass resolving power and mass accuracy are both crucial aspects of the spectrometer's performance. High-resolution mass spectrometers are preferred for metabolite detection based on their ability to separate metabolites with the same nominal mass but different monoisotopic mass and different chemical formulas. Resolution depends on the masses that must be resolved. For example, to resolve riboflavin 5-diphosphate ($C_8H_{13}N_4O_{11}P_2$ with 402.9944 m/z) from uridine 5-phosphate ($C_9H_{13}N_2O_{12}P_2$ with 403.0056 m/z) a resolution of around 36,000 is required.[95] This is calculated according to the Equation 1.1, where R is the resolving power, M is the m/z of the analyte of interest, Δm is the difference between the two masses.[104] The difference between these two compounds is 0.0112 Da. To resolve the same absolute difference in masses, minimum approximate resolving power of 9,000 and 90,000 is required for 100 and 1000 m/z respectively.

$$R = \frac{M}{\Delta m} \qquad \textbf{Equation 1.1}$$

Mass accuracy is defined as how close the experimentally measured m/z is to the true m/z of that ion, and good mass accuracy is important for correct metabolite identification. The two most common mass analyzers employed in global metabolomics are quadrupole time-of-flight (Q-TOF) and Orbitrap, both were used in this project.[35]

In metabolomics, Q-TOF mass spectrometers are commonly used because of their low full scan detection limits (as low as femtograms for highly-ionizable analytes) and good mass accuracy with internal mass calibration, both of which facilitate the detection and identification of very low-abundance compounds.[38,39] This translates to the ability to routinely detect metabolites present at nM to μM levels (for example 60 μM for glutamic acid and 0.3 μM for cortisol) in complex biological samples such as plasma, for metabolites with reasonable ionization efficiency. However, the exact detection limits depend strongly on many factors including the exact LC-MS method and instrument model used as well as analyte ionization efficiency and propensity to form adducts and/or multi-charged species. Quadrupole-time-of-flight mass spectrometers have an in-spectrum dynamic range of up to 5 orders of magnitude that can reveal trace level targets,

even in the presence of much more abundant compounds and have high resolution up to 40000. Fast data acquisition rates of up to 40 spectra/second ensure maximum compatibility with fast LC and high throughput methods. For a typical metabolomics analysis, one to three full scan spectra per second over a m/z range of 100-1500 is required.

Quadrupole-time-of-flight mass spectrometer consists of two mass analyzers; a quadrupole filter followed by a time-of-flight analyzer. As it is shown in Figure 1.3, LC eluent is sprayed (nebulized) into ESI. Ions generated in the ion source are transferred to the quadrupole analyzer via radiofrequency (RF) lens. Electrostatic force between positive ions generated in ESI and negative voltage, which is applied to RF lens, is used for ion transmission (for negative ions, small positive voltage is applied instead). [115]Quadrupole analyzer consists of four parallel rods arranged as a square. A pair of opposite rods is connected to negative and positive terminals of direct current (DC) source. Alternating current (AC) voltage is also applied to each pair and varied with (RF). At a given set of voltages (AC, DC) only ions with narrow range of m/z (typically 1 m/z) have a stable trajectory and are able to pass through, other ions are neutralized and swept away by the vacuum.[114] The ions that pass through quadrupole, then get into hexapole collision cell, which is filled with non-reactive collision gas such as helium or nitrogen and then fragmented using collision-induced dissociation to generate product ions and neutral fragments. Then, ions reach the pulser (a stack of plates), which bunches them into a tighter "pack" and accelerates them by pulse of high voltage (~20,000V) into the TOF drift tube. The pulser helps to measure the time of flight as it gives time zero for ions. The TOF mass analyzer is typically one meter in length and must have very high vacuum ($10E^{-7}$ psi) to minimize undesired fragmentation of flying ions and prevent ions from colliding with gaseous molecules. Within TOF drift tube there is no additional electric or magnetic field, so ions will undergo no further acceleration.[116, 117] At the opposite end of the flight tube is an ion "mirror", called "reflectron", which compensates for minor differences in initial kinetic energy, which occur in pulser. Faster ions penetrate deeper into the lens array and spend more time there while slower ions (with the same mass) will penetrate less, so that total flight times of ions with the same m/z will show less distribution in their flight times.[117] This means that in reflectron TOF these ions will reach the detector at same time, to achieve improved resolving power.

A microchannel plate (MCP), a thin plate punched by many microscopic channels, is the first stage of the detector. After an ion with adequate energy hits the MCP, one or more electrons are freed. Each microchannel acts as an electron multiplier. [39]The electrons exiting the MCP are accelerated onto a scintillator that will emit photons when it is struck

by the electrons. The photons from the scintillator are concentrated through optical lenses onto a photomultiplier tube (PMT) to produce an electrical signal proportional to the number of photons.[117] The amplified electronic signal is converted to photons and then backs to electrical signal in order to electrically isolate the signal. [108]

The flight time for each m/z is unique. The flight time is measured from the instant of the application of the high voltage pulse, which is applied to the plate of the ion pulser to the moment when the ion strikes the detector. There are two formulae that apply to time-of-flight analysis. One is the formula for kinetic energy. According to Equation 1.2, q is equal to ze, and corresponds to the total charge on ion (e is elementary charge), V is the accelerating potential applied to ions; m is mass of ion and $\boldsymbol{v}$ is the velocity of ion.[105]

$$\boldsymbol{KE} = qV = \frac{1}{2}\, m\, v^2 \qquad \textbf{Equation 1.2}$$

The second formula is the flight time of ion (t) or travel distance (d) which is given by:

$$t = d/v$$

$$t^2 = \frac{m}{z}\left[\frac{d^2}{2Ve}\right] \qquad \textbf{Equation 1.3}$$

For a given kinetic energy, low m/z ions will have higher velocity, shorter flight time and reach the detector faster.

The above description explains the operation of Q-TOF in MS/MS mode. For metabolomics applications, Q-TOF is most often operated in MS mode in which the quadrupole is operated as a focusing lens by applying RF voltage only and allows a wide range of ions to enter the TOF (typically m/z 100-1500), and no fragmentation is performed in the hexapole collision cell. In full scan MS mode, Q-TOF therefore provides a full mass spectrum of all analyte ions introduced into the ion source. For metabolite identification, MS/MS mode is required. In this case, the parent ion of interest is first isolated by the quadrupole, and then fragmented in the collision cell to produce product ions, which are then detected in the TOF analyzer. The full mass spectrum of all the product ions produced by dissociation of the selected parent ion provides information on the molecular structure of one particular ion at a time and is used to aid in metabolite identification.[39] In this study, metabolite identification was not performed, therefore all experiments were run using full scan MS mode.

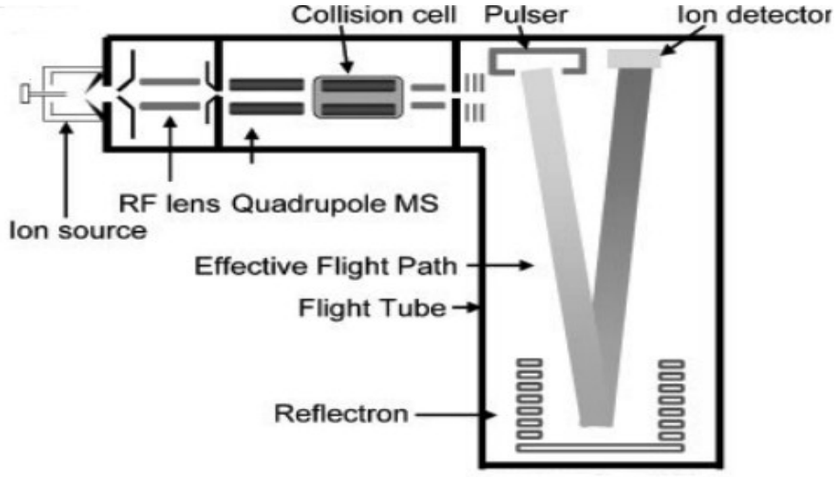

Figure 1.3 Schematic of a Q-TOF mass spectrometer. Figure from Reference 96 reprinted with permission from John Wiley and Sons publisher.

Linear Trap Quadrupole (LTQ) Orbitrap Velos is a hybrid mass spectrometer from Thermo Scientific which incorporates a linear ion trap and high-resolution Orbitrap analyzer.[40,41] Different compounds separated on the HPLC column are ionized in an electrospray ion source using similar principles as described for Q-TOF. The generated ions are next accelerated into s-lens and are transferred and guided using quadrupole and octapole. The ions then enter a dual-pressure ion trap assembly, which comprises of two identical ion traps separated by a center lens. Based on DC and AC voltages applied, only certain types of ions have stable trajectory in ion trap. Then, the ions are focused on multipole and ejected axially into the C-shaped storage trap to slow down the ions before injection into the Orbitrap. An Orbitrap consists of an inner and outer electrode. When voltage is applied between the outer and the central electrodes, the resulting electric field pushes ions to initiate harmonic axial oscillations. Ions rotate around the axis of central electrode of orbitrap and also simultaneously move from left to right along the z direction. Frequency of moving from left to right depends on their m/z. Outer electrodes are then used as receiver plates for image current detection of these axial oscillations to measure their frequency. Finally, these oscillation frequencies are converted into m/z values after Fourier transformation[97] as shown in Equation 1.4. where ω is frequency and k is force constant of the potential.[40]

$$\omega = \sqrt{z/m \times k} \qquad \textbf{Equation1.4}$$

The above description describes MS mode of operation of Orbitrap, which was used in current work. For identification, MS/MS mode is used whereby ions are passed from the C-Trap into HCD (Higher Energy Collisional Dissociation) cell to be fragmented. A softer CID fragmentation for MS/MS can also be performed in dual ion-trap. Linear ion trap includes a high and low pressure cells. High-pressure cell is used for trapping

injected ions, isolating precursor ions, and fragmenting precursor ions (there is collision gas in this cell to do fragmentation) and a low-pressure cell is used for scanning ions out.[113] Low pressure cell is equipped with detectors, therefore ions can be detected either in these detectors at low resolving power or analyzed in Orbitrap at higher resolving power.

The distinct benefits of LTQ-Orbitrap hybrid mass spectrometer include high mass accuracy ≤ 3 ppm, high mass resolution (100,000 for the model used in this thesis and up to 400,000 for more recent models), good dynamic range and low limits of detection. The high mass resolution achieved with this instrument is critical for lipid analysis because isotopic envelopes of some phospholipid classes have accurate monoisotopic masses that are close to each other[42] and require mass resolution beyond what can be achieved on Q-TOF. Therefore, in this study the Orbitrap instrument was used to measure lipid sub-metabolome.

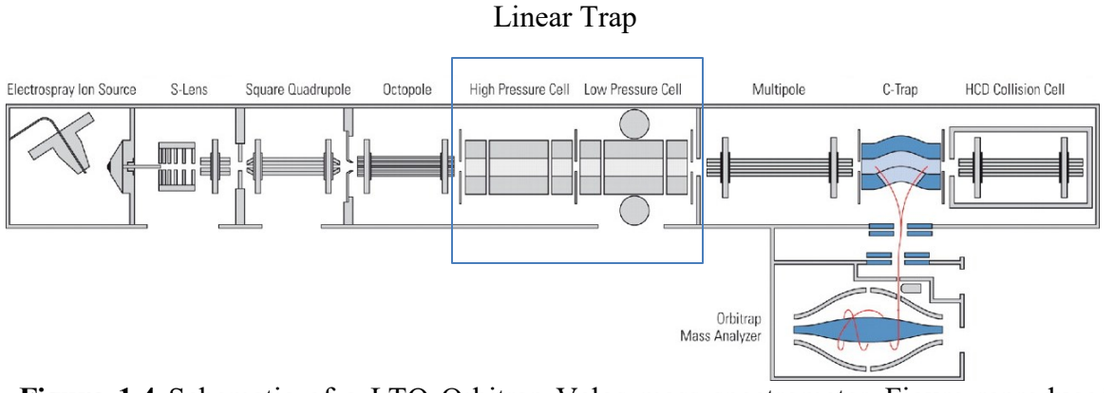

Figure 1.4 Schematic of a LTQ Orbitrap Velos mass spectrometer. Figure reproduced from website (ThermoFisher.com, 2016/08/10)

1.2.4 Data processing

After sample collection, preparation, and analysis by LC-MS, the data must be processed. The main steps of data processing for global metabolomics include (1) chromatographic alignment (2) peak picking or feature detection (3) removal of peaks that are present in blanks and extraction blanks (4) comparison of signal abundances among different conditions using statistical methods and (5) identification of components of interest using an accurate mass database search followed by confirmation using authentic standards.

In LC-MS-based metabolomics, statistical analysis is needed in order to discover the features of interest. Univariate techniques including Student's t-test assess the statistical significance of each peak independently, but they are not commonly used in global metabolomics studies because they can lead to high false positive rates due to multiple hypothesis testing when analyzing data sets containing thousands of metabolites.[43] A variety of multivariate statistics are currently in use for metabolomics studies and can be divided into two main categories: unsupervised and supervised methods. In unsupervised

techniques, no group classification is provided during data input, and the algorithm can identify hidden structures in the data without knowing the class labels. One of the most popular unsupervised techniques in LC-MS-based metabolomics studies is principal component analysis (PCA). It is a standard technique for data processing that can help to visualize high dimension data by reducing the dimensionality (the number of variables) of the data set. From a mathematical point of view, it converts a set of observations of correlated variables into a reduced set of uncorrelated variables that are called principal components. By using the first 2-3 principal components, instead of thousands of variables for each sample, similarities and differences between samples can be visually recognized using a scores plot. This plot is routinely used in metabolomics studies to evaluate the quality of data by examining whether quality control samples and/or replicates of study samples group closely together and how much of the study variability can be described by selected principal components. For this project, PCA can also be used to visually represent similarities and differences between different sample preparation methods that are under evaluation. The methods that can extract similar metabolites will group closely together, while the methods that are highly orthogonal will be shown far apart on PCA. Similarly, in a more typical metabolomics study, PCA is used to check whether treatment and control samples can be grouped or not, and distinguished from each other. In all of the above examples, loadings plot can then be used to examine which variables contribute the most to the observed difference(s) between samples, and these variables (metabolites) are then prioritized for identification and further follow-up. This helps to drastically reduce the number of metabolites for which identification is required, and focus the identification efforts on metabolites, which are changing the most in a given study. Supervised techniques such as partial least square-discriminant analysis (PLS-DA) are applicable to larger data sets and are beyond scope of this study.

1.2.5 Metabolite identification

The vast chemical complexity of metabolome makes the process of metabolite identification a very challenging task. Therefore, metabolomics studies typically only identify metabolites that are of particular interest to a given study (for example, metabolites that are highly up- or down-regulated in a given study). Two types of identification strategy are typically used in metabolomics: putative identification and definitive identification. In putative identification, the m/z of an analyte can be used to define the compound's molecular formula and to search for possible compound hits in databases such as NIST (http://www.nist.gov/srd/nist1.htm), KEGG (http://www.genome.jp/kegg/ligand.html), Human Cyc (http:// biocyc.org), LIPIDMAPS (http://www.lipidmaps.org/tools/index.html), HMDB (http://www.hmdb.ca), and

METLIN (http://metlin.scripps.edu). Putative identification using MS or MS/MS data is not sufficient confirmation of metabolite identity. This is due to the fact that many compounds can have the same, or similar, molecular weights that cannot be distinguished within the mass resolving power of a given mass spectrometer, and/or similar fragmentation pattern. Also, the same accurate mass and similar fragmentation spectra make the correct identification of isomers particularly difficult. Furthermore, metabolite databases are still incomplete, so not all metabolites have been included. Definitive identification verifies the mass-based search results and compares the observed retention time and mass spectrum of metabolites of interest to an authentic chemical standard analyzed under identical experimental conditions. By means of this comparison, the identities of the metabolites can be confirmed. Unfortunately, not all authentic standards are commercially available so in many cases definitive identification may also require synthesis and/or metabolite purification.

1.3 Challenges in sample preparation for global metabolomics

The main focus of this thesis is improving the sample preparation step of global metabolomics workflow, so in this section, the main challenges facing metabolomics sample preparation will be discussed in more detail.

1.3.1 Ionization suppression and matrix effects

Electrospray ionization is a competitive process because only a limited amount of charge is available at any given moment in the ion source. When there are molecules present at the same time as the analyte of interest in an ion source, they can compete for the charge available and decrease analyte signal. Therefore, the same analyte concentration can produce different signal intensity depending on whether co-eluting species are present, in what quantities and how well they can compete for ionization versus the analyte. This phenomenon is named ion suppression, and is one form of matrix effect that all LC-MS techniques suffer from. Analyte ion suppression (or enhancement which can also be observed) can also occur due to the change in the efficiency of droplet formation or droplet evaporation during the electrospray process in the presence of other components from the matrix.[44] This can affect the number of charged analyte ions in the gas phase that ultimately reach the detector, and thus change the analyte signal intensity even when analyte concentration is the same in two different samples. The main factors affecting ion suppression include the sample preparation method, the chromatographic method, the nature of the analyte, the amount of sample loaded, the presence of background interferences and the type of ionization method. Ion suppression can be evaluated by comparing the signal intensity of an analyte in the presence and absence of matrix

components. The presence of matrix effects adversely affects the determination of the analytes of interest (especially when present of small concentration) in complex samples such as biological fluids by reducing both the reproducibility and accuracy.[45,46]

Recent experiments involving ESI of biological extracts have shown that there are many possible reasons for ion suppression. It can arise from endogenous compounds (phospholipids in blood based samples) in the sample matrix or exogenous compounds from contamination. The latter can be introduced during the different steps of sample handling and preparation. For instance, contaminant peaks can arise even from the highest-purity solvents, reagents, anticoagulants, purified water, glassware and plasticizers from plastic ware. Very strong solvent contamination peaks may cause severe ionization suppression of the peaks eluting in the same retention time window. Therefore, it is recommended to run solvent blank and not use any batches of solvent that have prominent solvent contaminant peaks for sample preparation or mobile phase preparation.[47] The presence of nonvolatile species (e.g., salts, ion pairing agents, endogenous compounds) can also cause ion suppression. Consequently, matrix components can affect surface tension and viscosity of the drop and decrease efficiency of small droplet formation or evaporation, thus reducing the number of analyte ions reaching the gas phase.[47,48] These particular interfering compounds have high surface activity, in comparison to the analyte, so that the analyte cannot access the surface of the drop and prevents the analyte from reaching the gas phase.

Considering that there are multiple possible sources of ion suppression, there is no universal solution to address such matrix effects. This problem is more pronounced in global metabolomics methods due to the intentional use of non-selective sample preparation methods, which increase the complexity of the prepared sample. Minimizing the risk of ion suppression effects is possible but it involves careful optimization of sample preparation and chromatography techniques.

Various strategies are available to counter/measure ion suppression. The first strategy could be to switch the ionization mode. In this strategy, we do not need to change sample preparation or chromatography method but the analyte must be capable of ionizing in both positive and negative ESI. In negative mode fewer compounds can be ionized. Therefore, by changing the ionization mode to negative the extent of ion suppression can be reduced. Switching the ionization technique from ESI to atmospheric pressure chemical ionization can also reduce ion suppression.[36] Source geometries can also affect ion suppression; the Z-shape geometry is better than the perpendicular geometry.[49] Furthermore, the amount of interfering compounds entering the ion source can be decreased by dilution or minimizing the injection volume of sample. Clearly, improving the chromatographic method and resolution can also eliminate/reduce ion suppression.

Therefore, the chromatogram has to be checked to make sure analyte peaks are not eluting in regions of significant suppression.[50] For example, the region at the very beginning of chromatogram, in the void volume (where unretained compounds are eluted), or at the end of chromatogram (where the strongly retained compounds are eluted) are highly susceptible to ion suppression. Improving sample preparation by improving sample clean up and using more selective methods can also minimize ion suppression effects.[51] In fact, ion suppression is usually a more pronounced problem with protein precipitation methods (a non-selective method) as compared to SPE and LLE.[52] Finally, different calibration techniques can be used to compensate for matrix effects. Internal and external calibrations are the most popular techniques. External calibration involves the preparation of several standard solutions in the sample matrix to obtain the relationship between the analyte response and the target standard concentrations in the presence of matrix components. In this approach, the calibration standards have the same composition as the investigated samples (matrix-matched) so they would undergo the same extent of ionization suppression. However, blank matrix solutions free of the target analyte may not always be available. Both the calibration and test samples have to be analyzed to compensate for the effect of ion suppression so that this technique is time consuming. Isotopically-labelled internal standards are the most widely used technique to obtain highly quantitative results using MS. In this approach, an internal standard is used to compensate for possible variations during sample preparation and LC-MS such as losses of analytes, injection volume variability and matrix effects. To compensate for ion suppression, the internal standard must have ionization properties very similar to those of the analyte. This is why isotopically labelled analogs of the analyte are the best choice of internal standard because they have identical chemical and structural properties as the analyte, thus providing accurate quantitation. However, for global metabolomics methods it is not feasible to have isotopically-labelled internal standards for all analytes, so more selective sample preparation techniques can play an important role to adequately address ion suppression effects.

1.3.2 Improving coverage of metabolites

In global metabolomics, comprehensive metabolite coverage is needed to ensure good metabolite pathway coverage. The main approaches currently used for increasing metabolite coverage include:

(1) Performing adequate sample preparation prior to LC separation:[53] In order to increase detection sensitivity, coverage of metabolites and quantitation accuracy the use of an appropriate sample preparation before LC is required. One strategy to achieve this goal could be fractionation, which can improve signal to noise and reduce the effect of interference. It has generally been used in lipidomics[54] and

proteomics[55] but, is not commonly used in global metabolomics. In addition, multiple extraction methods can be employed on the same sample to boost metabolite coverage.

(2) *Improving chromatographic performance:* By moving from HPLC to ultra performance liquid chromatography (UPLC) performed at elevated pressures (15000 psi) using columns packed with small particles (<2 μm), separation efficiency can be increased. This can reduce ion suppression as a consequence of reducing co-eluting components. Also, by moving from HPLC to UPLC, better detection limits will be achieved as ESI is a concentration-dependent process, which will further improve metabolite coverage.[56]

(3) *Analyzing the biological sample in both positive and negative ionization ESI modes*:[57] One simple method is to record spectra in both positive- and negative-ion modes; this is easily done by re-analyzing the sample and will effectively increase the number of features identified, as not all metabolites can efficiently ionize in just one mode.

(4) *Re-analyzing the sample using APCI or analyze using nanoelectrospray as a second method of ionization*: This will reduce the ionization background interference and increase the number of features identified.[35] However, nanoLC and nanoESI can suffer from poor MS signal stability and retention time drifts over long analytical batches, so they are not yet routinely employed in metabolomics studies.

(5) *Use of long chromatographic run times and slow LC gradients:* This will maximize the separation and reduce co-elution which improves signal quality.[58]

(6) *Use different principles of chromatographic separation:* For example the use of both reversed-phase and HILIC chromatography, with the same sample set, optimizes the metabolite coverage and is currently the gold standard approach for metabolomics analysis[59] as discussed in Section 1.2.3.

1.4 Dispersive solid phase microextraction (D-SPME)

A recent and very efficient approach to sample preparation is solid-phase microextraction (SPME), invented by Pawliszyn and co-workers[60] in 1989 in order to address some of the limitations of other sample preparation methods like SPE and LLE.

1.4.1 Introduction

Solid phase microextraction (SPME) is similar to SPE, whereby solid sorbent is used to extract analytes from liquid or gaseous sample. Fiber format of SPME consists of a sorbent coating that is immobilized on a solid support such as a metal wire. The fiber is exposed to sample directly, or via headspace, and used to isolate and concentrate analytes in the coating. After extraction, the fibers are transferred to an analytical instrument for

separation and quantification of the target analytes or dissolved in solvent for LC-MS analysis. The amount of analyte extracted by the fiber depends on the thickness of the coating and on the distribution constant of the analyte. In the dispersive solid phase microextraction (D-SPME) format of SPME, the coating is not immobilized on the fiber. Instead it is dispersed throughout the sample, and then collected using centrifugation. The dispersion significantly increases the contact area between the sample and sorbent, which increases the extraction efficiency and reduces the time required to achieve equilibrium. Dispersive-solid phase microextraction also provides high flexibility in terms of sorbent selection and this low-cost configuration is single use so that there is no carryover issue to consider. In SPME, with the fiber configuration, some coatings are reused so that carry over is problematic because it is possible that some small amount of analyte remains in fiber after the desorption step.

Solid phase microextraction is an equilibrium-based technique, so exhaustive recovery of analyte from the matrix is not expected due to the fact that a small sorbent mass is used in comparison to the sample volume. This non-exhaustive microextraction means that high instrumental analytical sensitivity is required. In the context of this thesis, and more generally in mass spectrometry, sensitivity is the ability to detect and determine small amounts of an analyte in a sample. However, the lower signal intensities obtained in SPME methods, due to lower extraction efficiency, can also reduce ionization suppression, which can ultimately improve quantitation, data quality and metabolome coverage. The main disadvantage of this method is the need for strict control of extraction parameters to ensure good method precision.

SPME is an equilibrium extraction method where the amount of analyte extracted is proportional to its free concentration. In complex biological samples such as plasma, a number of different binding phases may contribute to the bound concentration of a given metabolite.[61, 127] The main carrier binding proteins include serum albumin and α 1-acid glycoprotein, and their average concentrations are ~ 670 and 16 μM in human plasma, respectively.[126] Typically, acidic compounds bind to albumin and basic compounds tend to bind α 1-acid glycoprotein, although they may often bind to albumin as well.[128] When a metabolite or other compound is bound to carrier proteins, it is not considered biologically active, and the extent of this binding regulates the free concentration of the metabolite. Metabolites can also bind to specific enzymes or receptors to carry out different biological functions, and the extent of this binding depends on free concentration of that metabolite. Thus, only the free metabolite is capable of diffusing through membranes or interacting with receptors/enzymes. For example, more than 80% of total cortisol is bound to carrier proteins, mainly corticosteroid-binding globulin, 10-15% binds to albumin and only ~5% is free and can enter tissues, diffuse through cell

membranes and bind to glucocorticoid receptor with high affinity.[130, 131]

If the amount of analyte extracted by SPME is very small, it will not significantly change free concentration of that analyte. This means that the binding equilibrium between that analyte and carrier proteins will not be affected. Under such SPME conditions, the amount of analyte extracted is proportional to the free analyte concentration, and this can provide highly relevant biological information during metabolomics studies.[129] If organic solvent, salt or pH are used to denature the proteins, analyte-protein binding will be disrupted, and SPME extraction of such samples can then provide information on total analyte concentration. In the latter case, the amount of analyte extracted by SPME would increase, especially for highly bound analytes, which could possibly result in the detection of more analytes. In current work, protein binding was not disrupted for any of SPME experiments.

Other features of SPME include high sample throughput, compatibility with microscale amounts of biological sample and reduced use of harmful solvents and sorbents. Therefore, SPME is said to be environmental friendly, and it also decreases purchase and disposal cost of solvents.

1.4.2 Theory of solid phase microextraction (SPME)

Solid phase microextraction is highly selective and its performance depends on the type of sorbent that is chosen. The partitioning of compounds between an aqueous sample and an extraction phase is the main principle of operation of SPME. The microextraction process is considered complete when the analyte concentration reaches equilibrium between the sample matrix and the fiber coating.

According to Equation 1.5, K_{fs} the distribution coefficient is defined as the ratio of analyte concentrations between the fiber coating and sample matrix at equilibrium.[61]

$$\boldsymbol{K_{fs} = \frac{C_f^{\infty}}{C_s^{\infty}}} \qquad \textbf{Equation 1.5}$$

Finally, the number of moles of analyte (n) extracted by the coating can be computed by Equation 1.6.[61]

$$\boldsymbol{n = C_f^{\infty} V_f = C_0 \frac{K_{fs} V_s V_f}{K_{fs} V_f + V_s}} \qquad \textbf{Equation 1.6}$$

Equation (1.6) shows that the number of moles of compound absorbed onto the coating (n) at equilibrium is directly related to its initial concentration in the sample (C_0), which is the analytical basis for quantification using SPME. In this equation, V_S is the volume of

the aqueous sample and V_f is the volume of the extraction (sorbent film) phase. When the sample volume is very large, i.e. $V_S >> K_{fS}V_f$ the amount of compound extracted by SPME can be simplified into Equation 1.7.[61,62]

$$\boldsymbol{n = K_{fs}V_fC_0} \qquad \textbf{Equation 1.7}$$

As a result, the amount of analyte extracted becomes independent of the sample volume. This feature is important and useful for in-the-field or *in vivo* sampling when the volume of sample is large and unknown.

1.4.3 SPME v*ersus* SPE

Solid phase microextraction (SPME) and SPE utilize similar three-step processes: In the first step, a sample interacts with the sorbent, and analytes are extracted from the sample. In the second step, a suitable solution passes through/over the sorbent to wash unwanted species from, while retaining desired analytes on, the sorbent. In the final step, an appropriate elution solvent is used to desorb the analytes of interest. However, there are major differences between SPE and SPME. In SPE, the main objective is to remove analytes completely from a sample and transfer them to the extraction phase. The capacity of the extraction phase for the extracted analytes must be significantly larger than the amount of analyte in the sample. It is difficult to select a wash solvent to remove unwanted compounds completely, without affecting on the retention of the compounds of interest. Therefore, unwanted compounds may remain in the sorbent. Because of low sorbent-to-sample ratio used in SPME in comparison to SPE, exhaustive extraction of the analytes will not be achieved in SPME. Solid phase extraction can therefore provide better detection limits than SPME due to its exhaustive extraction. Solid phase microextraction has less interferences and the amount extracted is proportional to the free concentration of analyte. Consequently, SPME can be a useful alternative to SPE for global metabolomics.

1.4.4 Ion exchange: cation and anion exchange

In 1850, agricultural chemists, Thompson and Way[63] recognized and described ion exchange process. The first practical industrial application of the ion exchange process occurred in 1905 by Gans[64] who synthesized sodium-aluminosilicate cation exchanger materials and used them to soften water. In 1935, Adams and Holms[65] in England, developed condensate polymers with various functional groups and produced both anion and cation exchange materials. Cation exchangers were prepared by attaching sulfonic acid groups ($-SO_3H^+$) to a phenol formaldehyde polymer matrix. On the other hand, anion exchangers were prepared by adding amine groups ($-NH_2$) to a similar matrix. Cation

exchange is used to retain and separate positively charged ions on a negative surface (exchange positively charged ions). On the other hand, anion exchange is used to retain and separate negatively charged ions on a positive surface (exchange negatively charged ions). Figure 1.5 shows these formats.

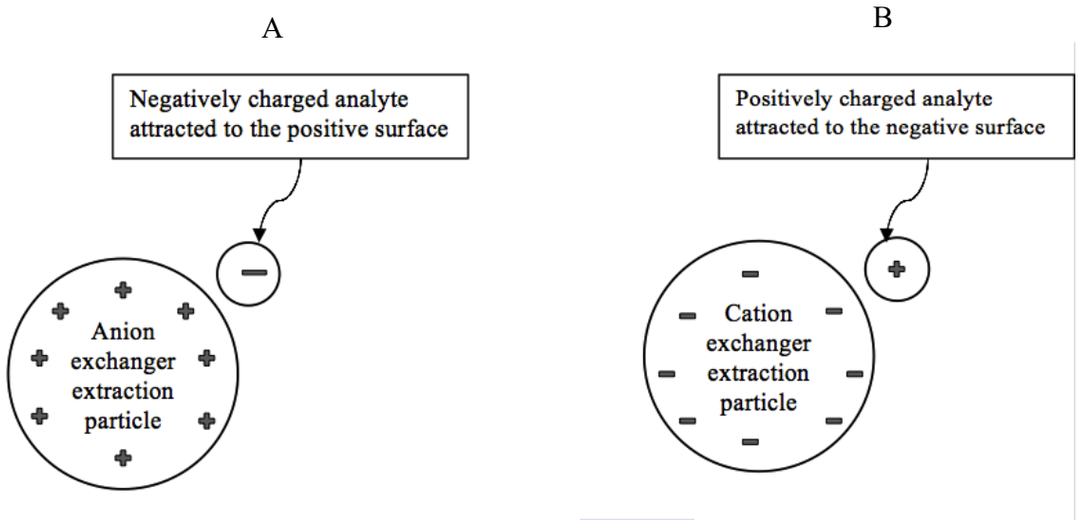

Figure 1.5 Types of ion exchanger. A: Anion exchange B: Cation exchange

Both exchangers can be further classified as strong and weak types. Strong ion exchangers have functional groups (e.g., quaternary amines, sulfonic acid) and are completely ionized regardless of pH, while weak ion exchangers have functional groups such as secondary amines or carboxylic acids, where the extent of ionization can be modified based on their pK_a and the mobile phase pH. Weak cation exchange materials lose their ion-exchange properties when the acidic exchanger group is protonated ($pH \leq 4$) and weak anion exchange materials lose their ion-exchange properties at high pH when they are deprotonated. As a result, weak base anion exchangers are very effective for the removal of acidic compounds and weak cation exchangers are effective for isolating basic compounds of interest. The ionization constant (pK_a) is the pH value at which 50% of the functional group is ionized and 50% is neutral. To ensure that analyte or particle surface are fully charged or neutral, the pH must be adjusted to a value at least 2 units below or above the pK_a.

1.5 Introduction to hydrogel particles

Hydrogels are three-dimensional networked structures of polymer chains which are able to absorb large amounts of water, including biological fluids.[66] Hydrogels can be termed "nano" or "micro" depending on their size which range from 10 nm to micrometer diameters respectively.[67] Hydrogels contain some hydrophilic groups in their structure such as –OH, –CONH–,–$CONH_2$, and –SO_3H that allow the hydrogel to absorb large amount of water. Specifically, Poly (N-isopropylacrylamide) (pNIPAm) based microgels

are hydrophilic and swell significantly in water when the temperature of the water they are dissolved in is below pNIPAm's lower critical solution temperature (LCST) of 32 °C. Above this temperature, the hydrogel is "deswollen" and has a much smaller water content.[68]

1.5.1 Properties of hydrogel

Hydrogels are a class of biocompatible materials, which enables their use for medical applications, including biological sensing, drug delivery, and tissue regeneration.[69] They have several promising properties: (1) These materials can absorb large amount of water (up to 90–99% water by weight) and have an elastic structure. The hydrophilic nature of the hydrogel can also reduce the nonspecific adsorption of proteins to the hydrogel.[70] (2) They have high surface area (within the particle size range of 10–1000 nm) so that mass transport on the microgels will be increased. (3) They have rapid volume changes in response to environmental factors, such as pH, temperature and ionic strength.[71] (4) They have controllable swelling process, which is shown in Figure 1.6. For a hydrogel with acidic groups bound to their polymer chains, the H^+ is removed in basic solutions and combines with OH^- to form H_2O. By changing the pH, the cation concentration is increased, which causes the gel to swell/deswell due to the osmotic pressure between the inside and outside of the gel. Some ions diffuse into the gel whereas others diffuse out of the hydrogel. The osmotic pressure inside the gel is higher than outside and therefore applies force in the outward direction throughout swelling. The extent of swelling depends on the ionization degree, quality of solvent, cross-link density, and ionic strength.[72] Usually, there are four inter-molecular forces involved in the swelling process: van der Waals, hydrogen bonding, hydrophobic, and electrostatic interactions. Van der Waals forces between the electric multipoles of the polymer monomers have the strength of the order of 10^{-2}–10^{-1} eV/atom and depend on the solvent composition.[73] Hydrogen bonding is a van der Waals interaction between fixed dipoles when a hydrogen atom is close to an atom of high electronegativity such as oxygen, nitrogen or fluorine and its strength is about 10^{-1} eV/atom. Hydrophobic interactions occur between nonpolar parts of polymer chains and their strength is 5.10^{-3}–5.10^{-2}eV/atom, so they are considered weak interactions. The electrostatic interactions occur between functional groups in the polymer gel and ions from the outside of the gel. Thus, it will lead to differential ion distributions inside and outside the gel and cause swelling or de-swelling of the gel.[74]

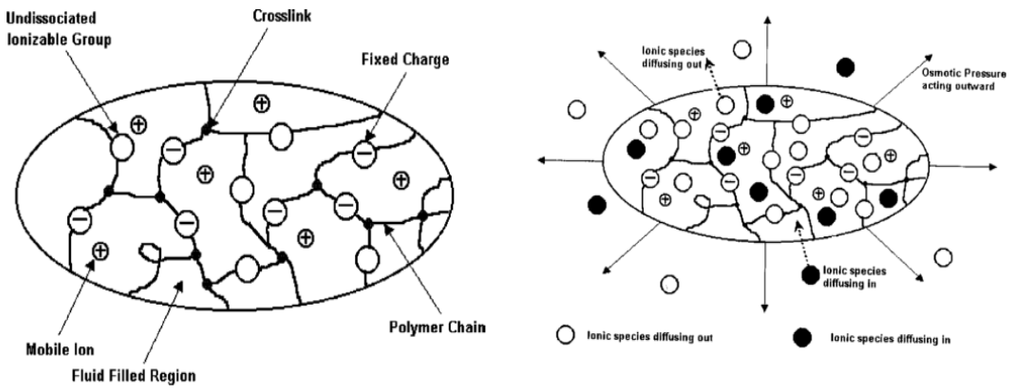

Figure 1.6 Hydrogel swelling process. Left-hand side shows hydrogel containing acidic groups bound to polymer chains. Changing pH can increase cation concentration and give rise to osmotic pressure that will cause the gel to swell/deswell as shown in right-hand panel. Figure from Sudipto *et al*. reprinted with permission from Reference 74. Figure copyright 2002 IEEE.

The most common polymer for hydrogel synthesis is Poly N-isopropylacrylamide (pNIPAm).[73] The main advantage of this polymer is that functional groups can be incorporated into pNIPAm microgels by simple copolymerization. As a result, hydrogel particles can have different chemistries and are compatible with different sample preparation approaches. Figure 1.7 shows the polymeric structure of cation and anion exchange hydrogel.

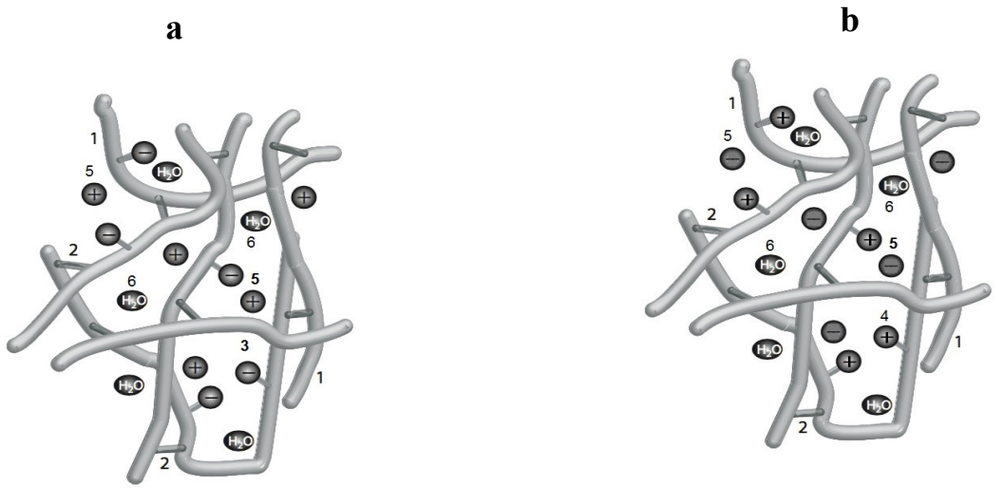

Figure 1.7 Schematic of polymeric ion exchanger (a) Cation exchange hydrogel (b) Anion exchange hydrogel. 1- polymeric chain 2- cross link 3- negatively charge cation exchange functionality attached to the chain 4- positively charge anion exchange functionally attached to the chain 5- counter ion 6- water (adopted from Andrei A. Zagorodni book)[75]

1.5.2 Microgels and nanogels as new materials in sample preparation

All global metabolomics studies to date, which have used the SPME format, rely on a fiber format where a metal wire is coated on the outside with a thin layer of an extracting phase. There have been no similar investigations using the D-SPME format or polymeric hydrogels for global metabolomics. However, commercially available core-shell hydrogel nanoparticles (CERES Nanotrap) have been used successfully for the exclusion of unwanted, abundant, proteins and enrichment of small protein biomarkers.[76,77] In this approach different high-affinity chemical baits are covalently incorporated into hydrogel nanoparticle cores or shells for protein and peptide harvesting, concentration, and preservation from body fluids. For instance, Tamburro *et al.*[76] used Poly (N-isopropylacrylamide-co-acrylic acid) and Cibacron Blue F3GA nanoparticles that were functionalized with amino-containing dyes via zero-length cross-linking amidation reactions. The shell contained vinyl sulfonic acid (VSA) and had an effective pore size that acted as a molecular sieve. Proteins and peptides small enough to enter to the core were captured by the high-affinity bait, while the shell prevented entry of unwanted molecules. Figure 1.8 shows the structure of core-shell hydrogel nanoparticles.

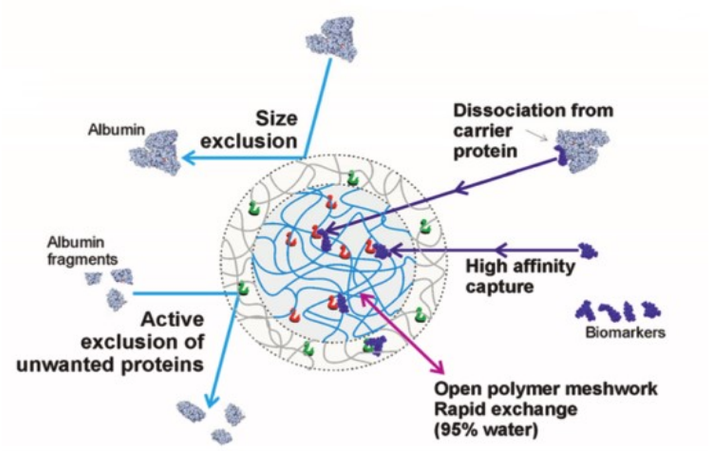

Figure 1.8 Structure of core-shell hydrogel nanoparticles. Figure reproduced from Reference 76 under ACS Author's Choice open access license for non-commercial use.

1.6 Research objective

Despite recent advances in instrumentation, the analytical approaches used in global metabolomics studies are not yet as well defined as in other "omics" studies and are currently an active area of research. Metabolomics aims at identification and quantitative analysis of wide range of metabolites in biological samples. However, due to the diverse range of chemical and physical properties, and the wide concentration range of metabolites within the metabolome, there is no single method can result in complete extraction of all metabolite classes. Sample preparation remains a major challenge in untargeted LC-MS metabolomics studies and coverage of low abundance metabolites generally remains poor. Also, many current standard preparation methods for metabolomics suffer from severe ion suppression issues. Due to its high selectivity and microextraction format, SPME may be able to address these two challenges. Therefore, the main goal of my project is to evaluate the potential of dispersive solid phase microextraction (D-SPME) using hydrogel micropaticles for global metabolomics of human plasma for the first time. To achieve this goal, three different types of hydrogel microparticles functionalized with vinyl acetate (VAC), acrylic acid (AAC) or N-3-aminopropyl methacrylamide hydrochloride (APMAH) will be evaluated and optimized D-SPME extraction protocols using these sorbents. The performance of these new extraction phases to commercial core-shell nanoparticles (CERES Nanotrap) with acrylic acid or cibachron blue cores will be compared and investigated their potential to reduce ion suppression effects thus improving analytical quality of metabolomics datasets. The optimized new method will also be compared to the conventional "gold standard" extraction method of solvent precipitation with methanol to evaluate its potential to boost the detection of low abundance metabolites. All methods will be developed and/or compared in combination with metabolomic profiling analysis using RPLC and HILIC

chromatography coupled to an LTQ-Orbitrap Velos or Q-TOF high resolution mass spectrometer via ESI.

Chapter 2

Development of dispersive solid phase microextraction method for global metabolomics using standard metabolite mixture

2.1 Introduction

The main goal of a typical metabolomics study is to compare the abundance of the small molecule metabolites in highly complex matrices such as body fluids. The greatest challenges for such analysis are the detection of low abundance metabolites among a massive background of interfering compounds and the ionization suppression. In this study we are using dispersive solid phase microextraction (D-SPME) to address these challenges. The focus of this chapter is to describe the development of novel D-SPME method for LC-MS global metabolomics using a standard metabolite mixture. Polymeric hydrogels were selected for this evaluation for their high permeability, low-cost and customizable functionalization. In particular, the introduction of ion-exchange functional groups such as vinyl acetate (VAC), acrylic acid (AAC) and N- (3-aminopropyl) methacrylamide hydrochloride (APMAH) within the polymer network will be tested in order to increase the number of interactions (such as ionic interaction) between analyte and sorbent.

Since this is the first time this type of hydrogel was investigated for its utility in global metabolomics, extensive optimization of the method using a metabolite test mixture as a simplified and controlled stand-in for a biological sample will be performed. This metabolite test mixture consisted of a diverse range of compounds including amino acids, amines, organic acids, hormones, sugars, nucleosides and lipids (at least one representative species per each of eight classes of lipids). The metabolite mixture was selected based on (1) commercial availability of authentic standards (2) wide molecular weight range (103-886 Da) (3) wide polarity range (log P range of -5.0 to 10.74) and (4) few representative low abundance metabolites. These analytes were dissolved in an appropriate buffer. The analyses were carried out using HPLC-Orbitrap and HPLC-Q-TOF with ESI ionization, in both positive and negative modes. In order to cover as much of the metabolome as possible, three different LC methods (HILIC, Pentafluorophenyl RP and Charged Surface Hybrid C18 RP) were used to provide good coverage of polar, intermediate and lipid metabolomes respectively. Finally, the optimum protocols for each of the three types of microgels tested are proposed.

2.2 Experimental

2.2.1 Chemicals and materials

Acetonitrile and methanol were purchased from Fisher Scientific (Ottawa, Canada). Isopropanol, dimethyl sulfoxide, ethanol, water (HPLC grade), all metabolite standards and buffer reagents were purchased from Sigma-Aldrich (Oakville, Canada). Lipid standards were purchased from Avanti Polar Lipids (Alabaster, Alabama, US). All microgels (AAC, VAC, APMAH) tested in this work were synthesized by the Michael Serpe group at the University of Alberta.

2.2.2 Preparation of standard mixture

In global metabolomics, the aim is to study the whole metabolome that consists of thousands of different compounds. Therefore, it is not possible to have a standard for each metabolite of interest. Consequently, for this optimization, one or a few analytes from each metabolite class are used, and considered to be representative for all the substances within that class. All metabolite standards and their properties are listed in Table 2.1 and their structures are shown in Figure 2.1.

Phosphate-buffered saline solution was prepared by dissolving 8.0 g of sodium chloride (137 mM), 0.2 g of potassium chloride (2.7 mM), 0.2 g of potassium phosphate, and 1.44 g of dibasic sodium phosphate (10 mM PO_4^{3-}) in 1 liter of purified water and adjusting the pH to 7.4, if necessary. Stock standard solutions were prepared in different solvents (water, methanol, ethanol and dimethyl sulfoxide) as described in Table 2.1 with sonication as appropriate to obtain the concentration of 1 mg/mL except for biotin and coenzyme Q10 that had concentration of 0.1 mg/mL and adenine with 0.2 mg/mL. Lipid standards were prepared in chloroform, methanol or chloroform: methanol: water (63/35/8, v/v) as appropriate depending on their solubility in order to obtain the concentration of 1 mg/ml. They were kept frozen at -80°C and were prepared fresh monthly. For extraction, metabolite standard solutions were prepared at 1 µg/mL concentration by dilution of stock standard in an appropriate buffer solution. For instrument calibration, working standard solutions with known concentration of metabolites were prepared by dilution of stock standard with desorption solvent used for each experiment. This calibration set was analyzed before and after each sample set to ensure method and instrument stability and used to calculate the recoveries.

Buffer solutions were prepared at different pH; ammonium formate and formic acid (pH=3.0), sodium phosphate dibasic and monobasic (pH=7.5), ammonium bicarbonate and ammonium hydroxide (pH=9.0) and pH was verified with pH meter (Accumet AB150, Fisher Scientific) to be within ±0.05 pH units experimentally.

Table 2.1 Physicochemical properties of 42 metabolites included in standard metabolite mixture.

Name of metabolite	Molecular formula	Molecular Weight (MW)	Log P	Dissolving solvent (v/v)	Lot number
Glutathione	$C_{10}H_{17}N_3O_6S$	307.3235	-4.9	Water	100K72763V
Lysine	$C_6H_{14}N_2O_2$	146.1055	-3.76	Water	BCBK3837V
Choline	$C_5H_{13}NO$	103.0997	-3.59	Water	SLBG5926V
Glutamic acid	$C_5H_9NO_4$	147.0531	-3.54	Methanol/Water (1/1)	SLBD1211V
Histidine	$C_6H_9N_3O_2$	155.0694	-2.67	Water	SLBF5674V
D-Glucose	$C_6H_{12}O_6$	180.1559	-2.6	Water	G8270
Ribose 5 phosphate*	$C_5H_{11}O_8P$	230.0191	-2.07	Water	BCBJ8213V
Glucose 6 phosphate	$C_6H_{13}O_9P$	260.0297	-2.06	Water	SLBD9319V
Creatinine	$C_4H_7N_3O$	113.0589	-1.65	Water	SLBD4664V
Phenylalanine	$C_9H_{11}NO_2$	165.0789	-1.35	Methanol/Water (1/1)	SLBB2703V
Adenosine	$C_{10}H_{13}N_5O_4$	267.0967	-1.21	Water	061M1410V
B-NAD	$C_{21}H_{29}K_2N_7O_{14}P_2$	663.1091	-1.18	Water	061M7005V
Tryptophan	$C_{11}H_{12}N_2O_2$	204.0898	-1.10	Methanol/Water (1/1)	SLBB6573V
Riboflavin	$C_{17}H_{20}N_4O_6$	376.1382	-1.05	Water	SLBC6522V
Epinephrine	$C_9H_{13}NO_3$	183.0895	-0.82	Methanol/Water (1/1)	BCBH9629V
Histamine	$C_5H_9N_3$	111.0796	-0.69	Water	BCBK5478V
Hydroxybutyric acid	$C_4H_8O_3$	104.0473	-0.50	Water	MKBL8779V
Nicotinamide	$C_6H_6N_2O$	122.0480	-0.45	Water	BCBK6434V
Adenine	$C_5H_5N_5$	135.0544	-0.38	Water	1181126V
Biotin	$C_{10}H_{16}N_2O_3S$	244.0881	0.17	Methanol/Water (1/1)	119K1533
Maleic acid	$C_4H_4O_4$	116.0109	0.21	Water	SLBC1970V
Taurocholic acid	$C_{26}H_{45}NO_7S$	515.2916	0.79	Water	091M0014V
Thyroxine	$C_{15}H_{11}I_4NO_4$	776.6867	1.15	Dimethyl Sulfoxide	BCBH4077V
Tryptamine	$C_{10}H_{12}N_2$	160.1000	1.21	Water	MKBH7797V
Cortisol	$C_{21}H_{30}O_5$	362.2093	1.79	Methanol	SLBD0859V
Estrone glucuronide	$C_{24}H_{29}O_8$	446.1941	1.92	Methanol	BGBB9162V
Cholic acid	$C_{24}H_{40}O_5$	408.2875	2.26	Methanol	SLBB1065V
Estradiol	$C_{18}H_{24}O_2$	272.1776	3.57	Methanol	SLBG0383V
D-erythro-Sphingosine	$C_{18}H_{37}NO_2$	299.2824	5.15	Chloroform/Methanol (9/1)	860490
17:0 Lyso PC	$C_{25}H_{52}NO_7P$	509.3481	5.43	Chloroform	855676
16:0 MG	$C_{19}H_{38}O_4$	330.5030	5.73	Chloroform	110606
19:0 PC	$C_{46}H_{92}NO_8P$	817.6560	6.15	Chloroform	850367
Cholesterol*	$C_{27}H_{46}O$	386.3548	7.02	Methanol	SLBC7554V
Palmitic acid*	$C_{16}H_{32}O_2$	256.4241	7.23	Methanol	SLBF5671V
Liver PI	$C_{47}H_{82}Na\ O_{13}P$	902.1330	7.79	Chloroform	840042
Vitamin K1	$C_{31}H_{46}O_2$	450.3498	8.48	Ethanol	BCBH2934V
17:0 PE	$C_{39}H_{78}NO_8P$	719.5464	8.59	Water/ Methanol/ Chloroform (65/35/8)	830756
18:0 PG	$C_{42}H_{83}O_{10}P$	778.5723	8.60	Water/ Methanol/ Chloroform (65/35/8)	840465
18:0 PA	$C_{39}H_{76}O_8P$	704.5356	9.14	Chloroform	830865
Coenzyme Q10	$C_{59}H_{90}O_4$	862.6839	9.94	Ethanol	SLBC559V
18:0-16:0 DG	$C_{37}H_{72}O_5$	596.5379	10.16	Chloroform	110883
18:1-16:0-18:1 TG	$C_{55}H_{102}O_6$	858.7676	10.74	Chloroform	111005

*Standards that were not detected by LC-MS methods

Glutathione

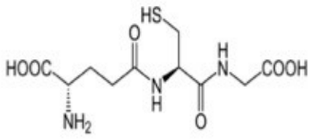

Lysine

Choline

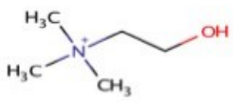

Creatinine

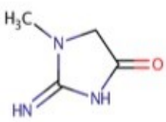

Glucose 6phosphate

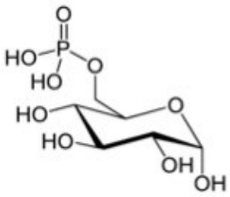

Adenosine

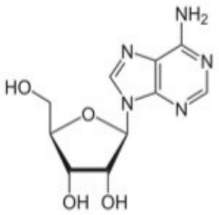

Glutamic acid

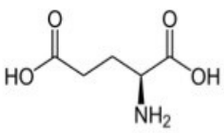

Histidine

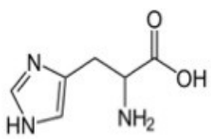

Histamine

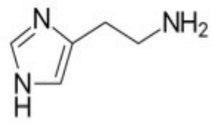

Ribose 5 phosphate

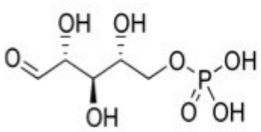

Tryptophan

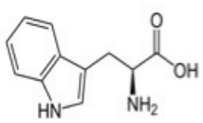

NAD

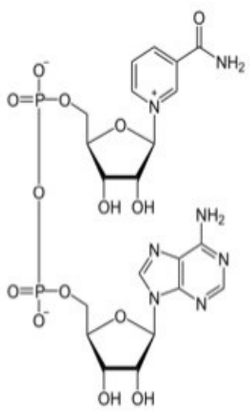

Riboflavin

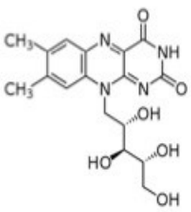

Hydroxybutyric acid

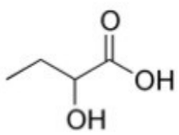

Phenylalanine

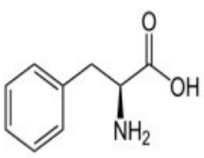

Glucose

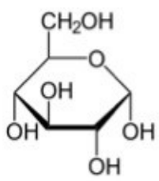

Thyroxine

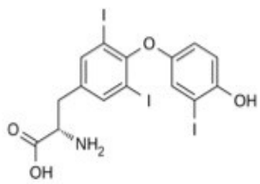

Adenine

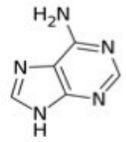

Nicotinamide

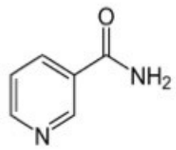

Biotin

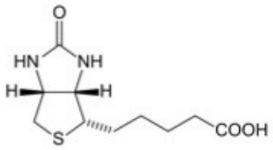

Maleic acid

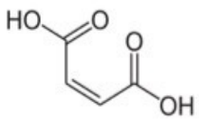

Taurocholic acid

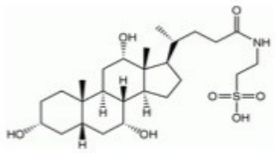

Tryptamine

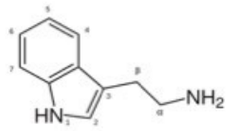

Cortisol

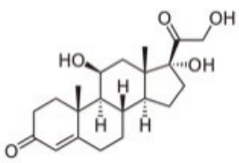

Epinephrine

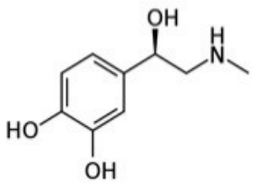

Estrone glucuronide

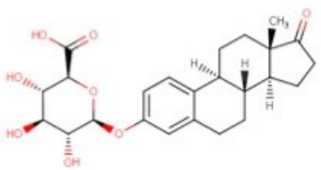

Vitamin K1

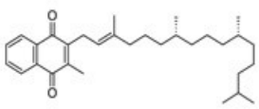

Cholic acid

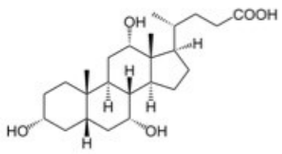

Estradiol

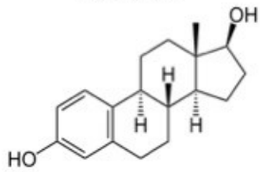

Palmitic acid

Cholesterol

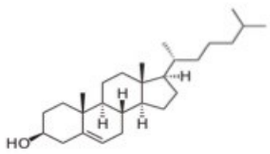

Coenzyme Q10

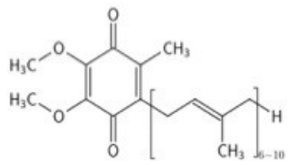

D-erythro-Sphingosine

1,2-dioctadecanoyl-sn-glycero-3-phospho-(1'-sn-glycerol) (18:0 PG)

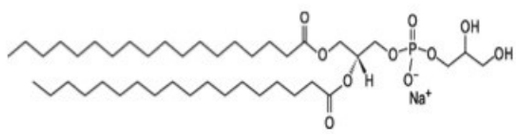

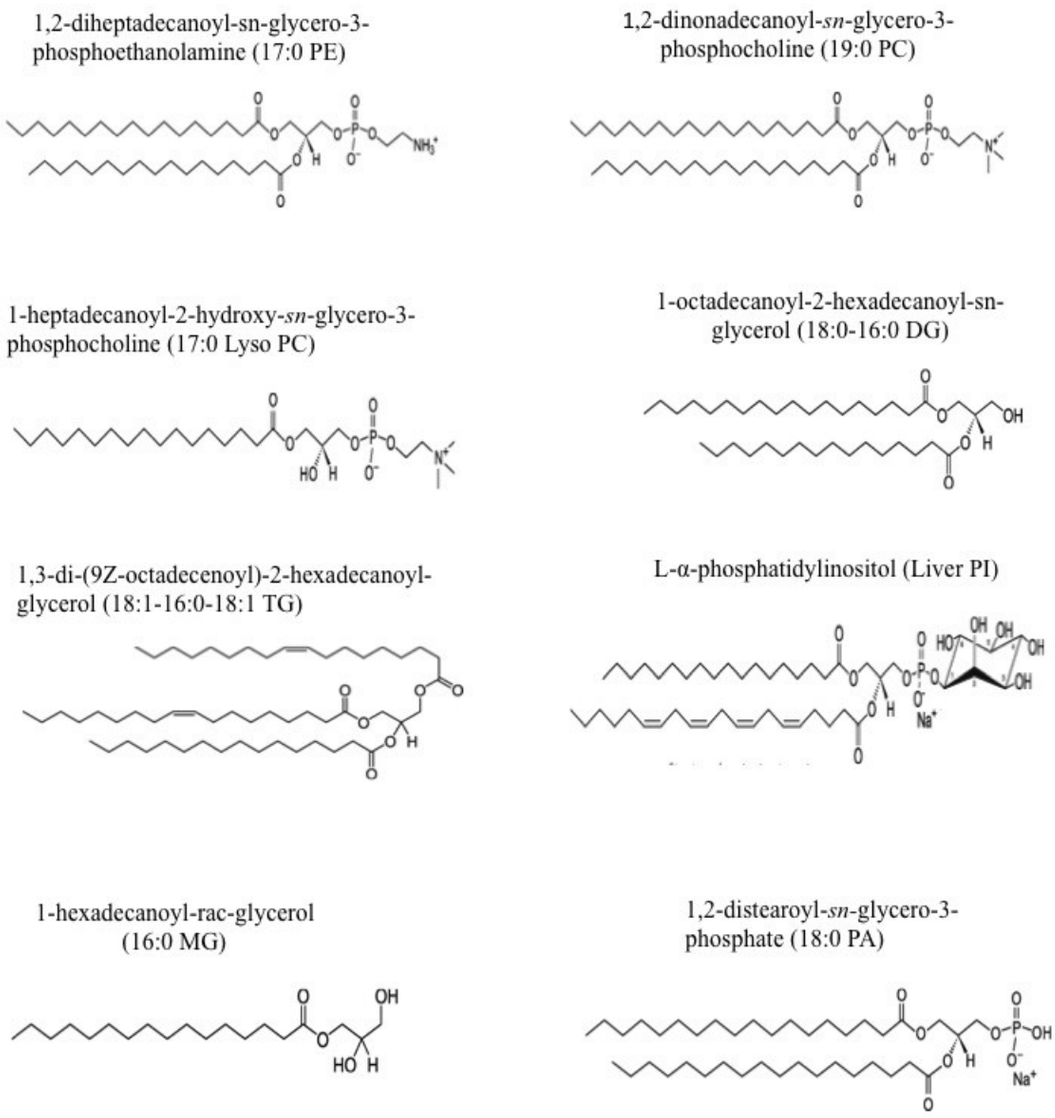

Figure 2.1 Structures of 42 metabolites included in metabolite standard test mixture.

2.2.3 D-SPME Procedure

2.2.3.1 Ion-exchange hydrogel microparticles: microgels

Different types and portions of ion-exchange functionality of microparticles (5, 10, 15% for AAC and VAC and 5, 10% for APMAH) were tested in this work to evaluate the effect of these properties to extract various metabolite classes. All microgels were about 1 μm in size unless otherwise indicated in the text. Their exact chemical composition is shown in Table 2.2. 15% APMAH was not available for testing due to the difficulty of attaching APMAH at such a high concentration in a stable hydrogel. Chemical structures of AAC, VAC and APMAH microgels are shown in Figure 2.2. NIPAm forms a three-dimensional network of polymer chains that are hydrophilic when crosslinked with methylenebisacrylamide (BIS). This network can be synthesized with a variety of functional groups, simply by adding functional co-monomers to the reaction solution via free radical precipitation polymerization.[78,67] The selected functionalized microgels can

act as ion-exchange sites to help extract basic or acidic compounds. AAC and VAC are negatively charged functional monomers containing acrylic acid and vinyl chain respectively and APMAH is a positively charged functional monomer prepared using N-(3-aminopropyl) methacrylamide hydrochloride co-monomer.

Table 2.2 Chemical compositions of microgels used in this study and synthesized at the University of Alberta.

Type of Microgel	Co-monomer	BIS	NIPAMm
AAC	5, 10, 15%	5%	90, 85, 80%
VAC	5, 10, 15%	5%	90, 85, 80%
APMAH	5, 10%	5%	90, 85%

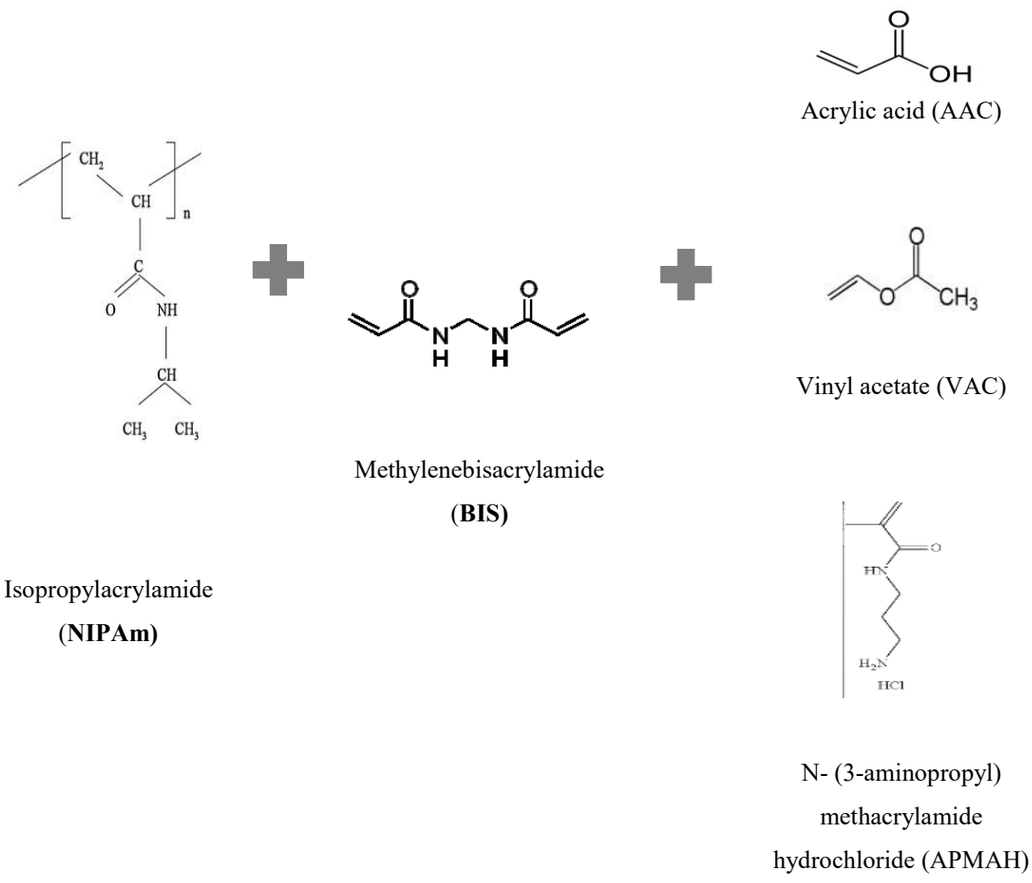

Figure 2.2 Schematic representation of AAC, VAC and APMAH microgel.

2.2.3.2 Polar metabolite extraction with D-SPME using microgel

The initial D-SPME protocol was as follows: 200 µL of standard metabolite mixture was added to 25 µL of appropriate microgel and incubated with shaking (Fisher Scientific™ Multi-Platform Shaker) for 60 minutes (450 rpm) at room temperature. After

centrifugation (25000 g, 4°C) for 10 minutes the supernatant was carefully removed. Then, the microparticles were washed (at room temperature) to remove any weakly bound compounds followed by another centrifugation step and removal of the wash solution. The wash solution was purified water unless otherwise specified. Finally, the microgels were then incubated with an elution solvent (at room temperature) for 1 hour with shaking (450 rpm) to elute the target analytes and 10-minute centrifugation (25000 g, 4°C) was applied for each elution step to separate the hydrogels from the supernatant. All parameters that affect extraction efficiency in SPME were systematically evaluated one-by-one to optimize the protocols for each of the three extraction phases tested. The final optimized protocol is summarized in Figure 2.33.

2.2.3.3 Lipid extraction with D-SPME using microgel

The initial D-SPME protocol for lipid extraction was as follows: 200 µL of lipid standard mixture [10 different standard lipids consisting of glycerolipids (18:0-16:0 DG, 16:0 MG, 18:1-16:0-18:1 TG); glycerophospholipids (19:0 PC, 17:0 PE, 17:0 Lyso PC, Liver PI, 18:0 PG, 18:0 PA) and sphingosine] at a concentration of 1 µg/mL each, which was dissolved in methanol/water (40/60, v/v), was added to 25 µL of microgel. The extraction was performed for 60 minutes with shaking (450 rpm) at room temperature, followed by 10-minute centrifugation (25000 g) at 4°C. After removing the supernatant, the particles were washed with 200 µL of methanol/water (20/80, v/v) and centrifuged again. 100 µL of an appropriate solvent was added into each microgel as an elution solvent. Desorption was performed with 1-hour shaking (450 rpm) followed by 10-minute centrifugation. 100 µL of supernatant was transferred to HPLC vial for LC-ESI-MS analysis. The final optimized protocol is summarized in Figure 2.33. Methanol/water (40/60, v/v) was required for this step of optimization to ensure lipid solubility across all classes. For plasma extractions described in Chapter 3, no methanol was used during extraction step, as lipids are well solubilized in plasma matrix.

2.2.4 Development of LC-MS conditions

Global LC–MS studies are typically performed using both reversed-phase chromatography and HILIC in both positive and negative ESI modes in parallel for the same sample sets in order to increase metabolome coverage[24] and this approach was used in this work as well.

2.2.4.1 Summary of LC methods

Overall, three different LC methods were used as shown in Table 2.3. HILIC method was used for metabolites of high polarity, PFP RP method for metabolites of intermediate polarity and CSH C18 RP method for lipids.

Table 2.3 Summary of optimized LC methods used in this study

LC parameter	HILIC method	PFP Reversed-Phase method	CSH C18 Reversed-Phase method
Column	Ascentis Si Express (Sigma-Aldrich)	Kinetex Pentafluorophenyl (Phenomenex)	CSH C18 (Waters)
Column dimensions	100 mm x 2.10 mm	50 mm × 2.10 mm	75 mm x 2.1 mm
Particle size	2.7 µm	2.6 µm	2.5 µm
Mobile phase A	acetonitrile/water (95/5, v/v) with 2 mM ammonium acetate total	water/formic acid (99.9/0.1, v/v)	water/methanol (60/40, v/v) with 10 mM ammonium acetate and 1 mM acetic acid total
Mobile phase B	acetonitrile/water (60/40, v/v) with 2 mM ammonium acetate total	acetonitrile/formic acid (99.9/0.1, v/v)	isopropanol/methanol (90/10, v/v) with10 mM ammonium acetate and 1 mM acetic acid total
Flow rate	300 µL/min	300 µL/min	150 µL/min
Run time	30 min	30 min	32 min
Injection volume	10 µL	10 µL	10 µL
Gradient program	0-2 min 100% A, 2-14 min linear gradient to 35% A, 14-18 min hold at 35% A, 18.10-30 min re-equilibration at 100% A	0-5 min 100% A, 5-15 min linear gradient to 20% A, 15-20 min hold at 20% A, 20.10-30 min re-equilibration at 100% A	0-2 min 60% A, 2-3 min linear gradient to 35% A, 3-16 min to 5% A, 16-24 min hold at 5% A, 24.10-32 min re-equilibration at 60% A
Temperature	22 ^{0}C	22 ^{0}C	55 ^{0}C

All 42 standard compounds were separated under these conditions except cholesterol and palmitic acid. Cholesterol had a poor detection limit due to poor ESI ionization efficiency so that it was removed from the standard mixture. Palmitic acid could only be observed on the PFP column in negative ESI mode with different mobile phase conditions and mobile phase additive [solvent A: water with 5 mM ammonium acetate, solvent B: methanol/water (90/10, v/v with 5 mM ammonium acetate)]. It was inappropriate to change the conditions for just one compound so palmitic acid was removed from the mixture as well. Ribose 5-phosphate was also omitted because it could not be eluted from HILIC column when using the above gradient conditions.

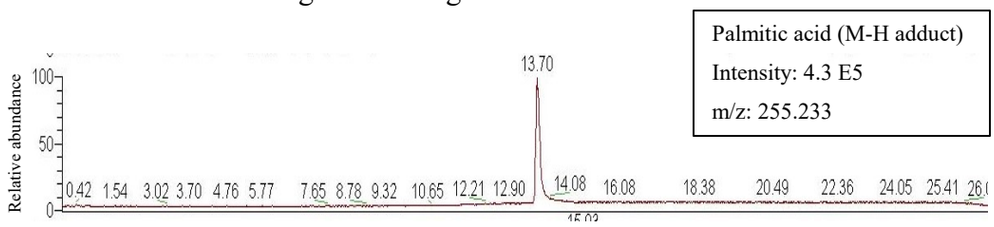

Figure 2.3 Example extracted ion chromatogram (XIC) of palmitic acid using PFP reversed-phase with water with 5 mM ammonium acetate as solvent A and methanol/water (90/10, v/v) with 5 mM ammonium acetate as solvent B.

2.2.4.2 HILIC LC conditions for analysis of polar metabolome

Separations were performed using an Ascentis Si Express HILIC 2.7 µm (100 mm × 2.1 mm) column at a flow rate of 300 µL/min.[79] Compounds were eluted using a mobile phase gradient that described in Table 2.3. Example extracted ion chromatograms of

some metabolite standards, at 200 ng/mL, using the HILIC method are shown in Figure 2.4.

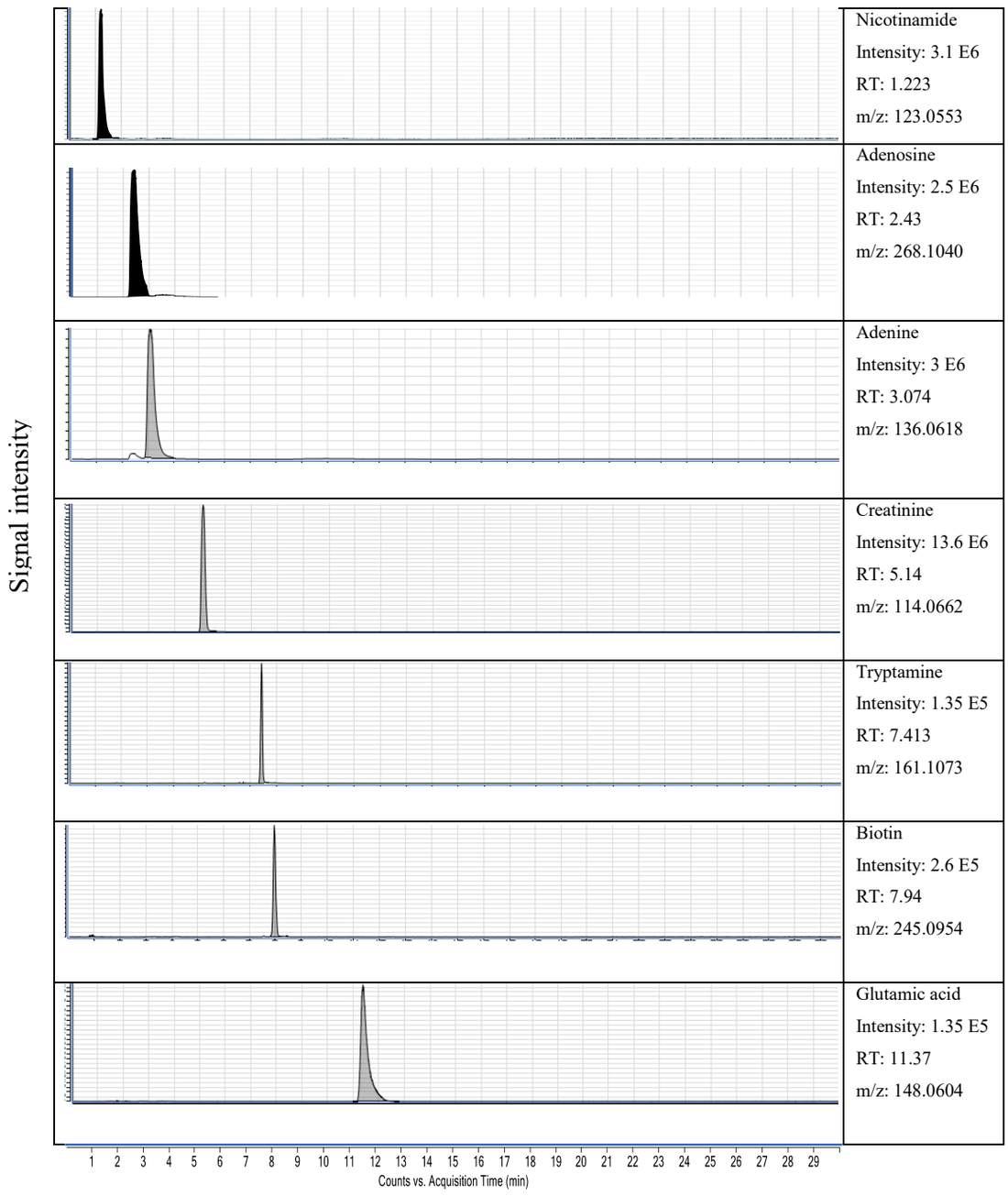

Figure 2.4 Example extracted ion chromatograms of $[M+H]^+$ ion of selected metabolites using HILIC LC-MS method with Ascentis HILIC silica column with solvent A (acetonitrile/ water (95/5, v/v) with 2 mM ammonium acetate and solvent B (acetonitrile/ water (60/ 40, v/v) with 2 mM ammonium acetate.

2.2.4.3 PFP RP method for analysis of intermediate polarity metabolome

Separations were performed using a Kinetex Pentafluorophenyl 2.6 µm (50 mm × 2.1 mm) column at a flow rate of 300 µL/min. Compounds were eluted using a mobile phase gradient that summarized in Table 2.3. Example extracted ion chromatograms of metabolite standards with concentration of 200 ng/mL analyzed using PFP reversed-phase method are shown in Figure 2.5.

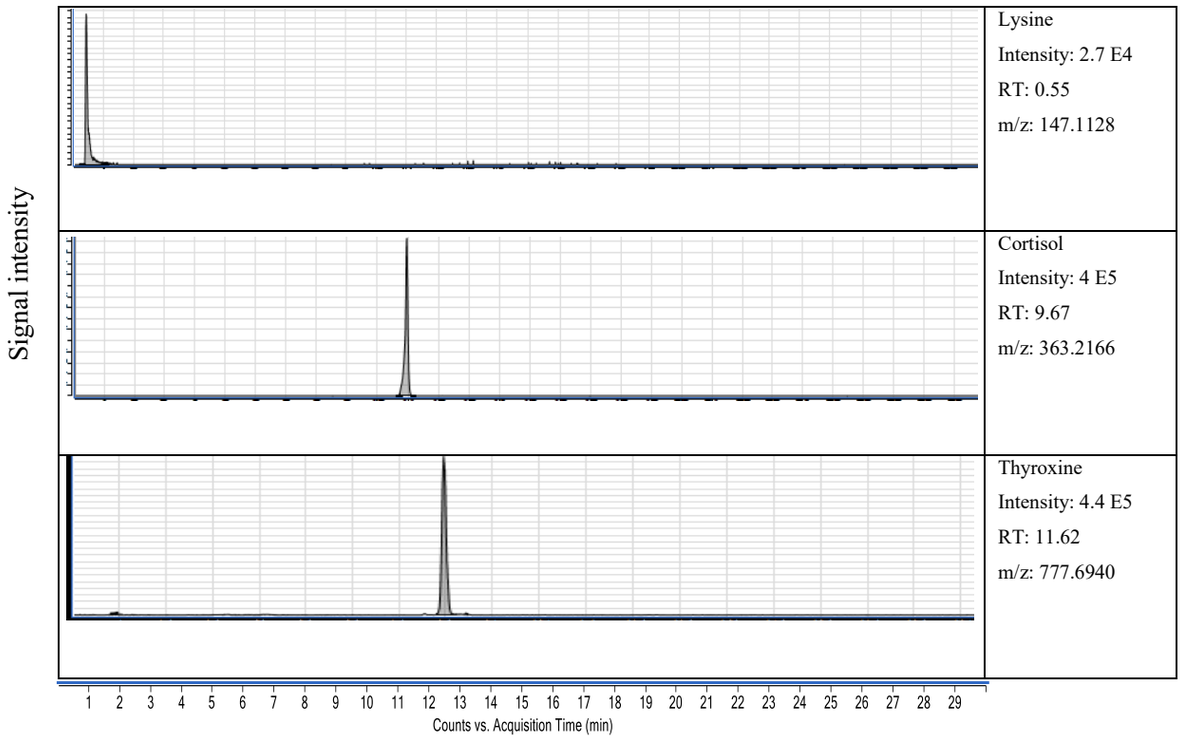

Figure 2.5 Example extracted ion chromatograms of $[M+H]^+$ ions of selected metabolites using reversed-phase LC-MS with PFP column with solvent A (water/formic acid, 99.90/0.1, v/v) and solvent B (acetonitrile/formic acid, 99.90/0.1, v/v)**.**

2.2.4.4 CSH C18 RP method for lipid separation

Lipids could not be properly separated and have good chromatographic peak shape with the developed PFP RP method presented in Section 2.2.4.3. Therefore, this separation was performed with a reversed-phase method using CSH (Charged Surface Hybrid) C18 stationary phase, elevated temperature and isopropanol containing mobile phase, all of which reduced tailing and thus improved both resolution and chromatographic peak shape for lipid analysis.[80,81] Charged surface hybrid particles are able to reduce the secondary interactions between silica in the column and basic compounds, therefore they provide excellent peak shape. Table 2.4 briefly summarizes the comparison of signals obtained for 1 µg/mL lipid standard mixture analyzed on PFP and CSH C18 columns, and shows better performance of all lipids on CSH C18 method except for the PE class, due to reduction in secondary interactions between analytes and the stationary. Separations

were performed using CSH C18, 2.5 µm (75 mm × 2.1 mm) column (Waters) at a flow rate of 150 µL/min. Compounds were eluted using a mobile phase gradient that summarized in Table 2.3. An example chromatogram of lipid standard analyzed using reversed phase method with CSH C18 column is shown in Figure 2.6.

Table 2.4 Comparison of 1 µg/mL lipid standard peak area with PFP and CSH C18 column.

Name of lipids	Peak area of 1 µg/mL standard in PFP column	Peak area of 1 µg/mL standard in CSH C18 column	Improvement
LYSO PC	4.8 E7 (M+H adduct)	7.3 E7 (M+H adduct)	1.54 fold
MG	1.6 E6 (M+H adduct)	3.6 E6 (M+Na adduct)	2.22 fold
Sphingosine	2.8 E8 (M+H adduct)	4.6 E8 (M+H adduct)	1.63 fold
PI	1.5 E6 (M+H adduct)	9.1 E6 (M+H adduct)	6.16 fold
PE	1.1 E7 (M+H adduct)	3.2 E6 (M+H adduct)	0.28 fold
PG	5.0 E5 (M+H adduct)	2.2 E6 (M+Na adduct)	4.45 fold
PA	1.6 E5 (M+H adduct)	9.8 E7 (M+NH4 adduct)	6.43 fold
PC	4.3 E7 (M+H adduct)	1.3 E8 (M+H adduct)	3.12 fold
DG	2.2 E7 (M+H adduct)	1.1 E8 (M+Na adduct)	5.08 fold
TG	4.4 E7 (M+H adduct)	1.1 E8 (M+H adduct)	2.71 fold

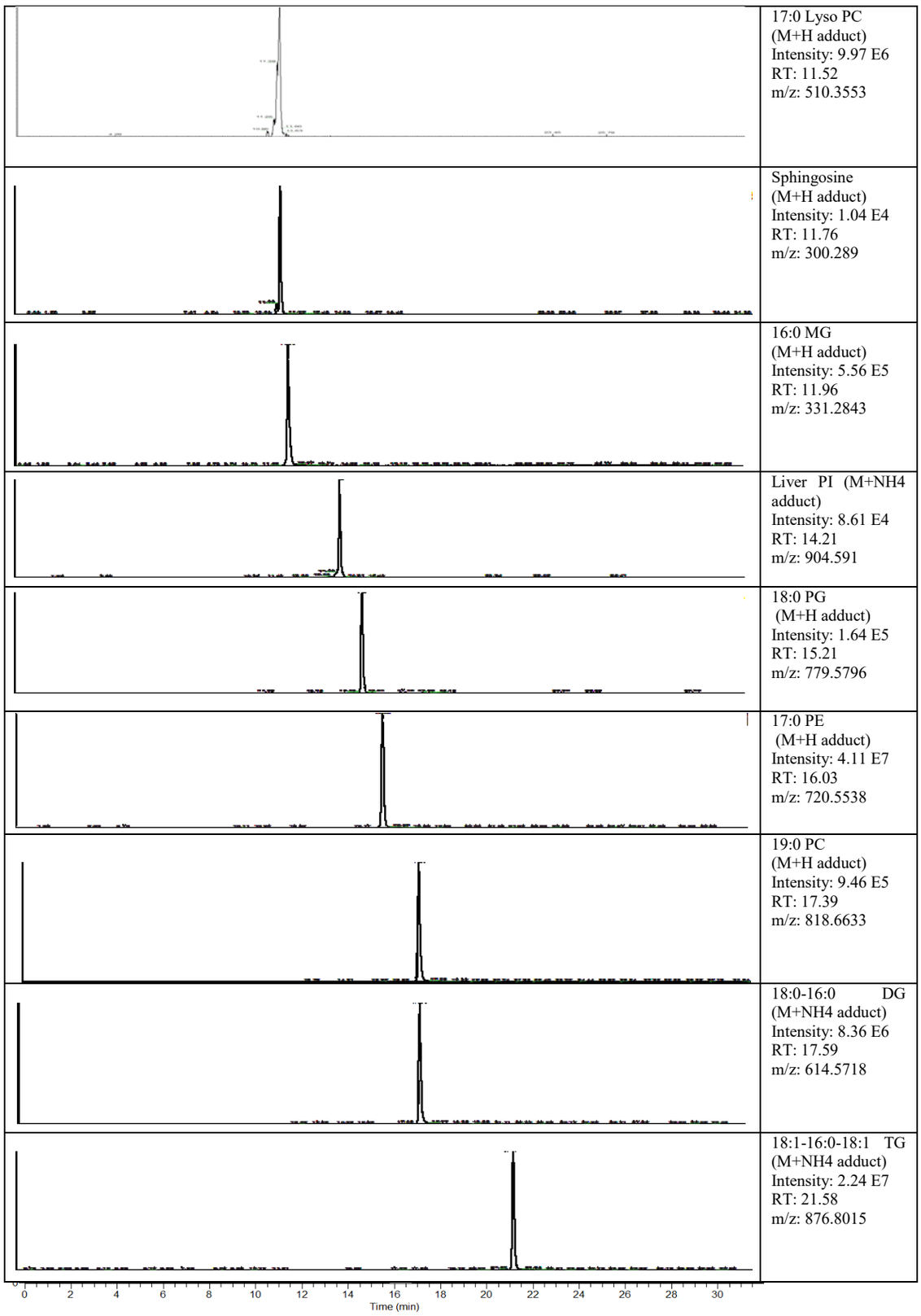

Figure 2.6 Example extracted ion chromatograms of lipid metabolite standards using reversed-phase method with CSH C18 column with solvent A (water/methanol (60/40, v/v) with 10 mM ammonium acetate and 1 mM acetic acid) and solvent B (isopropanol/ methanol (90/10, v/v) with 10 mM ammonium acetate and 1 mM acetic acid).

2.2.4.5 Development of MS conditions for all metabolites

All samples were analyzed on two instruments: an Agilent iFunnel 6550 Quadrupole Time-of-Flight mass spectrometer with the PFP RP and HILIC LC methods or on a Linear Trap Quadropole (LTQ) Orbitrap Velos (Thermo Fisher Scientific) with the CSH C18 RP method. The MS conditions used are listed in Tables 2.5 and 2.6.

2.2.4.5.1 Quadrupole Time-of-Flight (Q-TOF) MS parameters

An Agilent 1290 Infinity LC System equipped with a G4226A autosampler, a G42200A binary pump and a G1330B Thermal Column Compartment was coupled to an Agilent 6550 iFunnel Accurate-Mass Q-TOF LC-MS equipped with an ESI source with Agilent Jet Stream technology. Reference solution was introduced into the ESI source through an Agilent G1310B Isocratic Pump for reference ion mass correction. An external calibration solution was continuously sprayed in the ESI source of the Q-TOF system, employing purine at 112.050873 m/z, and "HP-0921" at 922.009798 m/z for positive mode and purine at 119.036320 m/z, HP-0921 (formate adduct) at 966.00072 m/z and HP-0921 (acetate adduct) at 980.016375 m/z for negative ESI to ensure mass accuracy throughout the chromatographic run. The instrument conditions are listed in Table 2.5. The Mass Hunter Workstation (Version B.07.00) LC-MS Data Acquisition software for Q-TOF was used to control all the acquisition parameters and also to process the obtained data.

Table 2.5 Q-TOF mass spectrometer conditions

MS conditions	
N_2 drying gas temperature	250 ^{0}C
N_2 drying gas flow	15 L/min
Nebulizer pressure	35 psig
Sheath gas temperature	275 ^{0}C
Sheath gas flow	12 L/min
Capillary voltage	3500 V
Nozzle voltage	400V
Oct RF voltage	750 V
Fragmentor voltage	175 V
Acquisition rate	2 spectra/s
Acquisition time	500 ms/spectrum
Mass range (Metabolites with high to intermediate polarity)	50-1100 m/z
Mass range (nonpolar metabolites)	250-1200 m/z

2.2.4.5.2 LTQ-Orbitrap MS parameters

LTQ-Orbitrap mass spectrometer was interfaced to an Agilent 1100 series HPLC equipped with a G1367A autosampler, a G1312A binary pump and G1322A degasser with a HESI source that was operated in both positive and negative ion electrospray modes. The MS conditions for LTQ-Orbitrap are listed in Table 2.6.

Table 2.6 LTQ-Orbitrap mass spectrometer conditions

MS conditions	
Capillary temperature	275 ^{0}C
Source heater temperature	300 ^{0}C
Sheath gas flow	10 L/min
Auxiliary gas flow	5 L/min
Source voltage	positive (4 kV) negative (-3kV)
S lens RF level (%)	62
Mass range	100-1000 m/z

Table 2.7 shows the retention time and the limit of quantification (LOQ) of each metabolite in PFP RP and HILIC in both positive and negative ESI modes. In reversed-phase, the compounds in the solvent front are highly suppressed but can typically be well retained in HILIC. The values highlighted in gray show the best method for that analyte and were used for inter-day and intra-day repeatability evaluations of the optimized method discussed in Section 2.3.12.

Table 2.7 Summary of retention time (RT), limit of quantitation (LOQ) and intensity obtained for various metabolites using different LC-MS methods.

Metabolites	Positive ESI-PFP-RP			Negative ESI-PFP-RP			Positive ESI-HILIC			Negative ESI-HILIC		
	RT (min)	LOQ (ng/mL)	Peak area intensity	RT (min)	LOQ (ng/mL)	Peak area intensity	RT (min)	LOQ (ng/mL)	Peak area intensity	RT (min)	LOQ (ng/mL)	Peak area intensity
Glutathione	0.50	0.87	2.7E4	0.49	0.87	4.4E3	12.20	3.12	1.4E3	NA		
Lysine	0.42	3.12	6.12E4	0.41	6.25	2.3E3	NA			NA		
Choline	0.47	6.25	5.6 E5	NA			NA			NA		
Glutamic acid	0.46	0.87	5.54E4	0.46	3.12	5.7E3	12.45	0.87	1.4E3	NA		
Histidine	0.42	0.87	4.77E4	0.44	0.87	1.0E3	NA			NA		
Glucose 6ph	0.50	3.12	5.60E3	NA			NA			NA		
Creatinine	0.48	0.87	6.2E4	0.47	25	1.3E3	5.63	0.87	1.8E4	5.68	6.25	2.4E3
Phenylalanine	0.49	3.12	2.26E5	0.42	0.87	2.2E3	NA			NA		
Adenosine	0.50	3.12	1.2E5	0.52	6.25	4.4E3	2.73	3.12	1.4E5	2.78	3.12	2.4E3
NAD	0.50	25	3.2E3	0.51	6.25	1.4E3	NA			NA		
Tryptophan	0.50	3.12	5.0E4	NA			NA			NA		
Riboflavin	8.01	0.87	5.8E3	7.99	25	5.6E3	2.64	0.87	4.4E3	2.70	0.87	1.2E3
Epinephrine	0.50	3.12	6.8E4	0.51	3.12	3.7E3	NA			NA		
Histamine	0.42	0.87	6.4E4	0.44	25	1.9E3	NA			NA		
Nicotinamide	0.49	3.12	1.1E5	NA			1.54	0.87	5.2 E4	NA		
Adenine	0.48	0.87	9.2E4	0.50	3.12	3.5E4	3.43	0.87	3E5	NA		
Biotin	7.96	0.87	9.9E3	7.97	3.12	1.4E4	NA			NA		
Maleic acid	NA			NA			NA			0.85	6.25	2.6E4
Taurocholic acid	10.61	25.0	3.8E3	10.70	0.87	3.8E3	3.13	0.87	7.5E2	NA		
Thyroxine	10.99	0.87	5.7E3	11.01	3.12	3.9E3	NA			6.86	6.25	1.7E3
Tryptamine	7.96	0.87	1.0E4	NA			6.16	6.25	8.3E3	NA		
Cortisol	9.66	0.87	5.8E3	NA			1.01	6.25	2.0E4	NA		
Estrone	NA			NA			NA			4.77	6.25	8.5E3
Cholic acid	10.83	0.87	3.5E3	10.81	0.87	8.9E3	NA			NA		
Estradiol	NA			NA			NA			NA		
Q10	NA			NA			0.77	0.87	1.2E3	NA		
Vitamin K1	NA			NA			0.82	25.0	5.6E3	NA		

*NA: metabolite not observed with the stated method at any of the concentrations tested

2.2.5 Data analysis and calculations

Extraction efficiency (or absolute recovery) was calculated by dividing the amount of analyte extracted by the coating (in ng) with the total amount of analyte spiked into sample (in ng). The amount of analyte extracted was determined using an external calibration curve of metabolite mixture prepared directly in desorption solvent (minimum of 6 concentration levels to cover the entire linear range of the instrument).

Calibration was performed using 1/x weighted linear regression using Thermo Xcalibur software (Version 2.2) and Agilent Mass Hunter workstation (Version B.07.00). Known metabolites were processed by extraction of theoretical monoisotopic mass (from

METLIN database) of the most intense ion with 10-ppm window tolerance. All integrated peaks were checked manually from the extracted ion chromatograms.

Mass accuracy of the measurement is defined as the ratio of mass error (difference between experimentally measured mass and theoretical mass of analyte) and the theoretical mass, and multiplied by 10^6 to convert it to ppm and can be calculated using Equation 2.1.

$$\textbf{Mass accuracy (ppm)} = \frac{m_{experimental} - m_{theoretical}}{m_{theoretical}} \times 1000000 \qquad \textbf{Equation 2.1}$$

2.3 Results and discussion

Sample preparation step is one of the most important and frequently the most time- and labor-consuming step in the entire analytical method, and one of critical steps in LC-MS global metabolomics workflow. The development of faster, simpler, inexpensive and more environmentally friendly sample preparation techniques is an important issue. As discussed in more detail in Chapter 1, solvent precipitation methods with methanol are currently gold standard methods for this application and there is generally a resistance in metabolomics community to employ more selective approaches for this application because the goal is to capture as many metabolites as possible in a single method. However, the few studies that explore more selective sample preparation methods for global metabolomics in plasma have found clear advantages of such methods including improving method precision, minimizing matrix effects and complementing metabolome coverage.[79,32] In this work, the potential of D-SPME for global metabolomics is explored. SPME has high selectivity because it is based on equilibrium process and even analytes with similar log P and pK_a values can have different K values based on the chemistry of selected sorbent. In addition, in this method small amount of extraction phase is used in comparison to sample volume, thus exhaustive recovery is not achieved. To date, SPME has only been explored in fiber format for LC-MS metabolomics studies.[32,82,83] D-SPME has not yet been tested for global metabolomics applications despite clear advantages in terms of sorbent flexibility, low cost per sample and fast extraction rates. In this study, we evaluated D-SPME method for the first time in combination with three different types of ion exchange functionalized hydrogel materials in order to evaluate its potential to increase the metabolite coverage. Considering this is the first use of these materials for global metabolomics, it was mandatory to first perform comprehensive optimization of the protocols to ensure the widest possible metabolite coverage and optimal achievable method performance. D-SPME is based on equilibrium process therefore all the parameters that affect equilibrium such as pH, solvent and time can affect extraction

efficiency as well. Figure 2.7 summarizes all the parameters that were optimized during method development in current study.

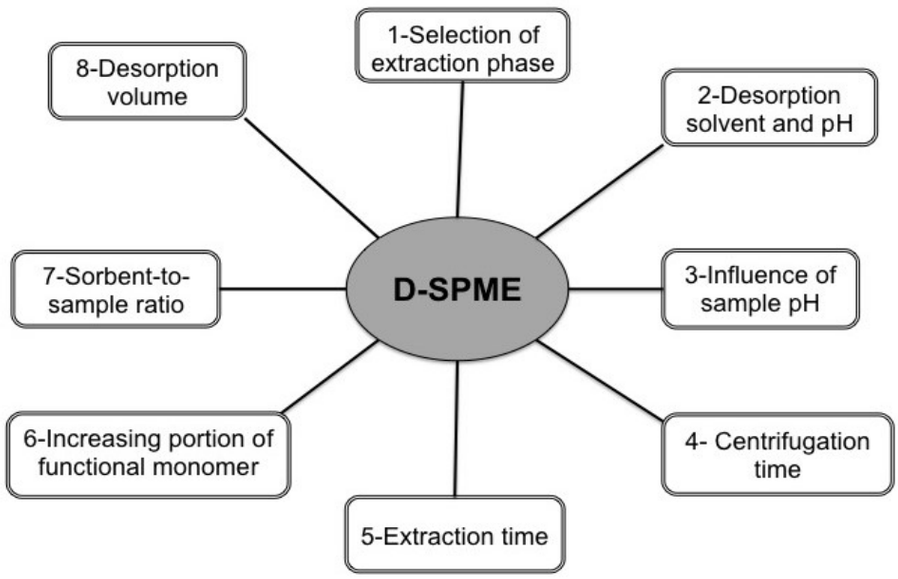

Figure 2.7 Overview of parameters that were optimized during D-SPME method development.

2.3.1 Selection of extraction phase for D-SPME

Selecting the appropriate coating is the first step in SPME method development and it depends on understanding the mechanism(s) of interaction and properties between the sorbent and analyte of interest. The most common mechanisms of interaction include, van der Waals forces (non-polar interactions), hydrogen bonding, dipole-dipole forces and cation-anion electrostatic interactions (ionic interactions). Polymer hydrogel nanoparticle can undergo facile functionalization at room temperature and be prepared at relatively low cost, therefore different molecular interactions are achievable. One of the main issues with existing SPME coatings is relatively poor extraction efficiency of polar compounds[79], so in this work we wanted to evaluate hydrogels enhanced with ion-exchange functionality to see how well these materials can perform for the extraction of metabolome and whether they can improve extraction of polar charged metabolome in particular. To enhance the extraction of anionic (negatively charged) compounds, hydrogels with tertiary amine group of N-(3-aminopropyl) methacrylamide hydrochloride (APMAH) were evaluated. Similarly, the effect of functionalization for the extraction of cationic compounds was evaluated using hydrogels functionalized with acrylic acid (AAC) or vinyl acetate (VAC) groups. Therefore, in the materials tested it was expected to observe both non-polar interactions and ion-exchange interactions based mainly on the electrostatic attraction of the charged functional group in the compound to the charged functional group in the microgel.

2.3.2 Effect of microgel particle size

Theoretically, using the smaller particle size of extraction phase will provide higher extraction efficiency due to the increase in surface area and volume. [98] The microgel particles used in this study were porous and may not be perfectly spherical. The results obtained for the experiment evaluating 400 nm and 1.1 µm sorbent particle sizes are shown in Figure 2.8. The extraction with 400 nm particles increased recovery for some compounds such glutamic acid (44%), biotin (20%) and thyroxine (67%). There was no difference for riboflavin, lysine and adenine. Assuming spherical shape and the same porosity of 1.1 µm and 400 nm particles, theoretical volume of the particles increased by 20 times for the smaller particle size, while theoretical surface area increased by 7 times. However, the differences in the recovery did not match theoretical calculation possibly due to the differences in network pore size, particle shape and/or incomplete sedimentation of the smaller particles. The volume calculation also excludes porosity and overestimates the enhancement. Both area and volume calculations also neglect the number of binding sites available and steric hindrance, so it is not surprising the observed enhancements are lower than expected. As it will be discussed in Section 2.3.8, smaller particle size also needs longer centrifugation times to sediment the particles and separate the supernatant. As a result, 1 µm particle size was selected for all further experiments because it requires shorter centrifugation times for sedimentation while providing good recoveries, which will make the overall workflow faster and more practical.

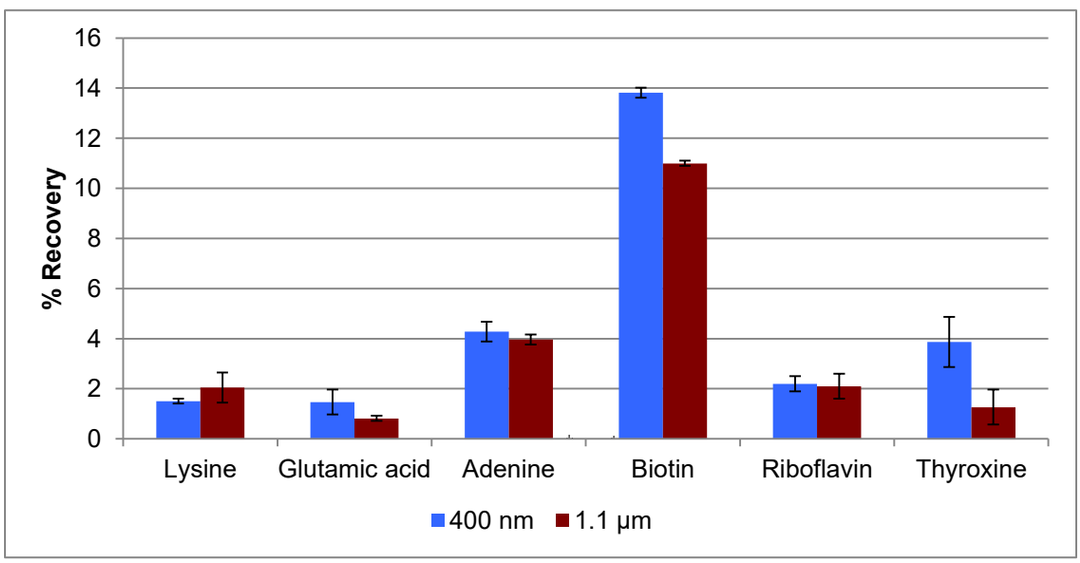

Figure 2.8 Effect of particle size (1.1 µm versus 400 nm) on extraction efficiency of 5% APMAH. The extraction was performed with adding 200 µL of 1 µg/mL metabolite standard in pH 7.5 PBS to 25 µL of 5% APMAH hydrogel according to procedure described in Section 2.2.3.2. The analytes were eluted using 100 µL of methanol. The samples were analyzed using PFP LC-MS method.

2.3.3 Optimization of desorption conditions for metabolites with high to intermediate polarity

Optimization of desorption solvent conditions during SPME method development relied on testing of different solvents (acetonitrile and methanol) and investigating the effect of pH adjustment in order to achieve efficient desorption of the analytes.

2.3.3.1 Effect of different solvents on elution for metabolites with high to intermediate polarity

This experiment was performed on 10% AAC hydrogels using the same extraction conditions described in Section 2.2.3.2. The efficiency of desorption step is highly dependent on the type of desorption solvent. In order to obtain a good recovery, the solvents should be capable to dissolve compounds of interest and be compatible with LC-MS. In current study, polar solvents such as methanol or acetonitrile were tested for their ability to desorb the analytes from the microgel. The results obtained are shown in Figure 2.9. Acetonitrile and methanol are both polar water-miscible solvents but the eluotropic strength of acetonitrile is higher than methanol so that it can better disrupt the interactions between analyte and microgel. As it is shown in Figure 2.9, the recovery was increased by using acetonitrile for all compounds within the experimental error except for thyroxine and cortisol. T-tests for cortisol and thyroxine were statistically significant (p-value <0.05) therefore; analyte solubility in methanol versus acetonitrile may have contributed to better performance of methanol. For phenylalanine, the observed difference between the two solvents was not significant (p-value: 0.1) indicating both solvents perform well for this analyte. According to these results acetonitrile was chosen as desorption solvent for metabolites with high to intermediate polarity.

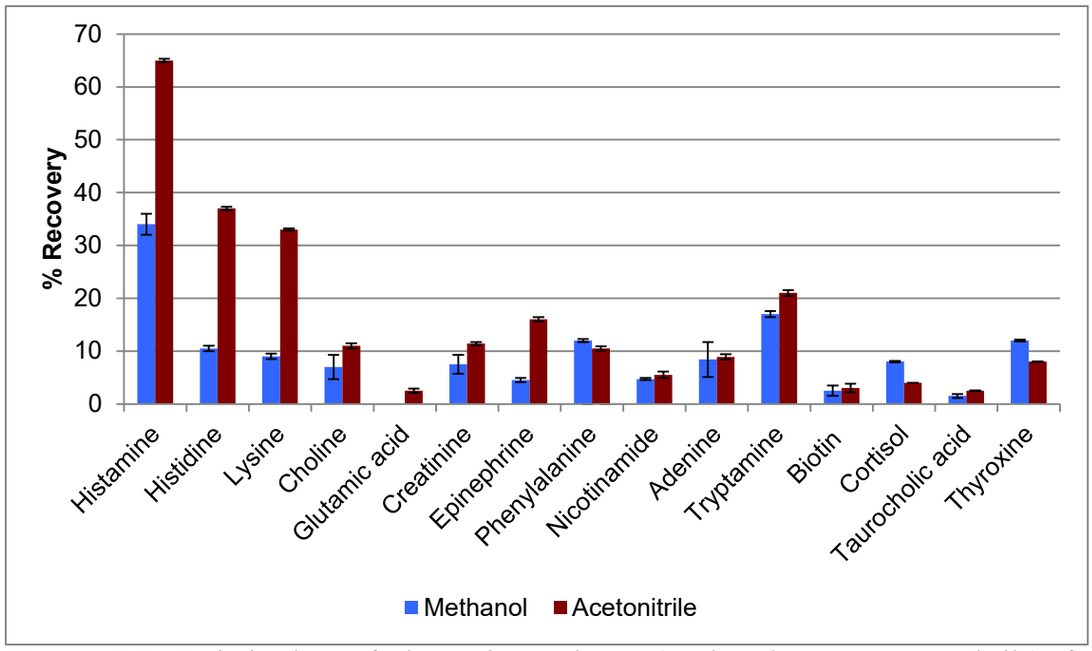

Figure 2.9 Optimization of desorption solvent (methanol versus acetonitrile) for metabolites with high to intermediate polarity on 10% AAC. The extraction was achieved with 1 µg/mL of metabolite standards in water. The analytes were eluted using 100 µL of methanol or acetonitrile. The samples were analyzed using PFP LC-MS method.

2.3.3.2 Effect of desorption pH on elution of metabolites with high to intermediate polarity

Adjustment of the desorption solvent pH can improve desorption efficiency of the method for basic and acidic analytes by disrupting electrostatic interactions. To elute the compound of interest that participates in ionic interactions, pH change can be used to neutralize either the functional group on the compound or the functional group on the sorbent surface. When one of these functional groups is neutralized, the electrostatic force that binds the two together is disrupted and the compound will elute. For AAC (pK_a= 4.25) and VAC (pK_a=5) the use of low pH will protonate the ion-exchange groups on the sorbent, while for APMAH (pK_a= 8.3) the use of high pH will deprotonate amine ion-exchange functionality. As it is shown in Figures 2.10 and 2.11 for AAC and VAC, the first desorption step was performed in acetonitrile so that it shows the disruption of van der Waals forces (e.g., dipole-dipole interaction, hydrogen bonding and London dispersion forces such as dipole-induced dipole interaction and induced dipole-induced dipole interaction), thus eluting neutral compounds. In the second step, 1% formic acid was added to acetonitrile to lower the pH of desorption solvent and disrupt the ionic interaction (the second bar shown in Figure 2.10 and 2.11 is the sum of first and second desorption step). By changing the pH of second desorption, the ionization of AAC and VAC microgel will be changed (surface will be protonated) and ionic interaction between compounds with amine functionality and AAC, VAC microgel (which has acidic functionality) will be disrupted. The results show that ionic interactions were clearly

present and could be efficiently disrupted by the change in pH. In the third desorption, acetonitrile with 5 mM ammonium acetate was used for AAC and VAC microgel to evaluate the effect of changing ionization of compounds, and investigate whether complete disruption of ionic interactions was achieved in the second desorption step (the third bar shown in figure 2.10 and 2.11 is the sum of second and third desorption step). It should be noted that we only used low ionic strength adjustment to maintain compatibility with direct LC-MS injection without causing significant decrease in analyte ionization during ESI. The extent of swelling depends on the degree of ionization, quality of solvent, cross-link density, and ionic strength.[106] Microgels exhibit different equilibrium degrees of swelling in response to various kinds of salts and concentration. In general, an increase in ionic strength decreases the repulsive electrostatic forces between the dissociated acrylic acid groups and decrease in the hydrodynamic radius which in turn lead to microgel deswelling .[101] The adjustment of ionic strength in the third desorption step did not increase the amount of metabolites desorbed, except for choline in AAC and epinephrine in VAC microgel. Therefore, third step desorption with salt did not improve extraction efficiency and was not used for following experiments.

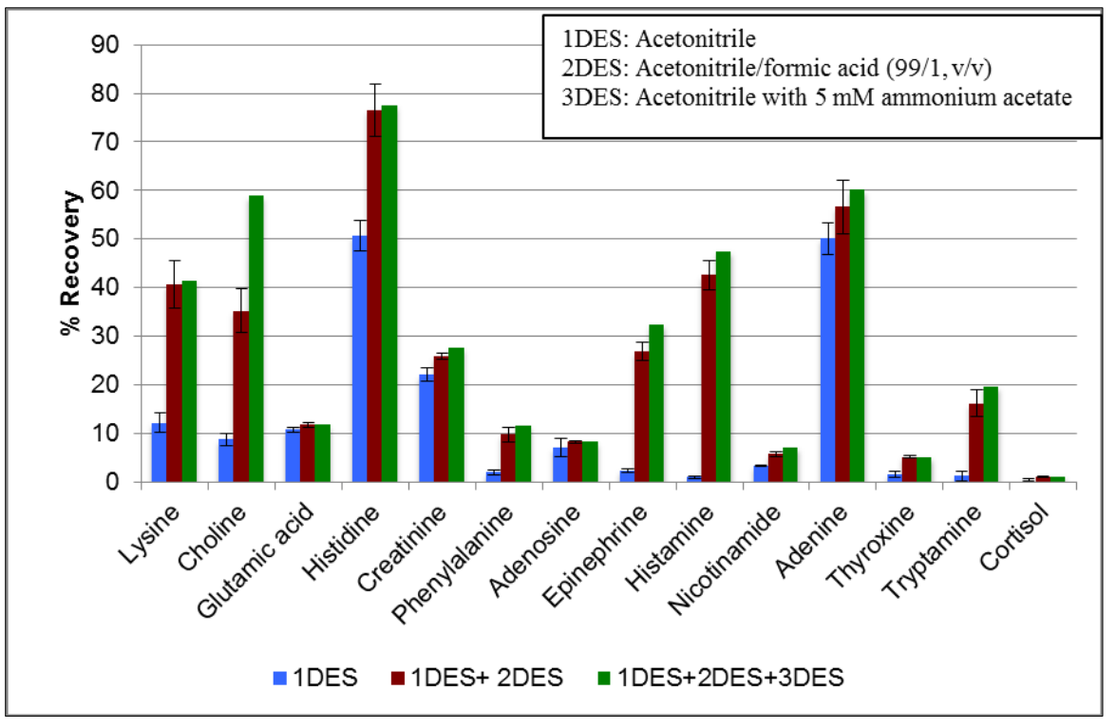

Figure 2.10 Effect of desorption pH on elution of metabolites with high to intermediate polarity on 10% AAC. The extraction was done as discussed in Section 2.2.3.3 with 1 µg/mL of metabolite standards in water. The first desorption step was in 100 µL of acetonitrile, the second desorption step was in 100 µL of acetonitrile/formic acid (99/1, v/v) and third step was in acetonitrile with 5 mM ammonium acetate (bars for subsequent desorption steps are cumulative). The samples were analyzed using PFP LC-MS method.

For metabolites such as epinephrine and histamine in AAC microgel and metabolites

such as lysine and histamine in VAC microgel, the use of acetonitrile in the first desorption solvent shows the effect of van der Waals forces and/or hydrogen bonding. In the second desorption step, the decrease of pH causes the protonation of the functional group of AAC and VAC microgels, thus eluting all analyte molecules that were held through ionic interactions. Therefore, for efficient elution of ACC and VAC microgels, pH adjustment is necessary.

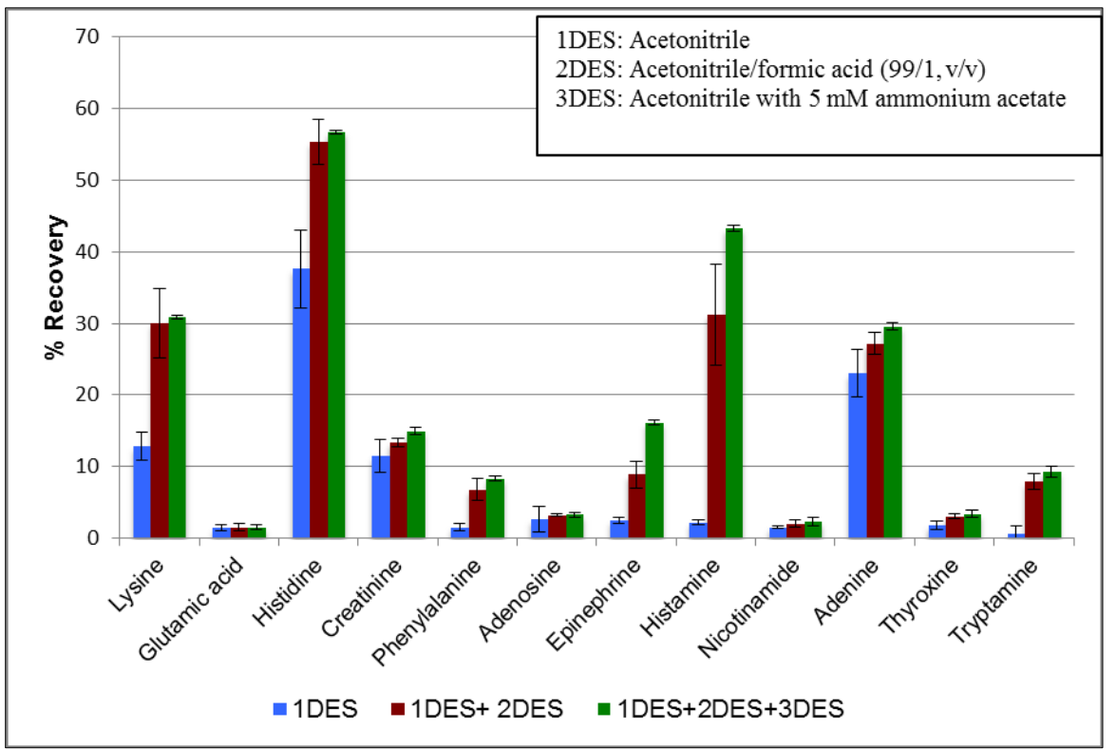

Figure 2.11 Effect of desorption pH on elution of metabolites with high to intermediate polarity from 10% VAC. The extraction was performed as discussed in Section 2.2.3.2 with 1 µg/mL of metabolite standards in water. The first desorption step was in 100 µL of acetonitrile, the second desorption step was in 100 µL of acetonitrile/formic acid (99/1, v/v) and third step was in acetonitrile with 5 mM ammonium acetate (bars for subsequent desorption steps are cumulative). The samples were analyzed using PFP LC-MS method.

Although acetonitrile generally outperformed methanol as desorption solvent, the solubility of some metabolites is going to be limited in acetonitrile. Therefore, in the next experiments the effect of using acetonitrile/water (9/1) versus pure acetonitrile was tested in combination with two-step desorption protocol. The first desorption was performed without pH adjustment as described in Section 2.3.3.2, and second desorption was with pH adjustment. The two steps were combined and subjected to LC-MS analysis. Figure 2.12 shows that a small amount of water (10%) in the desorption solvent helped to increase the recovery for almost all metabolites tested due to the better solubility of polar compounds in water. The addition of 10% water was selected to achieve optimum chromatographic peak shape in HILIC. Final sample extract should be dissolved in

solvent of weaker or equal strength to starting conditions. For HILIC chromatography, this means using acetonitrile/water (9/1, v/v) as injection solvent. Higher percentage of water in desorption solvent was not tested because it would result in poor peak shape and require evaporation/reconstitution to exchange solvent. Consequently, for the optimized method acetonitrile/water/formic acid (90/9/1, v/v) was selected as the best desorption solvent and is directly compatible with HILIC. This eliminates the need for evaporation/reconstitution of samples, and decreases the experimental error that arises from these manipulation steps.

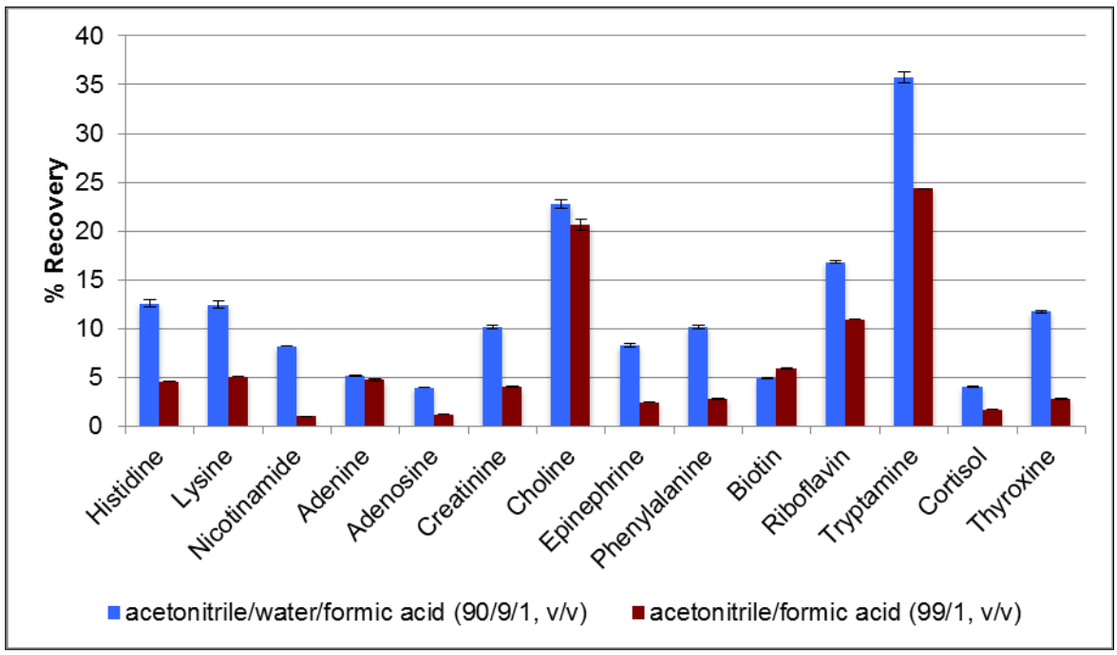

Figure 2.12 Comparison of acetonitrile versus acetonitrile/water (9/1, v/v) as desorption solvent for metabolites with high to intermediate polarity with 10% AAC. The first desorption was performed without pH adjustment as described in Section 2.3.3.2, and second desorption was with pH adjustment. Both desorption steps were combined and analyzed using PFP LC-MS method.

Figure 2.13 shows the effect of increasing desorption pH on analyte elution with 10% APMAH microgel. For the first desorption step, acetonitrile was used to see the effect of van der Waals forces and desorb neutral analytes. In the second step, ammonium hydroxide in acetonitrile was used to increase the pH of desorption solvent and disrupt the binding via ionic interactions. By changing the pH of second desorption, the ionization of amine functionality of APMAH microgel was changed. This disrupts the interaction of compounds with acidic functionality such as glutamic acid and taurocholic acid with APMAH microgel. The recovery of these compounds clearly increased when high pH was used in desorption solvent indicating presence of ionic interactions. It was also investigated if adding one more desorption step with acetonitrile and ammonium hydroxide would help to increase the extraction efficiency of acidic compounds but no further increase in recovery was observed. This means that one step desorption with pH

adjustment is sufficient to disrupt all the ionic interactions between compounds and microgel as predicted theoretically. Consequently, for the optimized method one step desorption with acetonitrile in ammonium hydroxide was selected for APMAH microgel.

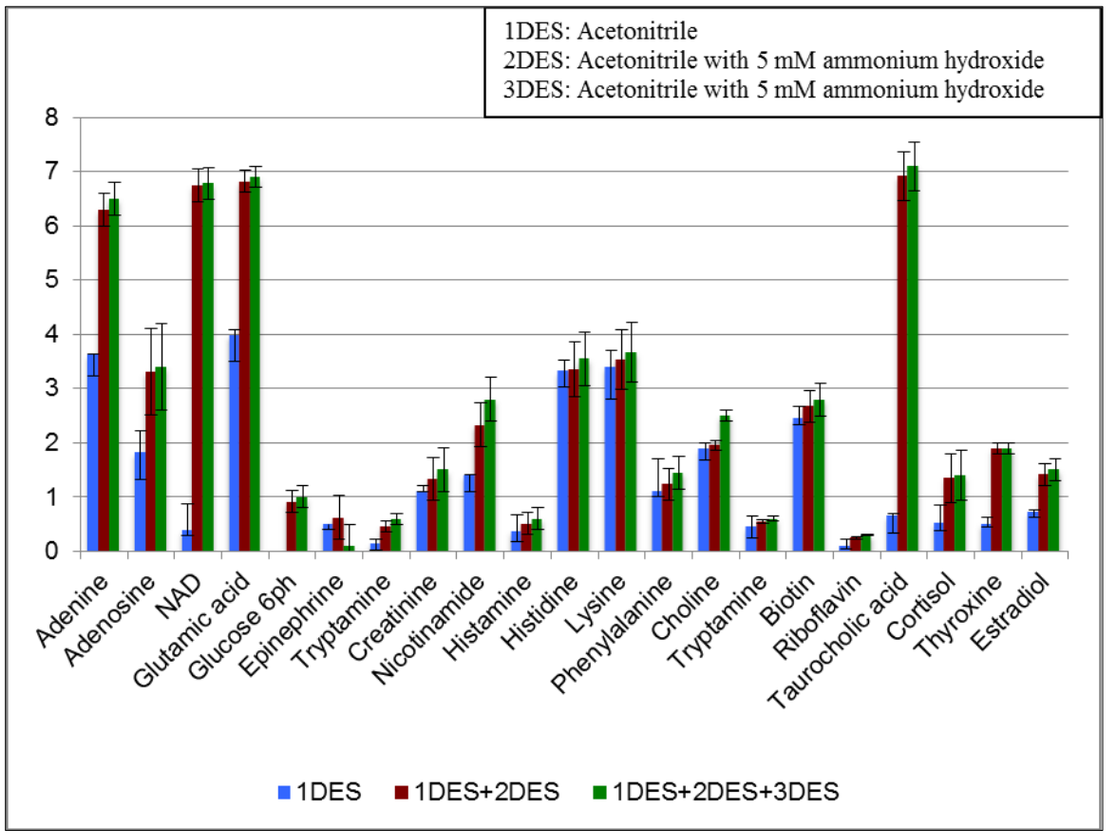

Figure 2.13 Effect of pH on elution of metabolites with high to intermediate polarity on 10% APMAH. Metabolite standards were prepared in water with the concentration 1 µg/mL. First desorption step was performed with 100 µL of acetonitrile and second desorption step was with 100 µL of acetonitrile with 5 mM ammonium hydroxide and third step desorption was the same as second step (bars for subsequent desorption steps are cumulative). They were analyzed using PFP LC-MS method. Samples were neutralized prior to injection.

2.3.4 Effect of increasing desorption volume

Increasing the volume of desorption solvent can help improve desorption process to ensure all analyte are effectively removed from the sorbent. In this experiment, the effect of increasing the desorption volume from 100 to 200 µL was investigated. The results obtained are shown in Figure 2.14. The extraction efficiency improved slightly for histidine, lysine, tryptamine, thyroxine, nicotinamide, creatinine, epinephrine and phenyalanine. However, precision deteriorated as shown by the higher error bars for 200 µL desorption volume. For this desorption solvent volume, the signal intensity for MS detection decreases due to dilution, which can also decrease method precision. Increasing desorption solvent can increase the recovery slightly and reduce the carryover, but the microgels are designed for single-use, therefore carryover is not primary issue.

Considering good method precision and metabolite coverage is crucial for metabolomics studies, 100 µL was chosen as desorption volume for D-SPME method due to better method precision and the fact that small improvements in recovery are offset by 2-fold dilution when larger desorption volume is used.

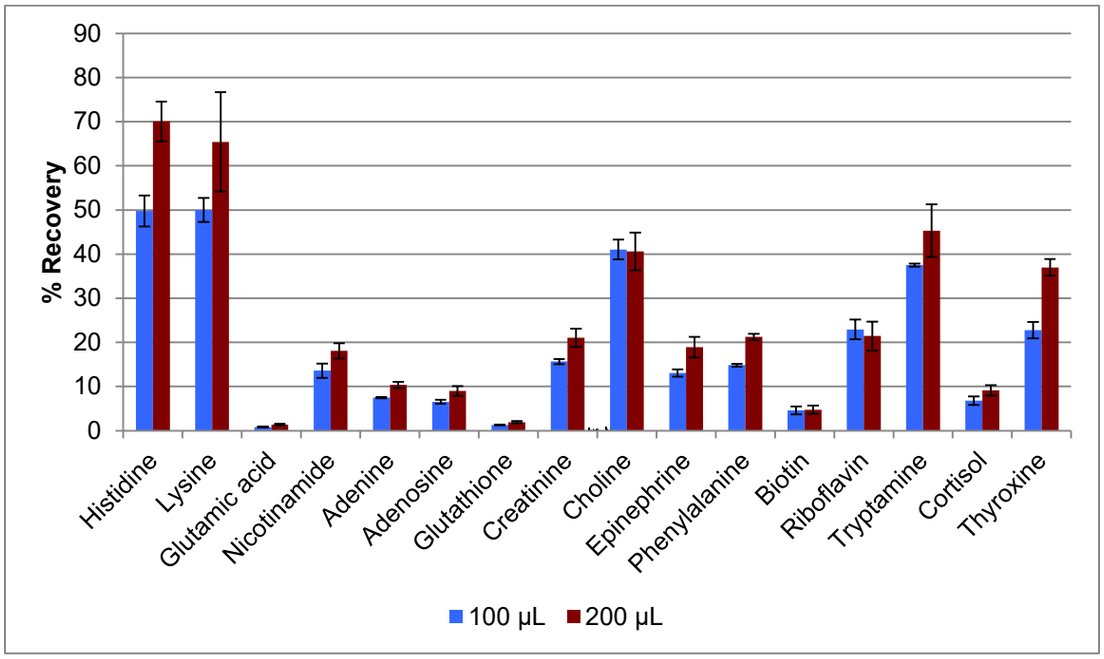

Figure 2.14 Effect of increasing desorption volume on 10% AAC. Extraction method is the same as Section 2.2.3.2. First and second desorption step was in acetonitrile/formic acid (99/1, v/v) and third desorption step was in acetonitrile/water (9/1, v/v). The samples were analyzed using PFP LC-MS method.

2.3.5 Optimization of desorption conditions for lipids

The effect of desorption solvent and pH was next evaluated for lipid metabolites.

2.3.5.1 Effect of different solvents on elution of lipids

The analytes considered here are relatively hydrophobic thus, a suitable organic solvent was needed for desorption. This experiment was performed on 10% AAC with different desorption solvents: methanol, acetonitrile and isopropanol as many lipid species are not very soluble in acetonitrile. Acetonitrile is a polar aprotic solvent with large dielectric constant (37 F/m) and large dipole moment (3.92 D), but that does not participate in hydrogen bonding. Methanol and isopropanol are polar protic solvents, which tend to have high dielectric constants (methanol: 33 F/m and isopropanol: 20 F/m) and high dipole moments (methanol: 1.70 D and isopropanol: 1.68 D). Furthermore, since they possess hydroxyl functionality, they can participate in hydrogen bonding. As shown in Figure 2.15, there was no significant difference observed between isopropanol and methanol in terms of desorption efficiency so either solvent can be selected. For this work, methanol was selected as desorption solvent for lipids. In addition, the figure

shows that neutral lipids such as MG, DG, and TG are soluble in acetonitrile, however phospholipids are not soluble in acetonitrile which opens up different possibilities for sequential desorption protocols. Such protocol would have the benefit of desorbing polar metabolites while most phospholipids would remain in the sorbent, which would decrease potential for ion suppression considering phospholipids are notorious for causing severe ion suppression problems.[84] Lyso PC and sphingosine are amphiphilic and easy to solubilize so that they were efficiently desorbed in acetonitrile as well.

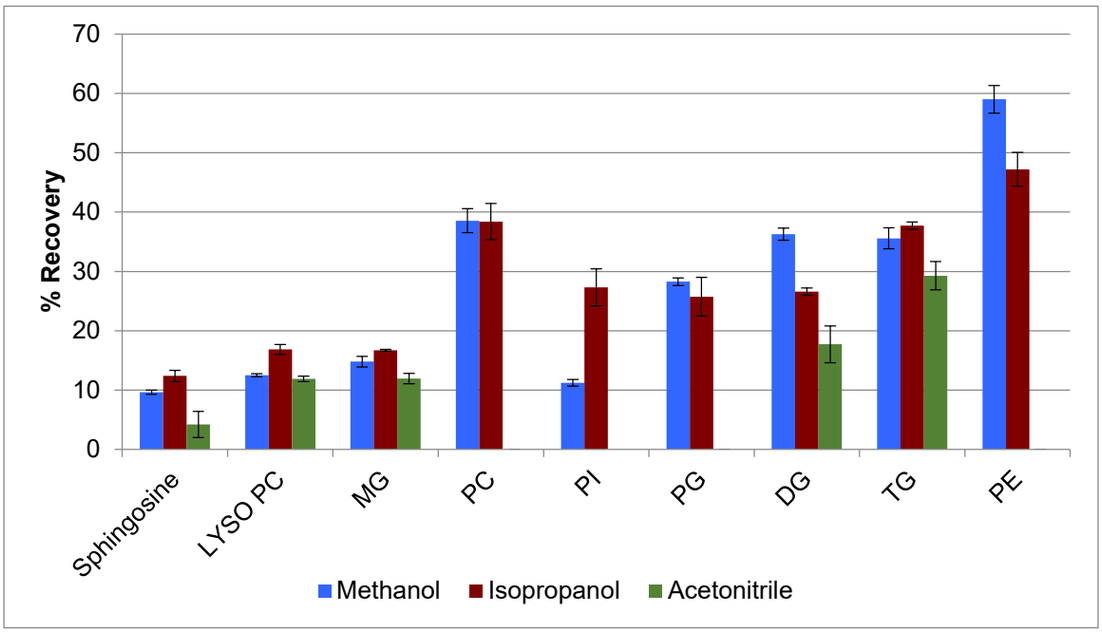

Figure 2.15 Optimization of desorption solvent (methanol versus acetonitrile versus isopropanol) for lipids on 10% AAC. Extraction was performed as described in Section 2.2.3.3 with 3-steps desorption using each of three different solvents. All desorption steps were combined prior to CSH C18 LC-MS analysis.

2.3.5.2 Effect of elution pH on lipid metabolites

After selecting methanol as an appropriate solvent for elution of lipids, the effect of pH adjustment during desorption step was evaluated in order to improve the recovery. For 10% AAC, 10% VAC and 5% APMAH, first and second step of desorption was performed using methanol. For AAC and VAC third and fourth desorption steps were performed using methanol/formic acid (99/1, v/v), whereas for APMAH, methanol with 5 mM ammonium hydroxide was used. The results obtained are shown in Figures 2.16, 2.17 and 2.18.

The two-step desorption with methanol was efficient to remove the majority of lipids extracted by the hydrogels. For AAC and VAC, low pH was used in the third and fourth step to see the effect of ionic interaction. By changing pH of the desorption solvent, AAC and VAC will be protonated so any ionic interactions with positively charged glycerophospholipids such as PE, PC and Lyso PC will be disrupted. According to the results shown in Figures 2.16 and 2.17, there was no significant contribution of ion-

exchange mechanism and recovery did not increase proportionally for these lipids. The slightly increasing trend, which is seen, can be the result of sequential desorption itself as neutral lipids such as TG exhibited the same trend. The lack of electrostatic interactions could be due to the repulsion between negatively charged phosphates on lipids and negatively charged acid groups on AAC and VAC microgel. In addition, the presence of 40% methanol during extraction to ensure lipid solubility could also minimize the extent of ionic interactions. According to Figure 2.16, increasing the number of desorption steps increases recovery of all lipids slightly except for sphingosine with AAC microgel where significant increase is observed. For VAC microgel as shown in Figure 2.17, recovery increased proportionally for all lipids by increasing the number of desorption steps. However, the use of four desorption steps considerably increases desorption time, so two-step desorption with methanol and methanol/formic acid (99/1, v/v) was selected as an acceptable compromise between desorption recovery and desorption time required.

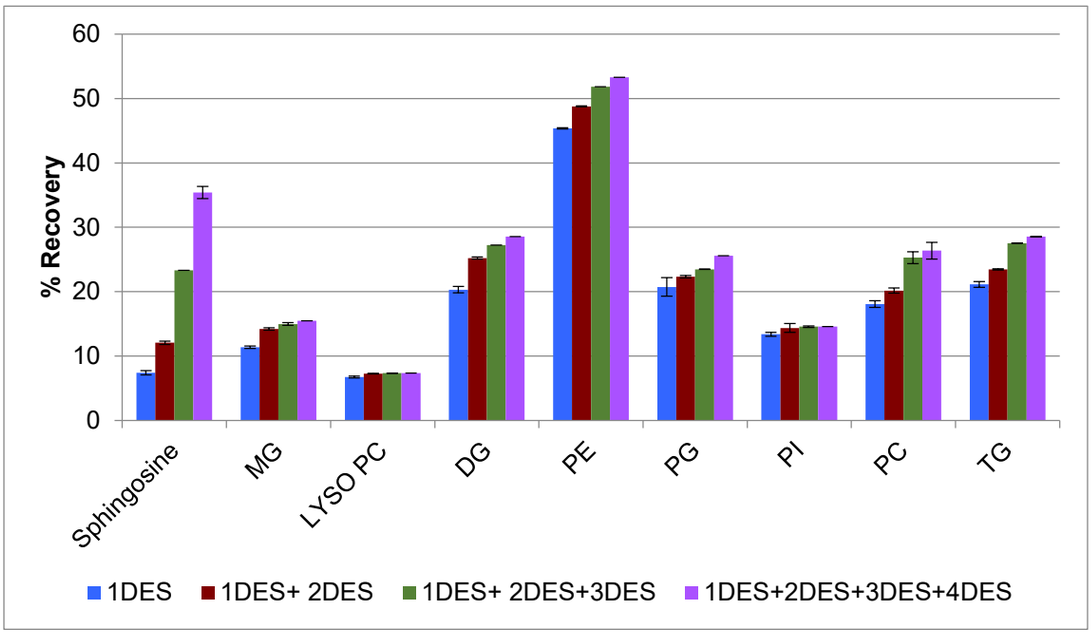

Figure 2.16 Effect of pH on elution of lipids with 10% AAC. Lipid standards were prepared in methanol/water (40/60, v/v) with the concentration of 1 µg/mL. First and second desorption steps were performed with 100 µL of methanol, third and fourth desorption steps were performed with 100 µL of methanol/formic acid (99/1, v/v). The samples were analyzed using CSH C18 LC-MS method. The bars for subsequent desorption steps are cumulative.

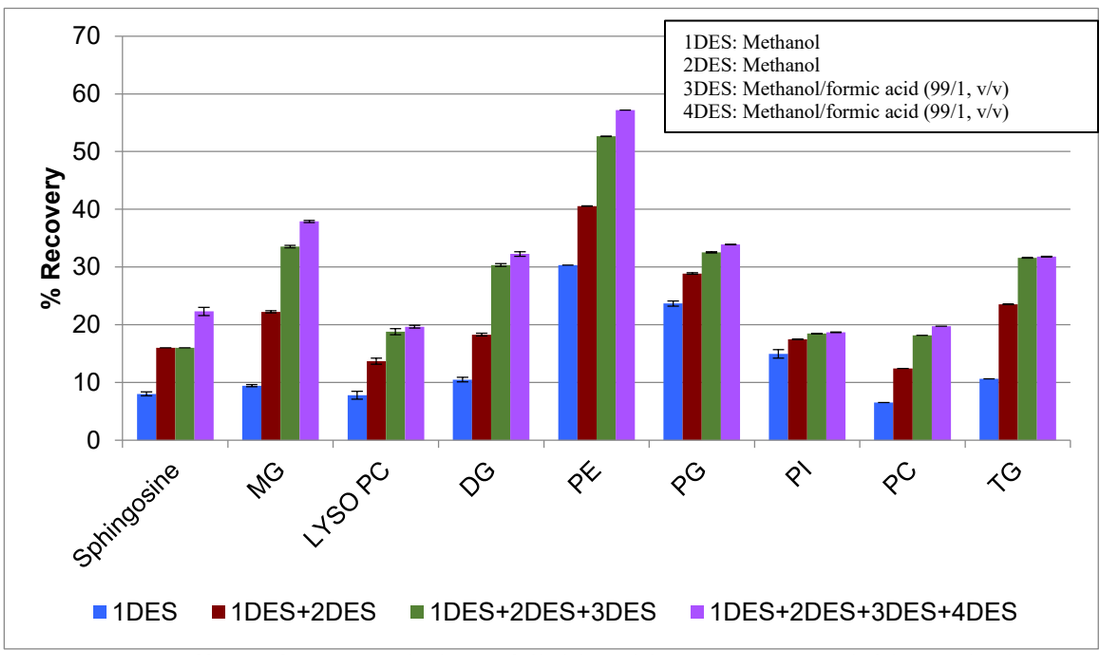

Figure 2.17 Effect of pH on elution of lipids with 10% VAC. Lipid standards were prepared in methanol/water (40/60, v/v) at the concentration of 1 µg/mL. First and second desorption steps were performed with 100 µL of methanol, third and fourth desorption steps were performed with 100 µL of methanol/formic acid (99/1, v/v). The samples were analyzed using CSH C18 LC-MS method. The bars for subsequent desorption steps are cumulative.

However, in contrast to AAC and VAC results, APMAH hydrogels showed clear contribution of ionic interactions for negatively charged glycerophospholipids such as PI, PG and PA. These lipids are negatively charged at high pH. By pH adjustment of desorption solvent, APMAH becomes deprotonated and ionic interactions will be disrupted. As shown in Figure 2.18, recovery increased proportionally for all lipids except for PI and PG, which showed significant jump in cumulative recovery after pH adjustment of the desorption solvent. This provides evidence that there are ionic interactions between PI and PG lipids in the APMAH microgel. Similar trend is expected to be observed for PA lipids. However, this experiment was run using reversed phase method in positive ESI mode and PA has good signal intensity only in negative mode. Because of this factor PA was not observed in this experiment.

By considering both sample throughput and reasonable extraction efficiency two-step desorption was selected for the optimized protocol. One step desorption with methanol and one step with methanol and pH adjustment. The pH adjustment is only critical for the recovery of negatively charged lipids such as PI and PG with APMAH hydrogel, while for AAC and VAC pH adjustment may be omitted.

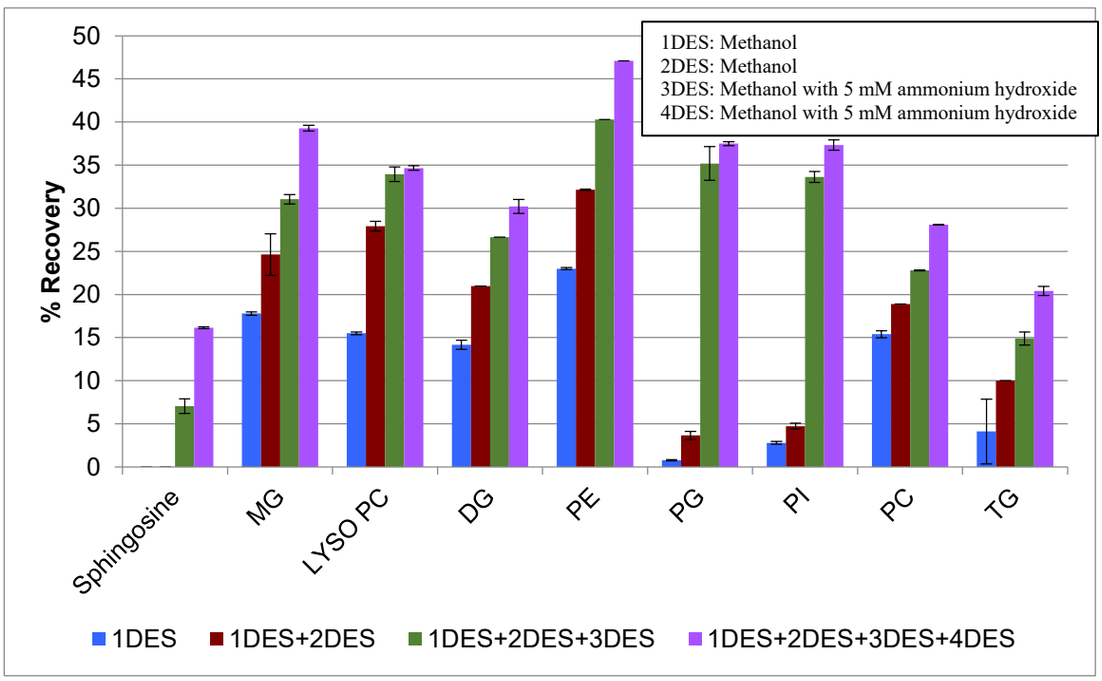

Figure 2.18 Effect of pH on elution of lipids with 5% PMAH. Lipid standards were prepared in methanol/water (40/60, v/v) at the concentration of 1 µg/mL. First and second desorption steps were performed with 100 µL of methanol, third and fourth desorption steps were performed with 100 µL of methanol with 5 mM ammonium hydroxide. The samples were analyzed using CSH C18 LC-MS method. The bars for subsequent desorption steps are cumulative. Samples were neutralized prior to injection.

2.3.6 Optimization of sample pH

In order to retain an analyte by ionic interaction, analyte must be ionized and therefore the sample pH as well as analyte pK_a values will affect the degree of analyte ionization. The pH of the sample matrix must be one at which both the compound of interest and the functional groups on the microgel are oppositely charged. Also, there is possibility that other species of the same charge as the compound in the matrix may interfere with the adsorption of the compound of interest, as there is only limited number of ion-exchange sites available within the sorbent.

2.3.6.1 Effect of sample pH for extraction of metabolites with high to intermediate polarity

In this experiment, the effect of different sample pH (3.0, 5.5, 7.5 and 9.0) on analyte recovery was tested. To increase the contribution of ionic interactions, it was required to choose the pH at which both microgel functionality and analyte functionality are charged. For instance, Figure 2.19 shows drastic increase in recovery of some metabolites at pH 5.5 such as histidine, lysine, creatinine, phenylalanine, adenine and tryptamine. AAC functionality on the hydrogel has pK_a of 4.25 so the extraction phase will be predominantly negatively charged at pH 5.5 and above. Reducing pH below this value results in the protonation of the extraction phase, which results in reduction of electrostatic interactions, increasing its hydrophobicity and expelling water that leads to shrinking of the hydrogel, a reduction of particle diameter and pore size and therefore the reduction in recovery. At pH 5.5 both microgel and many analytes of interest are charged leading to optimum extraction efficiency for this hydrogel. For example, Table 2.8 shows the percent of ionization of AAC microgel and lysine (considering pK_a of amine functionality) at different sample pH. It shows that at pH 5.5 and 7.5 both lysine and AAC microgel has the highest % of ionization, thus resulting in the highest extraction efficiency. On the other hand, in Figure 2.19, the recovery for lysine at pH 7.5 was decreased. Lysine is an amino acid and contains both amine and carboxylic acid groups; therefore, there may be repulsion between deprotonated carboxylic acid on AAC microgel and deprotonated carboxylic acid on lysine at high pH. This is probable cause of the observed difference in recovery at pH 5.5 and pH 7.5 in Figures 2.19 and 2.20. Furthermore, at pH 9.0, carboxylic acid with pK_a 9.0 is partially charged therefore it could be the reason of drop in recovery at pH 9.0 for lysine. As shown in Figure 2.19, the same trend was observed for other amino acids such as histidine and phenylalanine.

In one study, the hydrodynamic diameter of copolymer microgel particles (95% NIPAM-5% AAC) as a function of pH was investigated.[67] It was established that the hydrodynamic radius of AAC microgels dissolved at high pH is always greater than that

at low pH. This is due to deprotonation of the AAC groups at pH > ~4.25 (pK_a for AAC). The generated charges lead to intra-microgel coulombic repulsion and increased osmotic pressure, which in turn lead to microgel swelling, and an increase in the hydrodynamic radius and increase recovery. The largest increase in gel swelling occurs between pH 3.9 and 6, which is consistent with the acrylic acid pK_a of 4.25. Therefore, it would help explain the difference of recovery at pH 5.5 and 7.5 for compounds with amine functionality such as creatinine, adenine, tryptamine and amino acids due to the swelling of microgel but this requires further investigation. The phenomenon of swelling also explains the increases in extraction recovery for neutral analytes tested. For example, this effect can be clearly seen for cortisol, where increasing pH increases extraction efficiency due to gel swelling not the ionic interaction. In summary, pH 5.5 was selected as the optimum pH for AAC and VAC hydrogels as it provided good recoveries for both amine-containing and neutral metabolites.

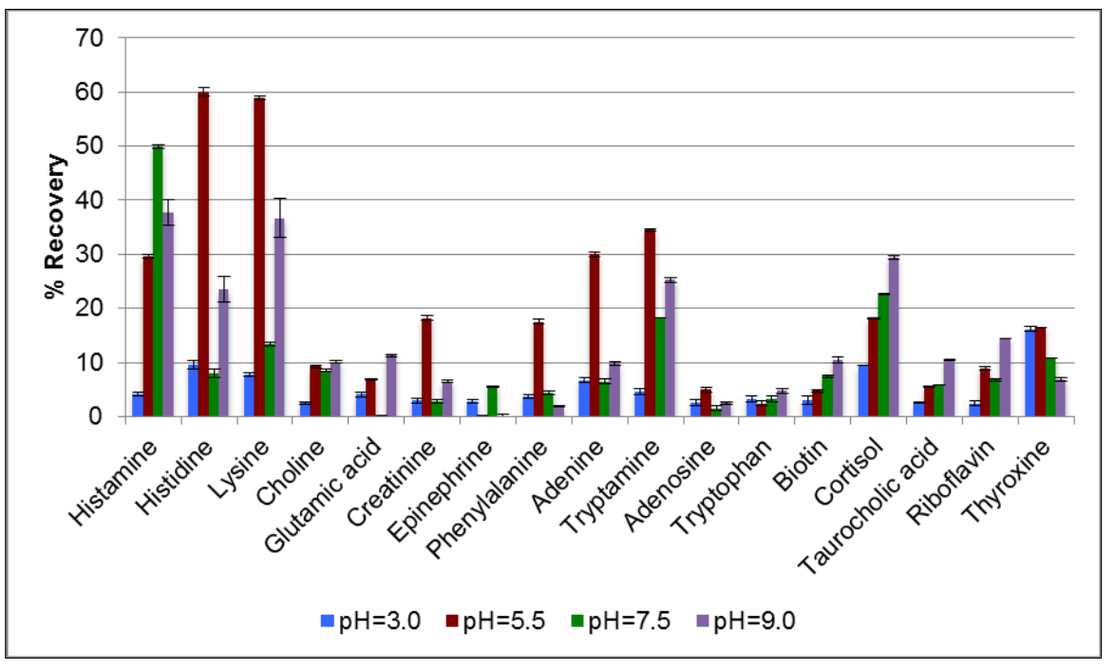

Figure 2.19 Effect of sample pH for metabolites with high to intermediate polarity on 10% AAC. Extraction was performed with 1 µg/mL metabolite standard, which was prepared in different buffers at pH 3.0, 5.5, 7.5 and 9.0. The first desorption step was in 100 µL acetonitrile, the second desorption step was in 100 µL of acetonitrile/formic acid (99/1, v/v) and third step was in acetonitrile with 5 mM ammonium acetate. All desorption steps were combined together prior to PFP LC-MS analysis.

Table 2.8 Percent ionization of AAC microgel and lysine at different pH

pH	Lysine		AAC microgel
	Pk_a =9.0	Pk_a =10.5	Pk_a= 4.25
pH= 3.0	99.99	99.99	5.32
pH= 5.5	99.96	99.99	94.67
pH= 7.5	96.93	99.90	99.94
pH= 9.0	50	96.93	99.99

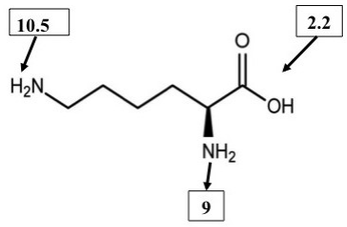

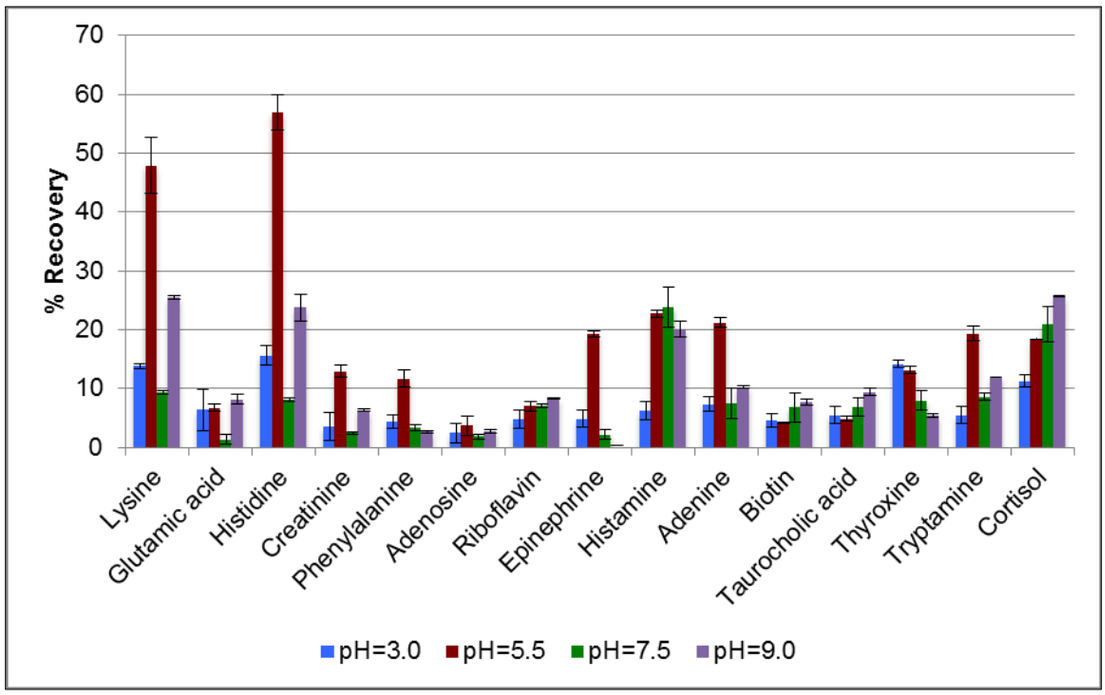

Figure 2.20 Effect of sample pH for metabolites with high to intermediate polarity on 10% VAC. Extraction was done with 1 µg/mL, which is prepared in different buffers at pH 3.0, 5.5, 7.5 and 9.0. The first desorption step was in 100 µL acetonitrile, the second desorption step was in 100 µL of acetonitrile/formic acid (99/1, v/v) and third step was in acetonitrile with 5 mM ammonium acetate. All desorption steps were combined together prior to PFP LC-MS analysis.

APMAH has basic functionality depending on the extraction pH employed; therefore, it can participate in electrostatic interactions with molecules that have acidic functionality such as taurocholic acid. In order to have the particle surface fully charged, the pH must be adjusted to value at least 2 units below the pK_a of APMAH microgel (8.3); therefore, pH 5.5 and pH 3.0 both are applicable. According to Figure 2.21, drastic increases in recovery of almost all metabolites were observed at pH 3.0 expect for glutamic acid for which pH 5.5 was optimal. Table 2.9 shows the percent of ionization of APMAH

microgel and glutamic acid with different pK_a (2.2 and 4.3) [102] at different sample pH. Acidic functionality of glutamic acid is mostly protonated at pH 3.0 whereas at pH 5.5 both acidic functionalities on glutamic acid are predominantly deprotonated while APMAH microgel is positively charged. This can facilitate electrostatic interactions and explains the observed increase of the recovery at pH 5.5 for glutamic acid as shown in Figure 2.21.

Furthermore, for neutral compounds such as thyroxine and cortisol, the increases in extraction recovery observed at pH 3.0 are due to gel swelling not the ionic interaction. Overall, the recovery of all compounds except glutamic acid increased at pH 3.0, therefore pH 3.0 was selected as the optimum pH for APMAH hydrogels.

Table 2.9 Percent ionization of APMAH microgel and glutamic acid at different pH

Glutamic acid	pK_a =2.2	pK_a= 4.3	pK_a= 8.3 (APMAH)
pH= 3.0	86.31	4.77	99.99
pH= 5.5	99.94	94.06	99.84
pH= 7.5	99.99	99.93	86.31

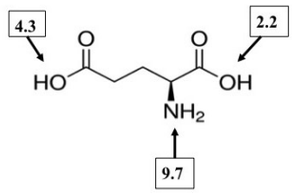

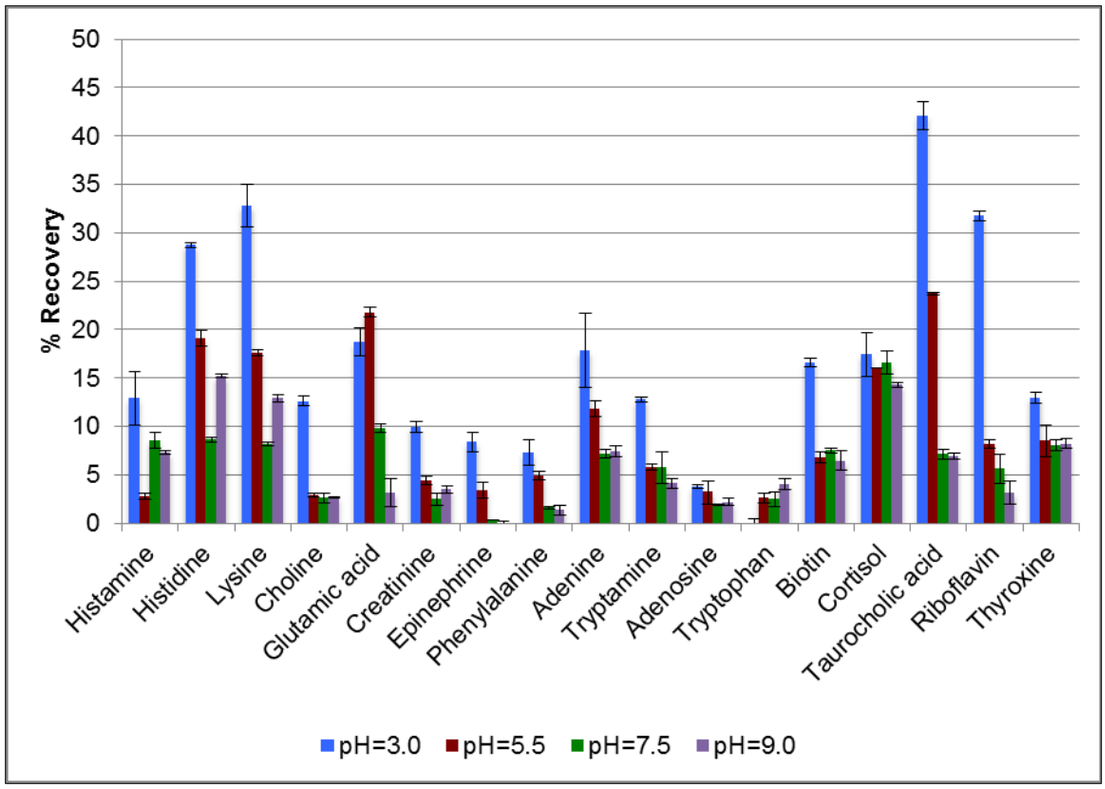

Figure 2.21 Effect of sample pH for metabolites with high to intermediate polarity on 10% APMAH. Extraction was performed with 1 µg/mL, which was prepared in different buffers at pH 3.0, 5.5, 7.5 and 9.0. First desorption step was done with 100 µL of acetonitrile and second desorption step was with 100 µL of acetonitrile with 5 mM ammonium hydroxide. All desorption steps were combined and neutralized prior to PFP LC-MS analysis.

2.3.6.2 Effect of sample pH for lipids

As shown in previous section, the pH of the solution plays a key role in the extraction of compound of interest on the microgel surface. In this experiment, the effect of pH on the extraction recovery for lipids was studied and the extraction method is the same as Section 2.2.3.3. The pH value was adjusted by using appropriate buffer solutions at given pH in water and then adding methanol to a final concentration of 40% to ensure lipid solubility.

When an organic modifier is added to an aqueous buffer to prepare sample solution, solvent pKa and autoprotolysis constant of the solvent change. Accordingly, pH of the organic mixture will be different than the measured aqueous pH of the buffer (for example the dissociation constant for methanol and water is 16.84 and 14 at 25^0C respectively, thus the neutral point of methanol at 25^0C will be pH 8.42). [112] The effect of organic solvent composition on the pH of mobile phase was tested in one study and they found that the true pH shifted to higher values in presence of methanol.[118] Although they did not use the same buffer composition as in current study, the extrapolation of their results to our buffer indicates that apparent pH in presence of organic solvent will be

higher than measured in aqueous buffer, but the expected difference would be less than 1 pH unit.

The results are shown in Figures 2.22, 23 and 24. In aqueous systems, AAC and VAC have negative charges above pH 5.5 which should enhance ionic interactions with lipids that have positively charged ions in their head group such as PE, PC and Lyso PC. In the present mixed solvent system, we are assuming that the pka's and pH's are largely the same, or at least scale together, as what is observed in an aqueous environment. However, these lipids also have phosphate groups in their structure that can cause repulsion. Because of that, an increasing trend in recovery was not observed for these lipids. These results further confirm our results in Section 2.3.3.2 that suggested there is no major contribution of ion-exchange mechanism for the extraction of lipids using ACC and VAC hydrogels.

In general, at pH 5.5 all lipids were detected in AAC and VAC microgel, so this pH was chosen as optimum based on its best performance for polar metabolome in Section 2.3.6.1.

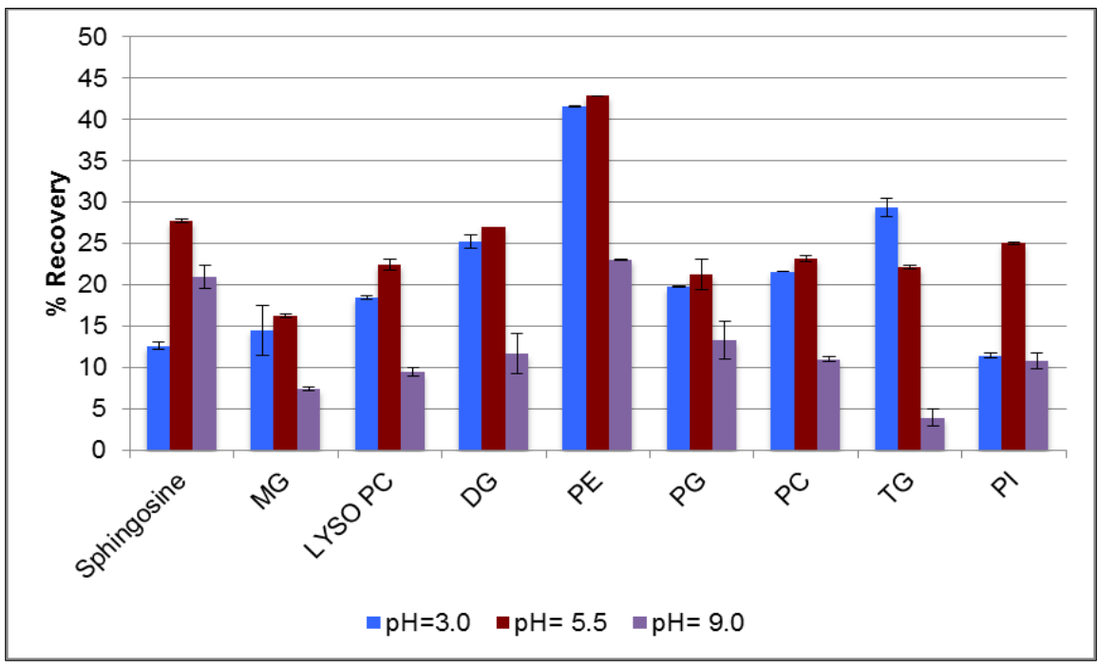

Figure 2.22 Effect of sample pH for lipids on 10% AAC. Lipid standards were prepared at the concentration of 1 µg/mL in different buffer solutions at given pH (3.0, 5.5 and 9.0) and then adding methanol to a final concentration of methanol/water (40/60, v/v). Three step desorption was performed in methanol, combined together and analyzed using CSH C18 LC-MS method.

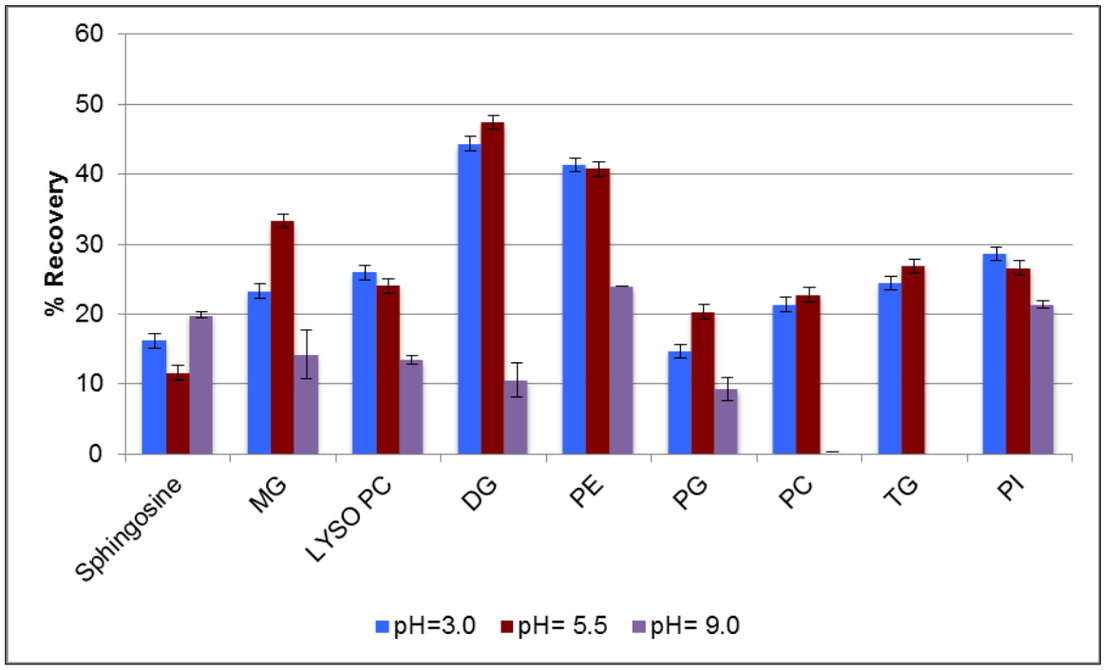

Figure 2.23 Effect of sample pH for lipids on 10% VAC. Lipid standards were prepared at the concentration of 1 µg/mL in different buffer solutions at given pH (3.0, 5.5 and 9.0) and then adding methanol to a final concentration of methanol/water (40/60, v/v). Three step desorption was performed in methanol, combined together and analyzed using CSH C18 LC-MS method.

APMAH which has positively charged functionality may interact with lipids that have negatively charged ions such as PI and PG via ionic interaction. As it is shown in Figure 2.24 at pH 3.0, the recovery for PG was increased, however for PI the recovery did not change within the experimental error. In general, at pH 3.0 all lipid classes were detected using APMAH microgel so this pH was chosen based on the results for polar metabolome.

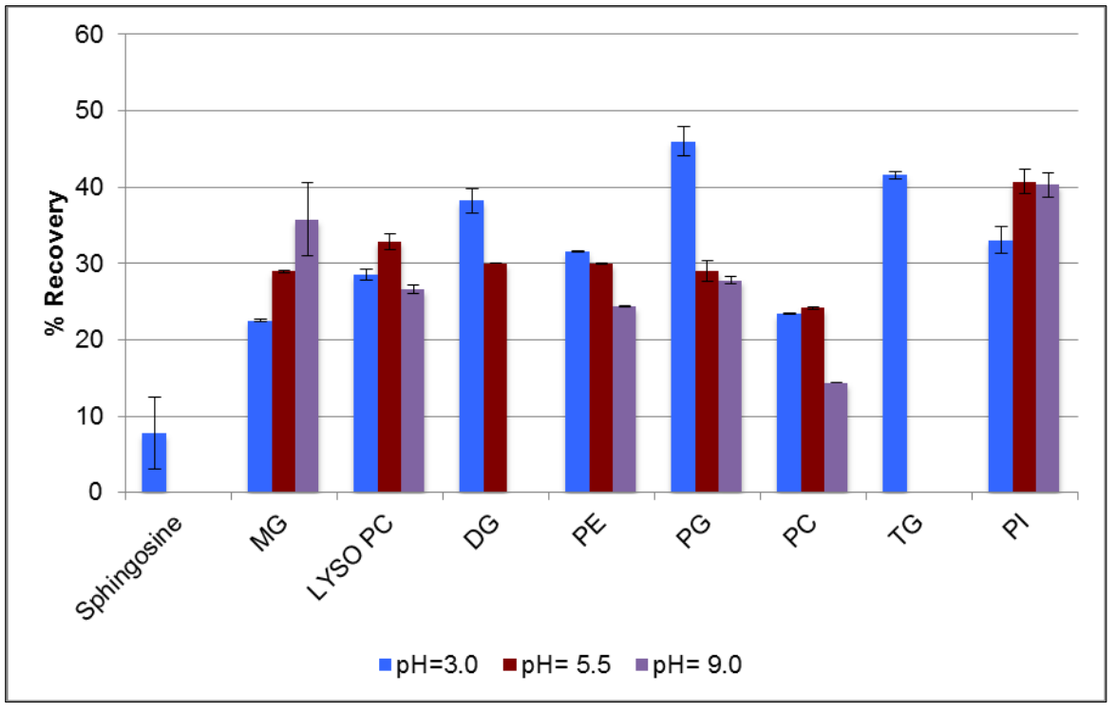

Figure 2.24 Effect of sample pH for lipids on 5% APMAH. Lipid standards were prepared at concentration of 1 µg/mL in different buffer solutions at given pH (3.0, 5.5 and 9.0) and then adding methanol to a final concentration of methanol/water (40/60, v/v). Three step desorption was performed in methanol, combined together and analyzed using CSH C18 LC-MS method.

2.3.7 Optimization of extraction time

Extraction time can affect extraction recovery in SPME because it takes time to achieve equilibrium. The microextraction process is considered complete when the analyte concentration reaches equilibrium in the sample and microgel. The time required is dependent on the partition coefficient of the analyte as well as its diffusion properties. The short diffusion path (which is very important when the matrix is highly viscous, such as plasma) will result in the shorter equilibration time. Extraction time also depends on geometry of the extracted phase (availability and number of extraction phase sites), temperature and agitation conditions. Once equilibrium is achieved, increasing extraction time further will result in no additional increases in analyte recovery. In the dispersive format of SPME, contact surface between the analytes and the support is higher and diffusion path is shorter, both of which increase the extraction rate and shorten the time required to reach equilibrium. This is in contrast to fiber format of SPME where thick commercial SPME coatings can take several hours to reach equilibrium.

2.3.7.1 Effect of extraction time for metabolites with high to intermediate polarity

In this experiment, extraction times were varied from 5 to 60 minutes using the same extraction conditions as Section 2.2.3.2. For almost all species tested equilibrium was reached within 5 minutes within the experimental error and no further increases in the

amount extracted were observed with subsequent increases in extraction time. Therefore, short extraction time of 5 minutes was chosen for D-SPME method. Such short equilibration time could be achieved due to the microgel size, structure and high degree of porosity. Moreover, in the dispersive format of SPME, contact between the analytes and the support is higher which increases the extraction rate and shortens the time required to reach equilibrium.

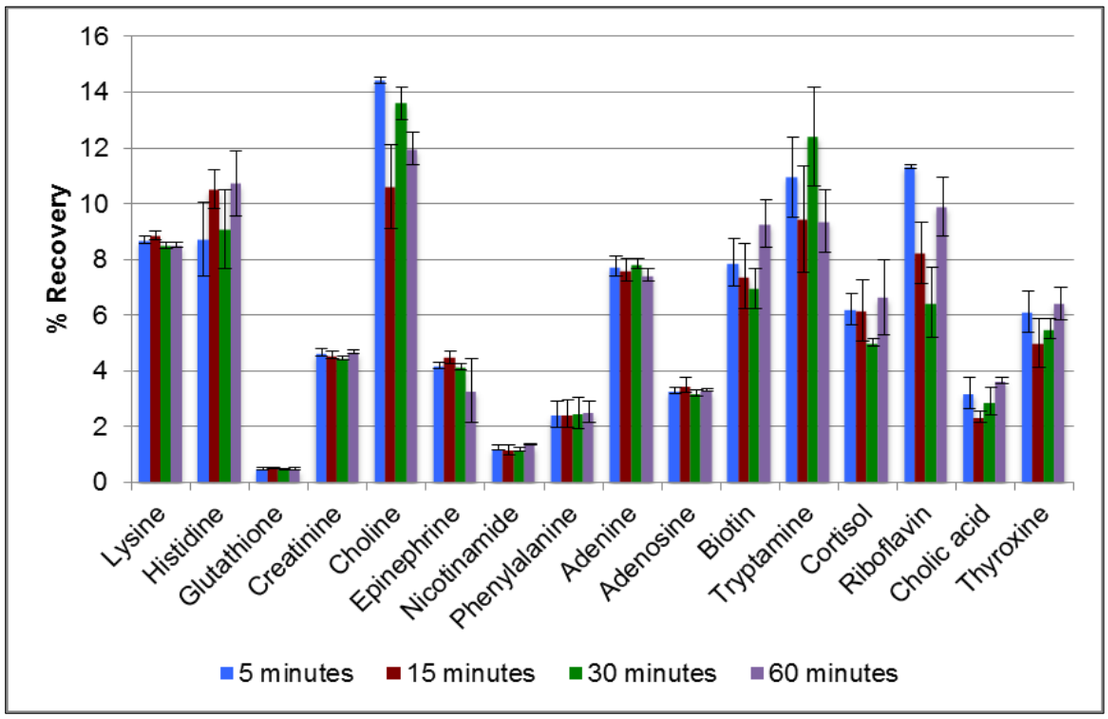

Figure 2.25 Effect of extraction time on 10% AAC for metabolites with high to intermediate polarity. Extraction was performed as described in Section 2.2.3.2. First and second desorption steps were in acetonitrile/formic acid (99/1, v/v) and third desorption step was in acetonitrile. The samples were combined and then analyzed using PFP LC-MS method.

2.3.7.2 Effect of extraction time for lipids

In this section the effect of extraction time on lipid compounds is evaluated according to the Section 2.2.3.3. Different extraction time from 5 to 60 minutes was used. An extraction time profile was determined by measuring the recovery is shown in Figure 2.26. As discussed in Section 1.4.2, the equilibration time is defined as the time after which the amount of analyte extracted remains constant within experimental error. According to these results 5 minutes was chosen as the extraction time for D-SPME method for lipids.

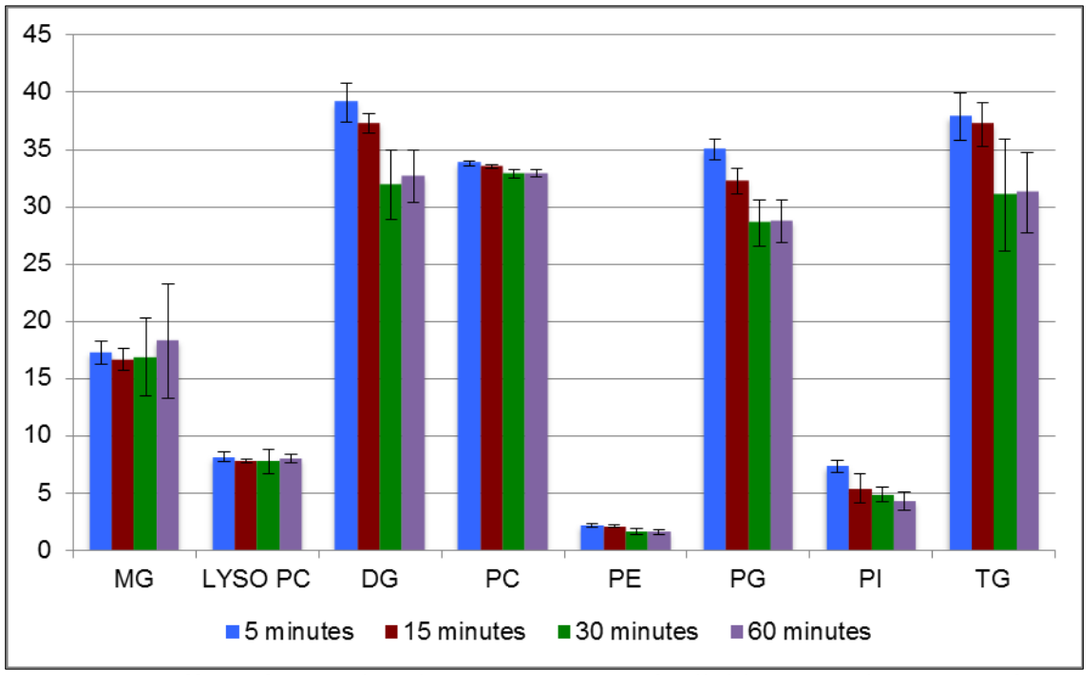

Figure 2.26 Effect of extraction time on 10% AAC for lipids. Extraction was performed as described in Section 2.2.3.3. Three step desorption with methanol was used. All desorption steps were combined and analyzed using CSH C18 LC-MS method.

2.3.8 Optimization of centrifugation time

Centrifugation is a process that involves the use of the centripetal force for the sedimentation of heterogeneous mixtures with a centrifuge. The separation efficacy of the centrifugation process depends on three variables, the centrifugation time, the relative centrifugation force (RCF) and the temperature.[109] Relative centrifugation speed is limited by the centrifuge rotor and in current study, maximum speed (25000g) was used. It was not suitable to switch to ultracentrifugation to achieve higher speeds, because this would limit the utility of protocol to only labs that have access to ultracentrifuges. The effect of temperature was also not explored due to the limited stability of analytes during extraction at elevated temperatures when working with biological samples. Therefore, only the centrifugation time was varied in this experiment to achieve the required separation of supernatant from microgel.

For D-SPME, centrifugation is used in all steps of extraction, wash and desorption to separate hydrogels from the supernatant. Therefore, the effect of centrifugation time was investigated using the same extraction method conditions as described for Section 2.2.3.2. Figures 2.27 and 2.28 show the comparison of 10- and 30-minute centrifugation time. As shown in Figure 2.27, for AAC and VAC microgels increasing centrifugation time did not improve the recovery or method precision within experimental error, indicating sedimentation process is complete within the 10 minutes. Therefore, 10-minute centrifugation time was chosen for all AAC and VAC hydrogels for D-SPME method. According to Figure 2.28 high variability was observed for APMAH with 10-minute centrifugation. For 10% APMAH longer centrifugation time was required to sediment microgel due to smaller size of APMAH microgel compared to other kind of microgels as shown by improved recovery and method precision when using 30-minute centrifugation time. Therefore, 30-minute centrifugation time was chosen for 10% APMAH with D-SPME method while for 5% APMAH 10-minute centrifugation time similar to AAC and VAC hydrogels was used for all subsequent experiments.

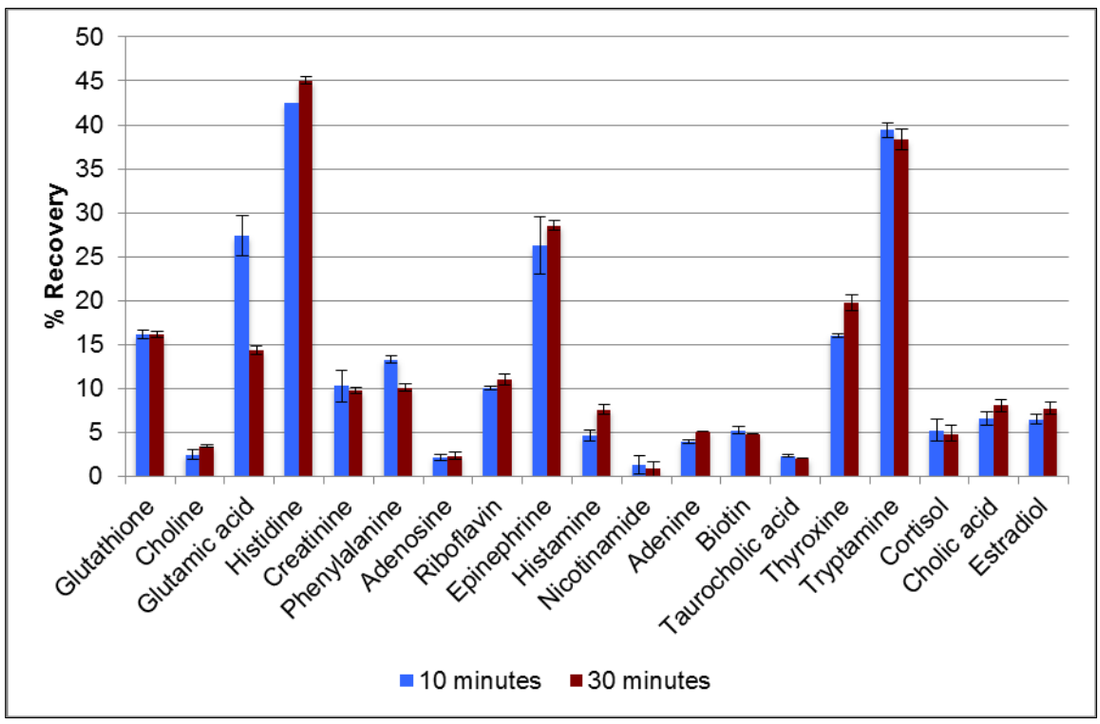

Figure 2.27 Optimization of centrifugation time for 5% AAC. Metabolite standards were prepared in water at the concentration of 1 µg/mL. Three step desorption was performed with acetonitrile/formic acid (99/1, v/v). The samples were analyzed using PFP LC-MS method.

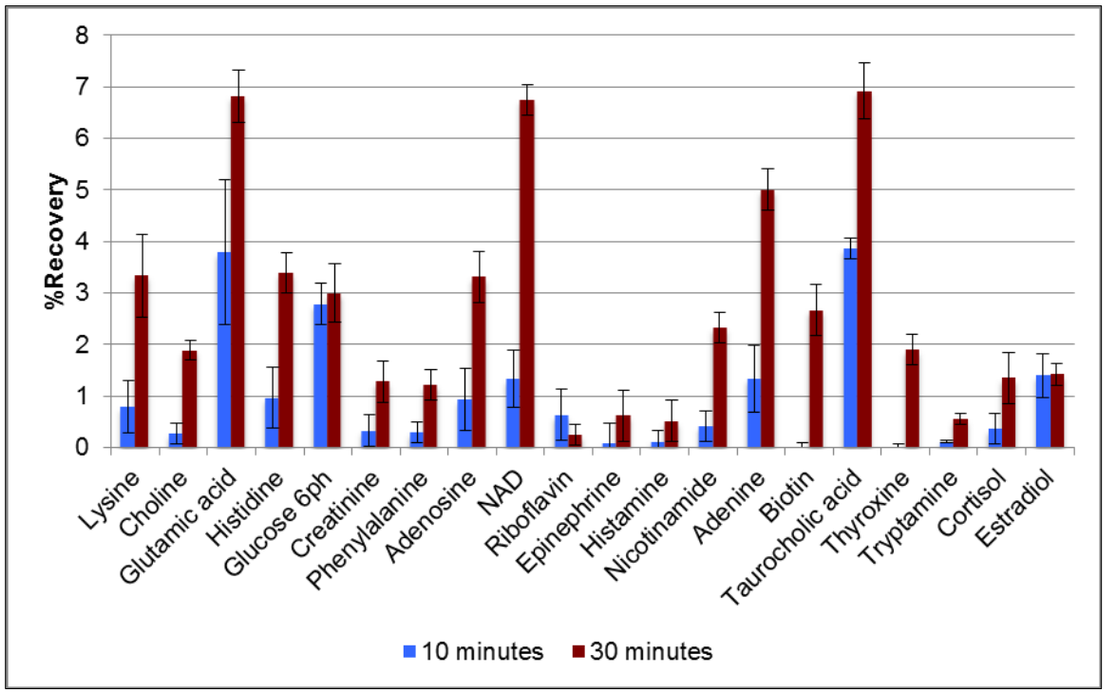

Figure 2.28 Optimization of centrifugation time for 10% APMAH. Metabolite standards were prepared at pH=3.0 with the concentration 1 µg/mL. First step desorption was performed using acetonitrile, second and third step desorption was with acetonitrile with 5 mM ammonium hydroxide. The samples were combined, neutralized and then analyzed using PFP LC-MS method.

2.3.9 Effect of increasing portion of functional monomer

For this experiment, the effect of having 5, 10 and 15% of functional monomer was evaluated. However, to ensure fair comparison, first the amount of sorbent in each hydrogel portion was determined. The solvent from 100 µL of each microgel was evaporated with Speedvac. The amount of sorbent for each microgel tested is tabulated in Table 2.10. As mentioned previously 15% APMAH microgel could not result in stable hydrogels, so this percentage was excluded for APMAH hydrogels only.

Table 2.10 Amount of sorbent for each portion of microgel after correction factor

Type of microgel		Weight of tube (g)	Weight of tube and gel after 3.5 hours evaporation (g)	Final weight of microgel (mg)	Amount of sorbent after correction factor (µL)
AAC	5%	0.9326	0.9386	6.0	25.0
	10%	0.9153	0.9190	3.7	40.5
	15%	0.9288	0.9314	2.6	57.6
VAC	5%	0.9332	0.9371	3.9	25.0
	10%	0.9207	0.9243	3.6	27.0
	15%	0.9230	0.9257	2.7	36.1
APMAH	5%	0.9089	0.9140	5.1	25.0
	10%	0.9267	0.9290	2.3	55.4

The extraction method was the same as Section 2.2.3.2 with the difference of using different portion of co-monomer in each microgel. The results obtained are shown in Figures 2.29 and 30. For AAC and VAC, the increase in ion-exchange sites is expected to primarily affect metabolites with amine functionality. This trend is in fact observed in Figures 2.29 and 2.30 where increasing the weight percentage of co-monomer, significantly increases the recovery for amine-containing metabolites such as lysine, histidine and epinephrine in AAC and metabolites such as lysine and choline in VAC microgel. According to the results of t-test (at the 95% confidence level), there was pronounced significant trend for most of the compounds with amine group that are expected to be charged at pH tested. Although a general trend is observed, the increase is not linear and some exceptions to the trend can be observed. The effect of increasing the amount of acrylic acid co-monomer on the porosity of AAC microgel was investigated using specific surface area and porosity analyzer and confocal laser scanning microscope. [111] The results showed that, total volume [V (m^3/g) 103] for microgel with 5, 10 and 15 % AAC functionality is 154.808, 63.104 and 56.184 respectively and the surface area (m^2/g) for 5, 10 and 15 % AAC functionality is 22.90, 13.10 and 18.46 respectively. Increasing from 10 to 15% AAC had very slight effect on volume and surface area of microgel. These results are in agreement with the recovery results shown in Figure 2.29. For instance, the recovery of creatinine in AAC microgel did not improve when increasing co-monomer portion from 10% to 15% within experimental error.

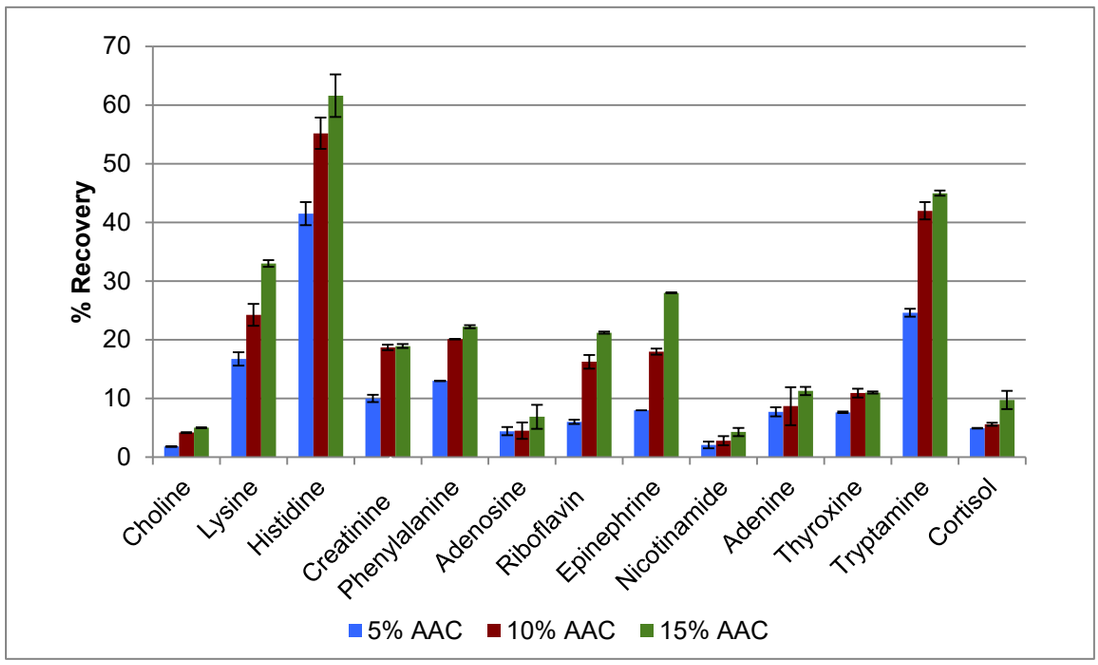

Figure 2.29 Effect of increasing portion of functional monomer for AAC microgel. Metabolite standards were prepared in water with the concentration of 1 µg/mL. First and second desorption steps were in acetonitrile/formic acid (99/1, v/v) and third desorption step was in acetonitrile. The samples were analyzed using PFP LC-MS method.

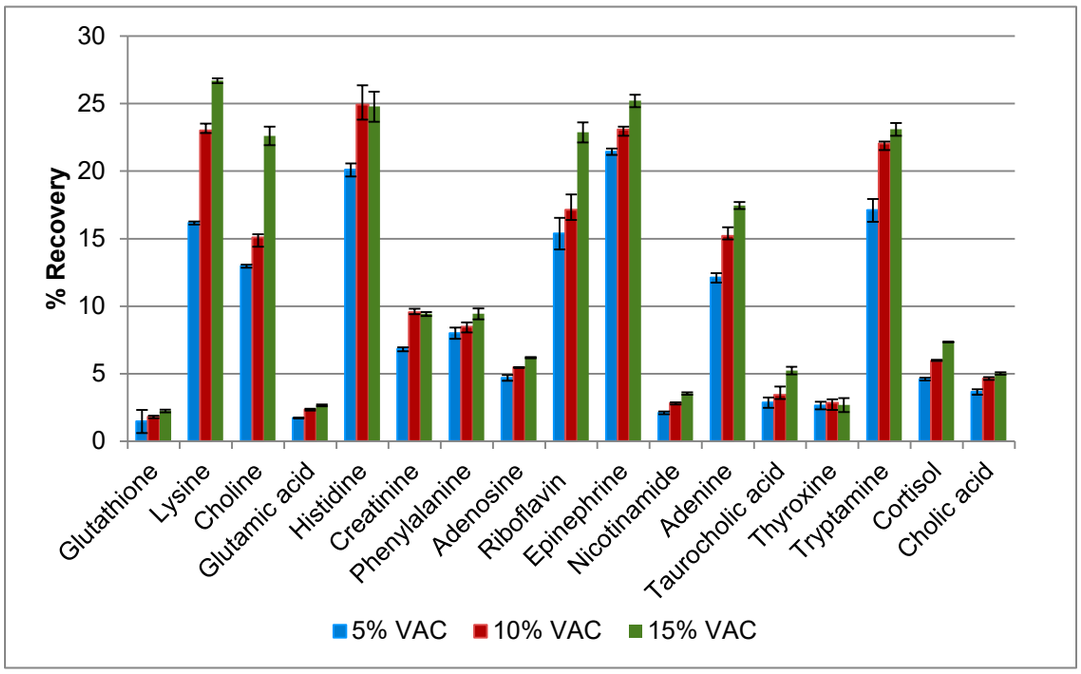

Figure 2.30 Effect of increasing portion of functional monomer for VAC microgel. Metabolite standards were prepared in water with the concentration of 1 µg/mL. First and second desorption step was in acetonitrile/formic acid (99/1, v/v) and third desorption step was in acetonitrile. The samples were analyzed using PFP LC-MS method.

For APMAH, it was expected to observe an increasing trend for the recovery of metabolites with acidic functionality. This is shown in Figure 2.31, where increasing the weight percentage of co-monomer increases the recovery for acid-containing metabolites such as taurocholic acid and glutamic acid. Increasing the amount of ion exchange functionality increases the size and number of pores and results in increasing the recovery of charged analytes as expected. However, the increase in ion-exchange contributions does not generally provide linear increase in extraction recovery due to presence of other interactions as well. In addition, as shown in Figure 2.31, the change in microgel porosity can impact extraction properties of all metabolites regardless of their charge and result in drastic increases in recovery. For this reason, 10% co-monomer is selected as the best co-monomer proportion for global metabolomics experiments to provide good extraction recovery across various metabolite classes.

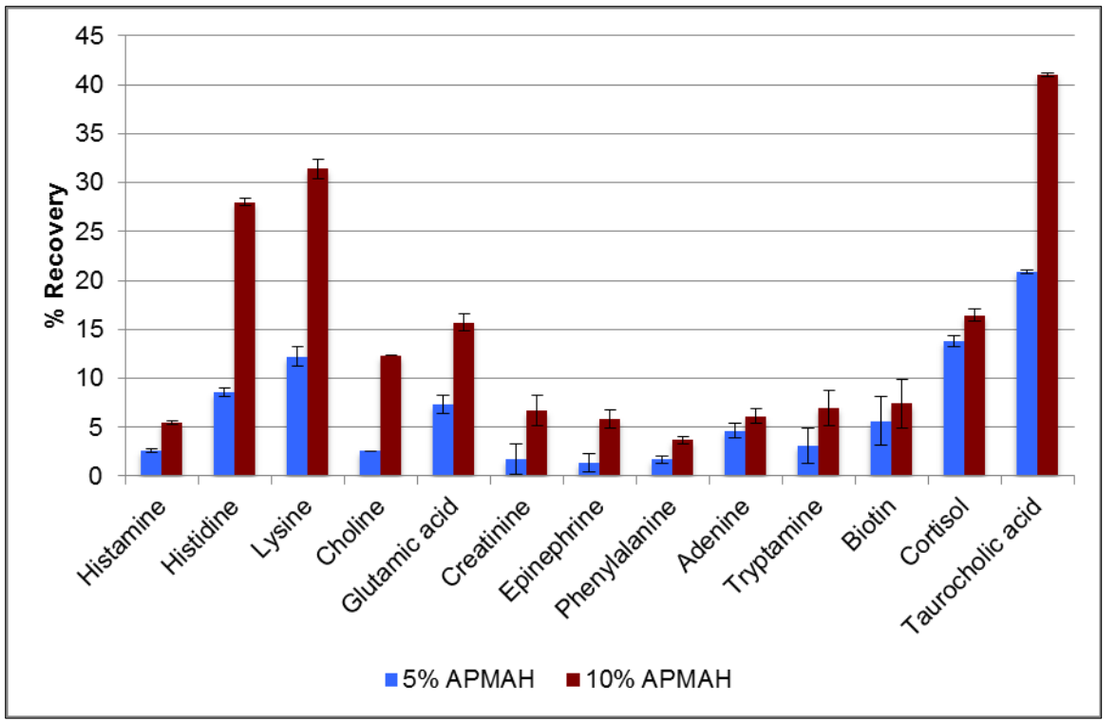

Figure 2.31 Effect of increasing portion of functional monomer for APMAH microgel. Metabolite standard was prepared at pH 3.0 with the concentration 1 µg/mL. First desorption step was performed with 100 µL of acetonitrile and second desorption step was with 100 µL of acetonitrile with 5 mM ammonium hydroxide and analyzed using PFP LC-MS method (samples are neutralized prior to injection).

2.3.10 Optimization of sorbent-to-sample ratio

The sensitivity of the SPME method is proportional to the number of moles of the analyte extracted from the sample. According to Equation 1.7, when the sample volume increases, the amount of analyte extracted also increases until the volume of the sample becomes significantly larger than the product of the distribution constant and volume of the coating. From that point onward, further increase in sample volume will not increase the recovery. In this experiment, sorbent-to-sample ratio was optimized using the extraction method conditions as presented in Section 2.2.3.2. For this experiment, the volume of microgel (25 µL) was kept constant, while the sample volume was increased. The results obtained are shown in Figure 2.32. The recovery was improved for amine-containing compounds (such as lysine, histidine and tryptamine) up to the ratio 1:25, beyond that the amount extracted did not increase anymore. Based on these results, the ratio of 1:25 was selected as the best choice for maximum sensitivity of the developed D-SPME method.

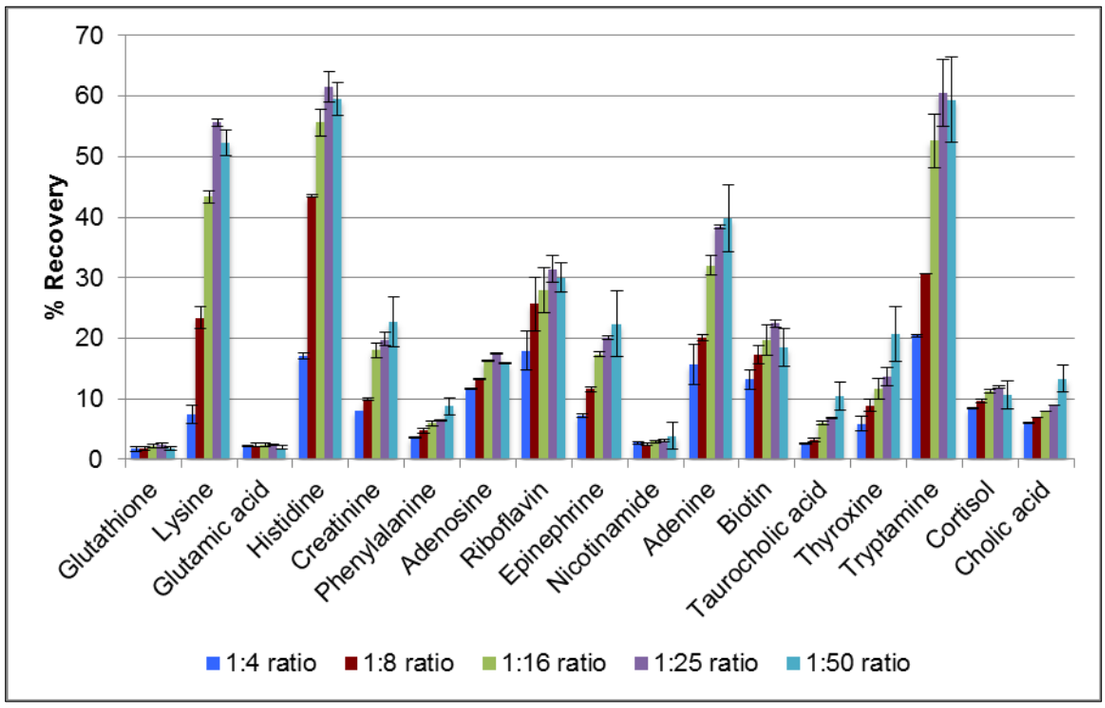

Figure 2.32 Effect of sorbent-to-sample ratio on 10% AAC. The extraction was performed with 1 µg/mL of metabolite standards in water. The wash step was performed using 200 µL of LC-MS water and analytes were eluted using three step desorption. First and second desorption in 100 µL of acetonitrile/formic acid (99/1, v/v) and third desorption was in acetonitrile. The samples were analyzed using PFP LC-MS method.

2.3.11 Evaluation of mean recovery and intra-day and inter-day repeatability

After selection and optimization of all relevant SPME parameters, the optimized D-SPME method was evaluated in order to demonstrate its suitability for global metabolomics. The main aspects of evaluation included intra- and inter-day method precision and recovery. For polar metabolites, extraction was the same as described in Section 2.2.3.2 but with three steps of desorption; first desorption, 100 µL of acetonitrile/formic acid (99/1, v/v); second desorption, 100 µL of acetonitrile/water/formic acid (90/9/1, v/v); third desorption, 100 µL of acetonitrile/water (9/1, v/v) which were all combined together for LC-MS analysis. Experiment for lipids was performed with 3-step desorption by methanol. In order to evaluate intra- and inter-day reproducibility, experiment was performed using 10% AAC on five different days and five replicates each day to establish method performance. Table 2.11 summarizes repeatability results obtained from five different days and calibration curves, as well as mean recovery of the metabolites tested. The results shown for each metabolite are obtained using the best LC-MS method for that analyte as previously described in Table 2.3 in Section 2.2.4.1

Table 2.11 Mean recovery, inter-day and intra-day repeatability of 10% AAC in 5 replicates and 5 different days

Metabolites	Method	Intra-day precision % RSD					Mean recovery (n=5)	Inter-day RSD% (n=5)
		(day 1)	(day 2)	(day 3)	(day 4)	(day 5)		
Glutathione	Positive ESI-HILIC	12.0	7.3	6.0	5.8	15	1.91	10.0
Glutamic acid		19.0	32.0	11.0	13.0	22.0	2.32	30.0
Creatinine		4.5	10.0	1.3	5.6	8.7	35.19	20.0
Adenosine		15.0	9.2	5.2	8.8	9.9	10.07	4.6
Riboflavin		7.3	15.0	11.0	34	16.0	4.15	26.0
Nicotinamide		6.2	4.3	0.6	8.6	3.6	17.72	7.0
Adenine		9.0	2.2	10.0	9.7	10.0	14.74	7.3
Qoenzyme Q10		17.0	3.7	18.0	6.5	17.0	10.39	9.0
Maleic acid	Negative ESI-HILIC	10.0	5.0	4.8	NA	NA	0.88	9.2
Estrone glucoronide		6.0	6.0	11.0	NA	NA	0.79	15.0
Tryptophan	Positive ESI-PFP-RP	7.8	8.7	3.6	10.0	14.0	1.72	10.0
Epinephrine		15.0	6.0	8.3	4.1	7.0	18.86	14.0
Biotin		9.0	10.0	9.5	7.1	9.3	4.89	11.0
Thyroxine		10.0	11.0	10.0	15	15.0	11.96	25.0
Tryptamine		35.0	6.1	12.0	6.7	7.6	23.55	19.0
Cortisol		15.0	7.2	9.4	9.5	13.0	6.44	22.0
Phenylalanine		8.9	2.5	7.2	5.4	8.0	10.62	10.0
Taurocholic acid	Negative ESI-PFP-RP	9.3	4.2	5.4	5.7	8.0	2.26	5.4
Cholic acid		13.0	9.1	10.7	4.7	8.7	6.21	15.0
Sphingosine	Positive ESI-CSH C18-RP	3.8	2.4	11.0	12.0	6.0	11.82	10.0
LYSO PC		2.1	2.1	5.8	7.3	6.0	12.00	7.1
MG		5.9	6.0	7.4	1.4	17.0	12.45	22.0
PC		5.3	5.7	12.0	12.0	4.4	38.25	23.0
PI		5.0	14.0	0.9	1.0	5.0	11.96	3.5
PG		2.3	5.7	17.0	3.2	6.4	16.21	18.0
DG		2.8	0.2	5.1	0.2	3.7	36.89	14.0
TG		5.0	5.1	5.6	3.7	4	31.92	17.0
PE		3.3	2.0	3.3	6.3	7.6	57.90	12.0

Acceptable variability in regulated quantitative LC-MS according to Food and Drug Administration (FDA) guidelines is 15% at all levels except for LOQ where 20% RSD is allowed.[110] For metabolomics methods, there are no established acceptance criteria, but due to its semi-quantitative nature many authors use RSD cut-off of 30%. For all compounds, the precision of the results did not exceed acceptance criteria of 30% RSD therefore, inter-day and intra-day repeatability are acceptable for metabolomics. In general, mean recovery of lipids was higher than polar metabolites, unless polar metabolites could also participate in ionic interactions.

Mass accuracy is crucial aspect of MS performance and it is defined as the difference between the theoretical (calculated) mass of a compound and the mass measured by the mass spectrometer (described in Equation 2.1). Table 2.12 shows the mass accuracy of representative metabolites over five different days in PFP reversed phase method. All compounds exhibited mass accuracy < 10 ppm showing suitability of 10 ppm extraction window for data processing.

Table 2.12 Summary of mass accuracy in positive ESI mode during reversed phase chromatography with PFP column using metabolite standard mixture analyzed on five different days**.**

Metabolite	Mass accuracy results (ppm)				
	Replicate 1	Replicate 2	Replicate 3	Replicate 4	Replicate 5
Choline	4.80	1.92	6.72	5.76	5.40
Creatinine	3.51	2.63	0.88	4.38	3.51
Nicotinamide	3.45	2.32	3.25	2.44	1.63
Adenine	0.73	1.47	3.67	2.94	5.14
Lysine	1.36	2.04	6.80	5.44	2.04
Glutamic acid	2.70	4.05	3.38	5.40	4.73
Histidine	1.92	2.56	6.41	5.77	0.64
Phenylalanine	2.41	1.81	5.42	4.82	3.61
Biotin	1.22	2.86	0.82	0.41	6.12
Adenosine	4.10	3.36	4.48	5.22	1.86
Cortisol	1.38	0.28	0.83	1.10	0.28
Thyroxine	1.03	1.16	0.31	0.13	0.26

2.3.12 Conclusions and optimized method

Solid phase microextraction in dispersive format has not yet been used in global LC-MS metabolomics. Here, for the first time we developed a new D-SPME method for comprehensive coverage of metabolome. The optimized protocol with D-SPME sample preparation for AAC, VAC and APMAH microgels is shown in Figure 2.33. The optimized D-SPME was found to perform well for acidic and basic metabolites and for lipid metabolites across all lipid classes. Acidic metabolites (such as organic acids) are

extracted well using N-3-aminopropyl methacrylamide hydrochloride (APMAH) functionalized microgel, while basic metabolites (such as amines) are extracted better using vinyl acetate (VAC) and acrylic acid (AAC) functionalized microgels.

The optimum sorbent-to-sample ratio was found to be 1:25, while the optimum sample pH for extractions using AAC and VAC was pH=5.5 and for APMAH phase was pH=3.0. 10-minute centrifugation time was sufficient for complete and reproducible sedimentation of all microgels except 10% APMAH where 30-minute centrifugation time was required due to slightly smaller particle size compared to other microgels. 5-minute extraction time was found sufficient to reach equilibrium for all metabolites illustrating good potential of hydrogels as extraction phases in SPME. 20% methanol wash solvent was found suitable for this application, although some losses of very polar metabolites will be observed using these more stringent wash conditions. Overall, acetonitrile was found to be better solvent for desorption of polar metabolites, while methanol performed better for lipid compounds. One-step desorption with acetonitrile/water (9/1, v/v) containing appropriate additives was sufficient to recover the majority of polar metabolites but additional two desorption steps in method are needed to effectively recover lipids. The proposed desorption scheme is highly compatible with the complementary LC methods used in this study. Polar metabolites that are desorbed during the first desorption step in acetonitrile/water (9/1, v/v) with pH adjustment can be directly injected in HILIC method thus avoiding need for evaporation/reconstitution step. Furthermore, as shown in our work this fraction will not contain many phospholipids, which should improve data quality by minimizing ion suppression by co-eluting interferences. Metabolites with intermediate polarity could be effectively desorbed both using acetonitrile and methanol desorption steps. To avoid signal splitting of such metabolites and ensure good method precision one aliquot of first desorption and one aliquot of second desorption should be combined and analyzed in reversed phase method with PFP column, after appropriate adjustment of injection solvent strength through either dilution or preferably evaporation/reconstitution. Finally, the obtained lipid fraction from desorptions 2 and 3 is compatible with direct analysis in reversed phase method with CSH C18 column after appropriate adjustment of injection solvent strength by dilution with water.

The results for optimized protocol indicate that good metabolite coverage can be achieved using D-SPME formats with hydrogel extraction phases. The next chapter will be examining the performance of these materials in human plasma and compare their performance against traditional “gold standard” method of methanol solvent precipitation.

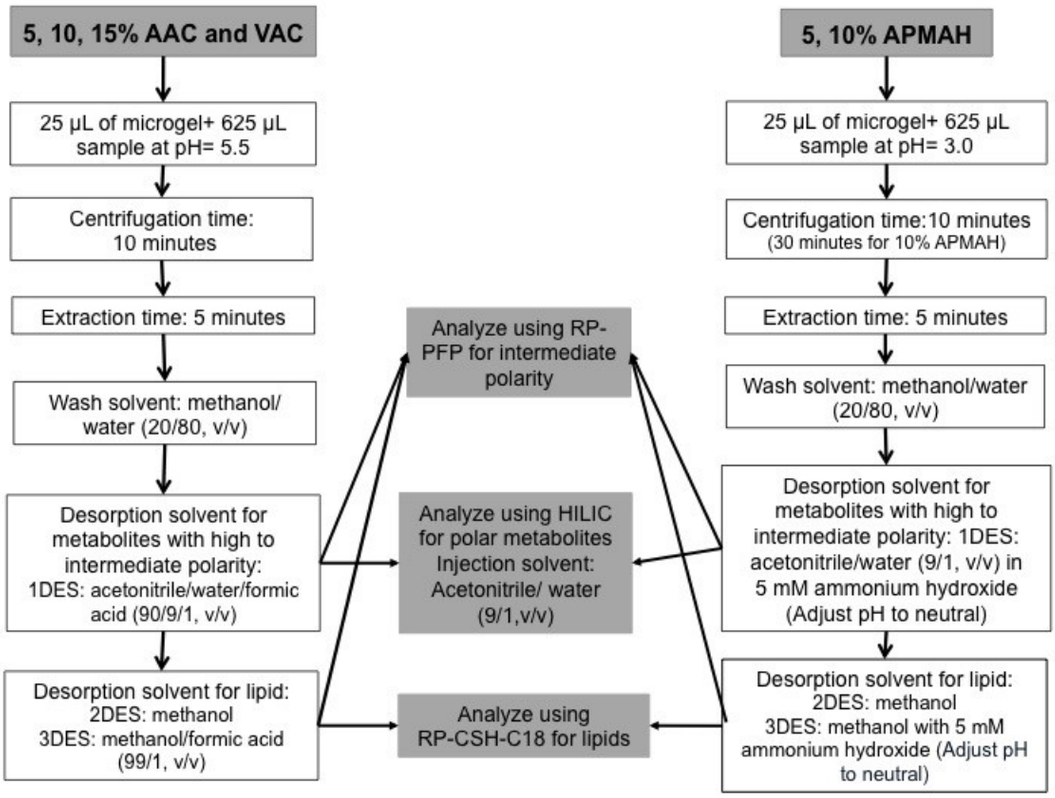

Figure 2.33 Optimized D-SPME protocols for AAC, VAC and APMAH microgels

Chapter 3

Metabolomics of human plasma: comparison of optimized D-SPME to traditional method of methanol protein precipitation and to nanotrap extraction

3.1 Introduction

There is an increased interest in recent years in the evaluation of different sample preparation methods for global LC-MS metabolomics. No single analytical method can provide complete metabolome coverage, so it is important to investigate new sample preparation methods and compare their coverage to the traditional method of solvent precipitation. In this chapter we present a novel application of hydrogel particles for sample preparation of human blood plasma samples for the first time. The objective of this chapter is to use optimized D-SPME method presented in Chapter 2 in order to extract human plasma and compare the results obtained against commercial nanotrap particles used for protein enrichment and the most common "gold standard" method of global metabolomics (methanol solvent precipitation). The methods were compared according to the following criteria: metabolome coverage, the repeatability of extraction, and the susceptibility to ion suppression.

Blood is composed of two parts: a cellular component consisting of red and white blood cells and platelets, and liquid component, called plasma which accounts for approximately 50–55% of blood volume. Plasma consists mostly of water (~ 95 % by volume); the rest is composed of proteins, peptides and metabolites.[86] Prior to LC-MS analysis of a plasma sample, the proteins must be removed, because the presence of proteins can drastically affect properties of chromatographic column employed for analysis, reduce column lifetime as well as interfere with metabolite signal detection. Plasma also contains many enzymes that can chemically modify metabolites. The optimal temperature for the enzymes is 37 °C and the enzymatic activity decreases when the temperature is reduced.[87] Therefore, plasma samples should be stored and handled as cold as possible until proteins are removed to prevent enzymatic conversion of metabolites.

The best traditional method to use for this comparison was selected from literature based on high number of observed metabolites and reproducibility. For instance, Polson *et al.*[88] compared different protein precipitation techniques (organic solvent, acid, salt and metal) in plasma using LC-MS. Among the tested methods, the precipitation with methanol was found to perform the best in terms of metabolite coverage and method reproducibility. Want *et al.*[29] compared 14 different protein precipitation methods and also showed that 100% methanol and methanol- containing solvent mixtures is the most effective methods

for the detection of the largest number and broadest range of serum metabolite features. In summary, protein precipitation with methanol is the most widely used method for global metabolomics of plasma[89,90], so our newly developed method presented in Chapter 2 is compared against this gold standard method.

Although protein precipitation with organic solvent provides high number of metabolite features and reproducibility, precipitation methods provide incomplete protein removal with an estimate of 1-10% protein remaining in the sample, which can cause shortening of column lifetimes for metabolomic studies.[26] Another challenging issue with protein precipitation is ion suppression or enhancement, which is change of analyte signal in the presence of co-eluting interferences that alter its ionization behavior during electrospray process. SPME can provide improved sample cleanup due to the use of small volume of extraction phase, which leads to the extraction of smaller amounts of analytes and potential interferences. This could help improve both ion suppression and metabolite coverage and will be investigated in detail in this chapter.

Nanotrap particles are comprised of N-isopropylacrylamide hydrogel with a porous outer shell and internal core containing chemical affinity baits as discussed in Section 1.5.2. These charge-based affinity baits are incorporated into the Nanotrap particles by copolymerization and covalent binding. The affinity baits can be positively or negatively charged and interact with analytes that can diffuse through the outer shell through multiple types of interactions. The patented Nanotrap particles are designed for optimal protein size sieving and harvesting of proteins from complex biological samples.[76] Nanotrap particles which are used in this work are hydrogel particles of about 800 nanometers in size that have a shell made of polymers of N- isopropylacrylamide (NIPAm) and co-monomers such as acrylic acid (AAC) and Cibacron blue which are called white and blue nanotrap respectively with crosslinkers of N, N9-methylenebisacrylamide (BIS). These nanoparticles are expensive and have shown excellent performance for the enrichment of small protein biomarkers from plasma, but have not been explored for metabolite extraction.[76] White nanotrap has the same functionality (acrylic acid) as AAC microgel and in this chapter these two hydrogels will be compared together. The comparison of white nanotraps and AAC hydrogels will help explore if core-shell geometry is advantageous for the extraction of metabolites.

3.2 Experimental

3.2.1 Chemicals and materials

Human plasma with sodium citrate as anticoagulant was obtained from Bioreclamation IVT Laboratories (Lot # BRH957197). Core-shell nanoparticles were purchased from Ceres Nanosciences (Manassas, Virginia, US) and other materials and reagents are the

same as described in Section 2.2.1.

3.2.2 Extraction of metabolite standard mixture using nanotraps and comparison to microgel extraction

The exact composition of nanotraps is not known but based on published paper[76], Figure 3.1 is the likely structure of nanotraps. There is shell that has NIPAm network and high affinity bait such as vinyl sulfuric acid (VSA) that acts as a molecular sieve and prevents unwanted molecules to enter to the core. This shell with VSA works as a size exclusion cut-off and excludes large unwanted abundant molecules such as immunoglobulins and albumin. Inside the core there is NIPAm network, and either acrylic acid or cibacron blue co-monomer and methylenebisacrylamide (BIS) crosslinker.[76]

In terms of experiment, 50 µL of 1 µg/mL standard mixture in PBS buffer was mixed with 50 µL of blue or white nanotrap (ratio 1:1) as appropriate with 30-minute shaking (700 rpm) at room temperature. After 10-minute centrifugation (25000 g at 4^0C). The particles were washed with 200 µL of LC-MS water and centrifuged again to remove the supernatant. 100 µL of acetonitrile/acetic acid/water (60/2/38 v/v) was added to white nanotrap and 100 µL of acetonitrile/ammonium hydroxide/water (70/10/20 v/v) was added as an elution solvent to blue nanotrap. It was incubated for 18 hours, and then centrifuged. 100 µL of supernatant was transferred to HPLC vial, and blue nanotrap sample pH was adjusted to neutral with formic acid prior to PFP LC-MS analysis. Extraction method for 10% AAC microgel is the same as described in Section 2.2.3.2 with two step desorption using 100 µL of acetonitrile and acetonitrile/ formic acid (99/1, v/v) with the sorbent to sample ratio of 1:8.

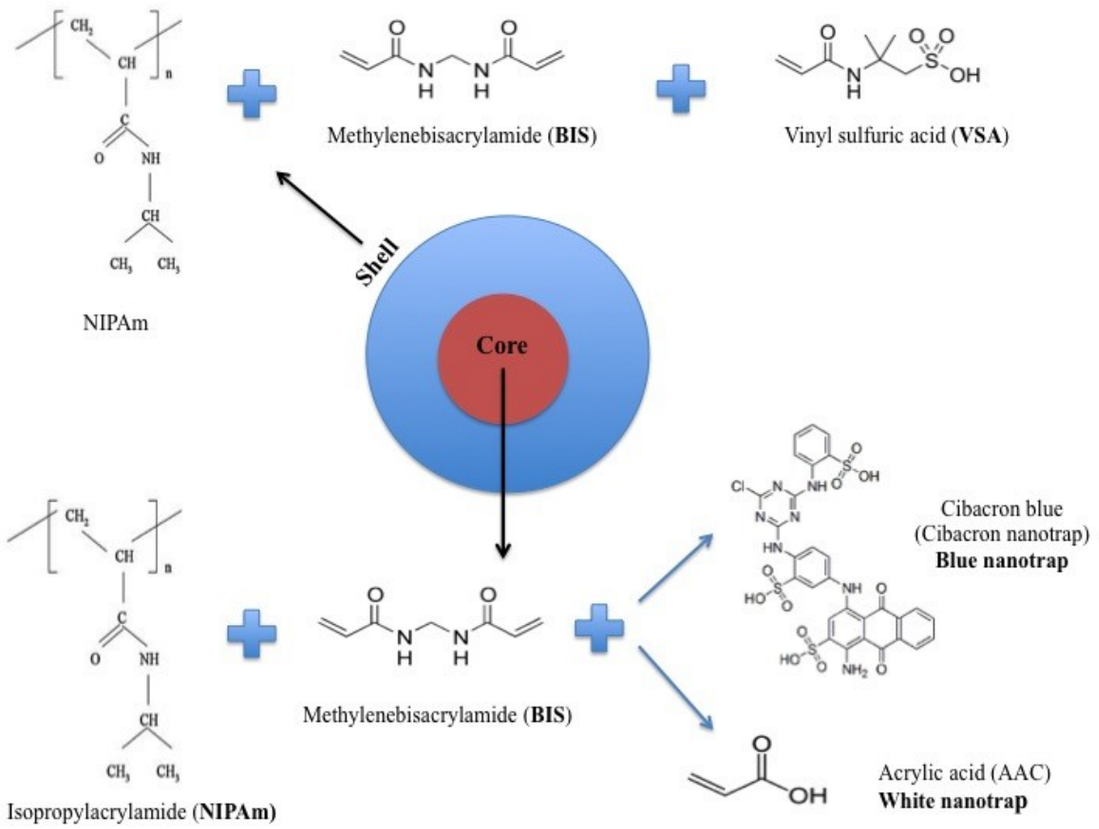

Figure 3.1 Schematic representation of white (AAC) and blue (Cibachron Blue) nanotrap

3.2.3 Protein precipitation with methanol for human plasma

Plasma to precipitant ratio of 1 to 4 was selected for the comparison, as recommended in literature.[91] For this experiment, 400 µL of cold methanol (kept for 10 minutes in freezer at -80^0 C) was added to 100 µL plasma. After 2-minute vortexing, plasma samples were placed on ice for 15 minutes, followed by centrifugation at 25000 g at 4 °C for 10 minutes. Afterward 400 µL of the supernatant was removed and divided into three portions. The first portion was evaporated to dryness using Speedvac (Thermo Scientific™ SPD121P) and at the time of LC-MS analysis reconstituted in 100 µL of 40% methanol (in this chapter called protein precipitation with evaporation/reconstitution). Second portion was diluted with 100 µL of water (in this chapter called protein precipitation with dilution) to have the composition of 40% methanol. First and second portions were injected in reversed phase method with PFP column in both positive and negative ESI mode. Third portion was evaporated to dryness and finally reconstituted in 100 µL of 90% acetonitrile: water to analyze with HILIC method in both positive and negative ESI mode. All samples were stored in freezer at temperature -80^0 C until LC-MS analysis. All samples were prepared in 5 replicates. For blank, the same experiment was performed but instead of plasma an equivalent volume of LC-MS water was used to perform the extraction procedure. The main steps of protein precipitation with methanol are shown in

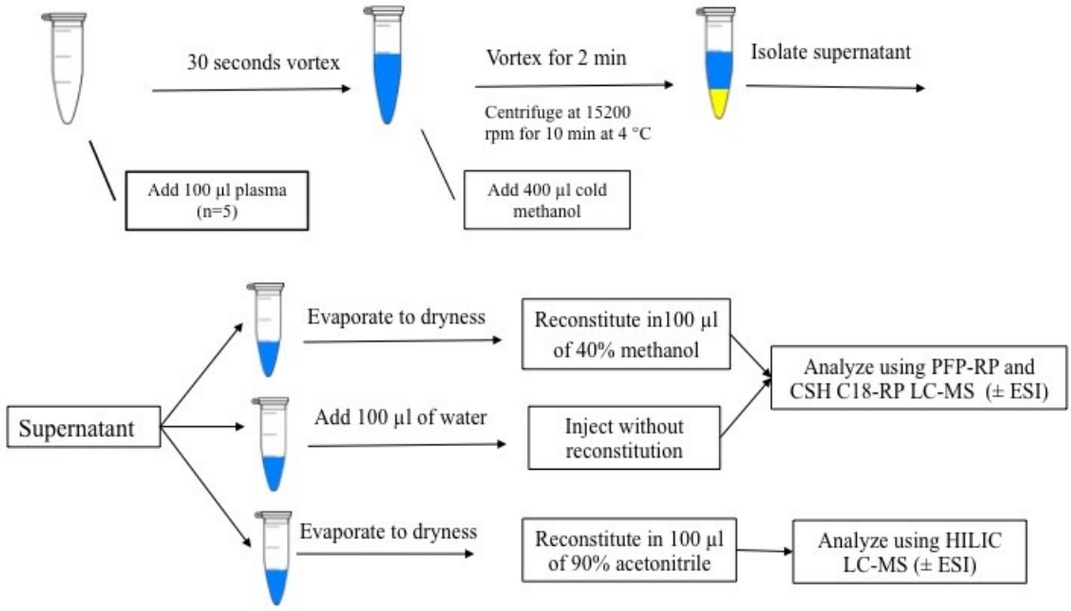

Figure 3.2 Overview of protein precipitation method with methanol for plasma.

3.2.4 Sample preparation with commercial nanotraps for human plasma

This protocol was performed according to manufacturer's instructions that were optimized for small protein biomarker enrichment. The overall procedure using nanotraps is shown in Figure 3.3. Briefly, 50 µL of plasma was added to 50 µL of either white or blue nanotrap (1:1 ratio) in 5 replicates, then incubated with shaking for 30 minutes at 4500 rpm. Afterwards samples were centrifuged for 10 minutes at 4°C and supernatant removed. After the sample had been washed with 200 µL of water, analytes were eluted from nanotraps as follows: 100 µL of acetonitrile/acetic acid/water (60/2/38 v/v) was added to white nanotrap and 100 µL of acetonitrile/ammonium hydroxide/water (70/10/20 v/v) was used for elution of blue nanotrap and followed by pH adjustment with 10 µL formic acid. Next, samples were incubated for overnight (18 hour) and centrifuged for 10 minutes at 4 °C. Finally, the resulting supernatants were diluted to total volume of 178 µL to keep the amount of plasma consistent across all sample preparation methods. The samples were divided into two portions. One portion was used directly for reversed phase LC-MS analysis with PFP column in both positive and negative ESI mode. Other portion was evaporated to dryness and reconstituted in acetonitrile/water (9/1, v/v) to analyze in HILIC method in both positive and negative ESI mode. All samples were stored in freezer at temperature -80^0 C until LC-MS analysis. For blank, the same experiment was performed but instead of plasma LC-MS water was used.

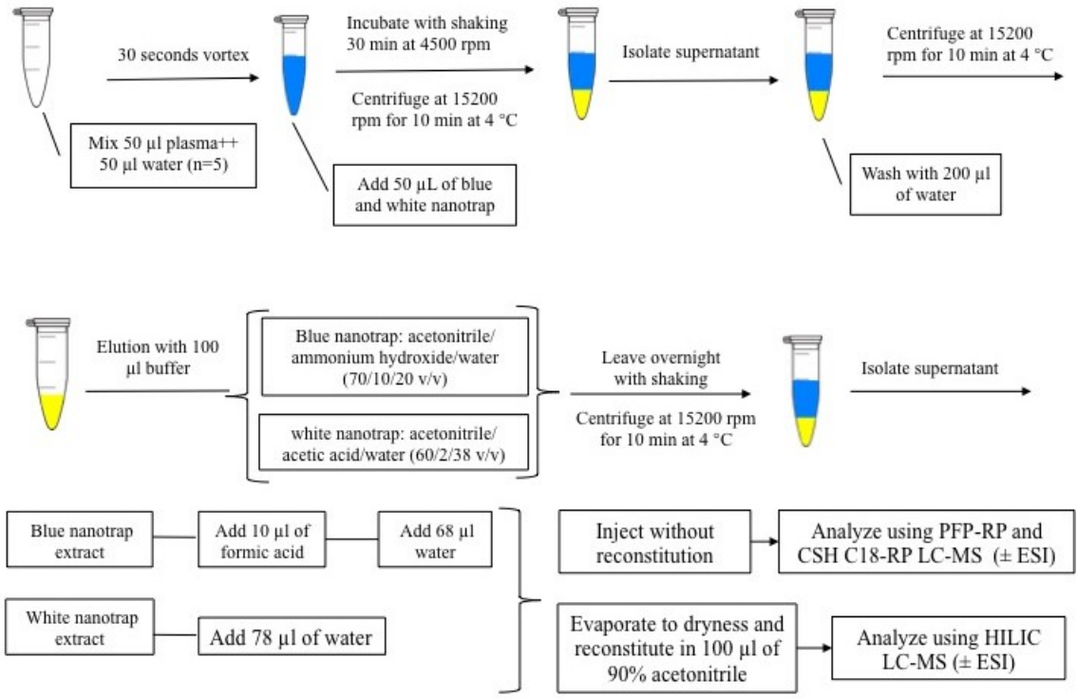

Figure 3.3 Overview of extraction procedure using white and blue core-shell nanotraps for plasma.

3.2.5 D-SPME sample preparation with ion-exchange microgel (10% AAC) for human plasma

Dispersive-solid phase microextraction samples (n=5) were prepared according to the developed method described in detail in Chapter 2. This experiment was performed with 10% AAC microgel according to the procedure shown in Figure 3.4. First, pH of plasma was adjusted to 5.5 using formic acid, then 200 µL of plasma was added to 25 µL of 10% AAC microgel. Samples were shaken for 30 minutes at 4500 rpm followed by 10-minute centrifugation at 4 °C and removing supernatant. The particles were washed with 200 µL of methanol/water (20/80, v/v) and centrifuged again for 10 minutes at 4°C. Sequential desorption was performed in three steps with 60-minute shaking and 10-minute centrifugation per each step. For first, second and third step desorption, 100 µL of acetonitrile/water/formic acid (90/9/1, v/v), 100 µL of methanol and 100 µL of methanol/formic acid (99/1, v/v) was used respectively. All elutes were mixed and divided to two portions. First portion was included of 150 µL of the mix of elutes which was diluted to 250 µL of water to keep the amount of plasma consistent across all sample preparation methods. This portion was directly analyzed using pentafluorophenyl reversed-phase in both positive and negative mode. Second portion was reconstituted in 150 µL of acetonitrile/water (9/1, v/v) to analyze with HILIC method in both positive and negative ESI modes. For blank, the same experiment was performed but instead of plasma LC-MS water was used.

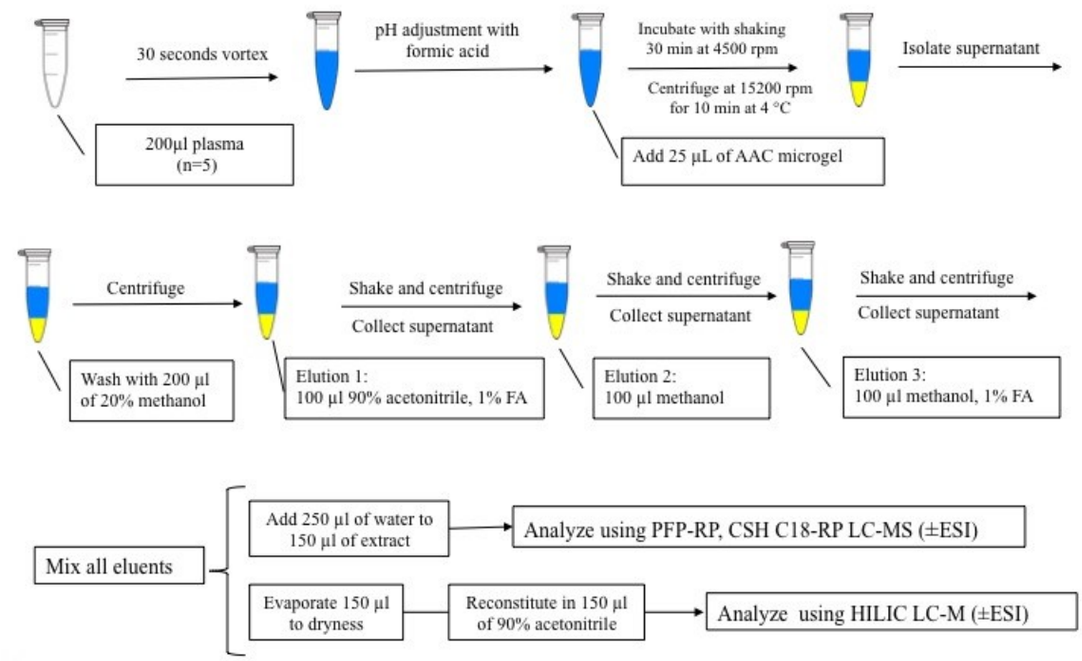

Figure 3.4 Overview of dispersive solid phase microextraction using microgel with acrylic acid ion exchange functionality (10% AAC) for plasma

3.2.6 LC-MS analysis

All samples were analyzed separately in positive and negative ionization modes using RP PFP LC-MS on Orbitrap. For reversed-phase chromatography, final injection solvent was 40% organic to help solubilize any lipids present in the samples. Under these conditions, very polar compounds would not have any retention, but these compounds will subsequently be analyzed by HILIC.

Appropriate quality controls were used throughout all the metabolomics LC-MS analyses described in this chapter. Appropriate blank solutions were used for each sample preparation method throughout the run to eliminate peaks originating from blank solution and not the plasma samples themselves during data processing. Known metabolite standard mixture (200 ng/mL) was also analyzed throughout each sample set to check retention time, peak shapes and MS sensitivity prior and throughout all analytical batches. QC sample (prepared by combining 10 μL aliquots of all study samples) was used throughout all analytical batches mainly for two reasons. First, it was used to condition the column (15 injections of QC at the beginning of the run) before the actual samples are run according to standard recommended metabolomics practices.[92] It is extremely important in metabolomics that the column is properly conditioned beforehand in order to obtain reproducible LC-MS result. Secondly, pooled QC was injected after every eight-sample injections to check the stability of the system. The QC samples were then examined using principal component analysis (PCA) to give an assessment of the quality of the data in that analytical batch. Ideally, the QC samples should be clustered closely together if the system was stable over the whole analysis.

The analytical batches consisted of five preparation replicates of each sample preparation method tested. Samples were run in randomized order. In metabolomic studies, factors such as changes in instrument signal over time and small changes in sample concentration because of storage in auto-sampler while waiting for injection may affect sample analysis and cause systematic error in the data. Full randomization of run order is performed in order to randomize these factors, so they will not appear as one a principal components and lead to possible erroneous identification of putative biomarkers, which are not relevant to the study in question but originate from the variables during an analysis.

In this study as mentioned before in Section 2.2.4.1 in Table 2.3, three different LC-MS methods (HILIC, PFP Reversed-Phase and CSH C18 Reversed-Phase) are planned to be used. For this thesis, only the results of PFP method are reported. However, HILIC and CSH C18 LC-MS analyses will be performed as future work on the same samples and are beyond scope of current thesis.

3.2.7 Data analysis and calculations

Global metabolomics analysis was performed using SIEVE software version 2.2 (Thermo Fisher). The main steps of SIEVE workflow include (1) chromatographic alignment (2) feature detection; (3) removal of background noise (4) deisotoping and combining adducts (M+H, M+K, M+Na, M+NH_4, M-H, M-H_2O-H) that belong to the same metabolite. The following parameters were used for SIEVE processing: 0.01-minute retention time start, 25-minute retention time stop (5-minute column re-equilibration time was excluded from processing), minimum signal intensity of 10000, maximum m/z 1000, minimum m/z 100 and 15 ppm m/z width were used for feature detection. In this study, chromatographic alignment bypass was applied because total ion chromatograms from different sample preparation methods are too different so that the automatic chromatographic alignment does not work properly. The data set obtained from SIEVE is a matrix described by three parameters: retention time, m/z and signal intensity in each sample. This dataset was then evaluated manually to eliminate any incorrect entries, which represented approximately ~ 20% of peaks as the software in some instances has trouble to distinguish between real chromatographic peaks and baseline noise. Final step was filtering of the data to include only (i) all the peaks that are present with signal intensity of at least 5 times greater than in blank extract and(ii) peaks which are present in minimum of 4 out of 5 replicates. This final curated dataset was used to report the number of metabolites detected by each sample method, to produce ion maps, to evaluate method orthogonality and to calculate the median RSD. Median RSD is defined as the ratio of the standard deviation obtained for the five extraction replicates to the mean of the signal intensity and multiplied by 100%, to express as percentage. Targeted analysis was performed as described in Section 2.2.5. The final manually verified dataset was also used to perform PCA using SIMCA software version 14 after Pareto-scaling.

3.3 Results and discussion

The performance of optimized D-SPME method with microgel was compared versus traditional gold standard method of protein precipitation using methanol and nanoparticle extraction with commercially available nanotraps for global metabolomics of human plasma. The main criteria used for the comparison were number of detected features, precision and ionization suppression.

3.3.1 Comparison of AAC microgel to nanotrap in metabolite standard mixture

The comparison of the extraction efficiency between commercially available blue and white nanotraps is shown in Figure 3.5. The exact amount of acrylic acid or Cibachron blue residing in the core is not known, as the nanotraps are proprietary materials. Therefore, the results are shown after the normalization of the extraction phase by

weight. In general, white nanotrap (with AAC carboxylic acid functionality) had significantly better recovery than blue nanotraps (with amine and aromatic functionality) for amines like tryptamine, adenine and histamine and almost all other metabolites tested except thyroxine.

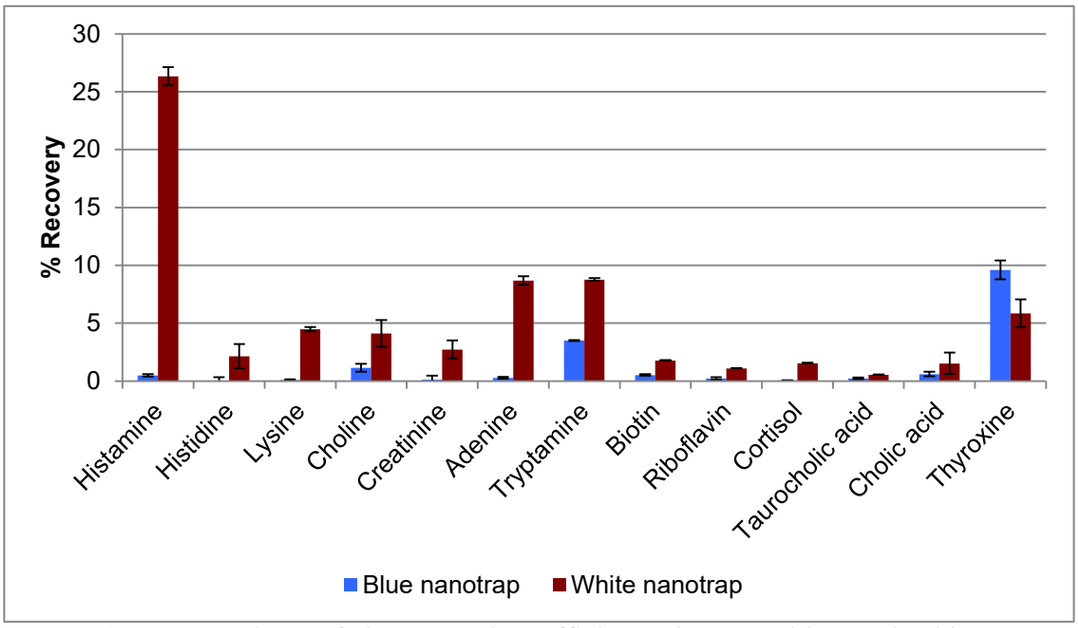

Figure 3.5 Comparison of the extraction efficiency between blue and white nanotrap using metabolite standard mixture. Samples prepared as described in Section 3.2.2.

The comparison of extraction efficiency between 10% AAC microgel and white nanotrap is shown in Figure 3.6. These two hydrogels share the same ion-exchange functionality (acrylic acid) and the same polyNIPAm hydrogel polymer network. In terms of structure, in nanotrap, there is shell that has high affinity bait like vinyl sulfuric acid (VSA) that acts as a molecular sieve and it prevents unwanted molecules to enter to the core that has acrylic acid co-monomer.[76] With nanotraps, the access to the core is available only to the molecules that can diffuse through the shell. The pore size of nanotrap shell is also proprietary although previous studies have clearly shown larger proteins such as human serum albumin cannot enter the core.[76] Thus, for this comparison the recovery was calculated after normalization of extraction phase by weight. AAC microgel is homogenous, so acrylic acid functionality is more available for extraction and direct contact with analytes in plasma. Figure 3.6 shows that AAC microgel has better recovery for amines like tryptamine and histamine than white nanotrap, and for the majority of other metabolites tested including neutral metabolites such as cortisol that would not participate in ion-exchange interactions. The direct comparison of the two materials is difficult due to lack of information on nanotraps, however lower extraction efficiency for nanotraps may be due to the nanotrap structure, which makes it harder for metabolites to extract into and desorb from the core. In addition, presence of VSA bait in nanotrap shell network could also change the selectivity of this material versus microgels. Overall, AAC

microgel performed better than white nanotrap in terms of both recovery and metabolite coverage.

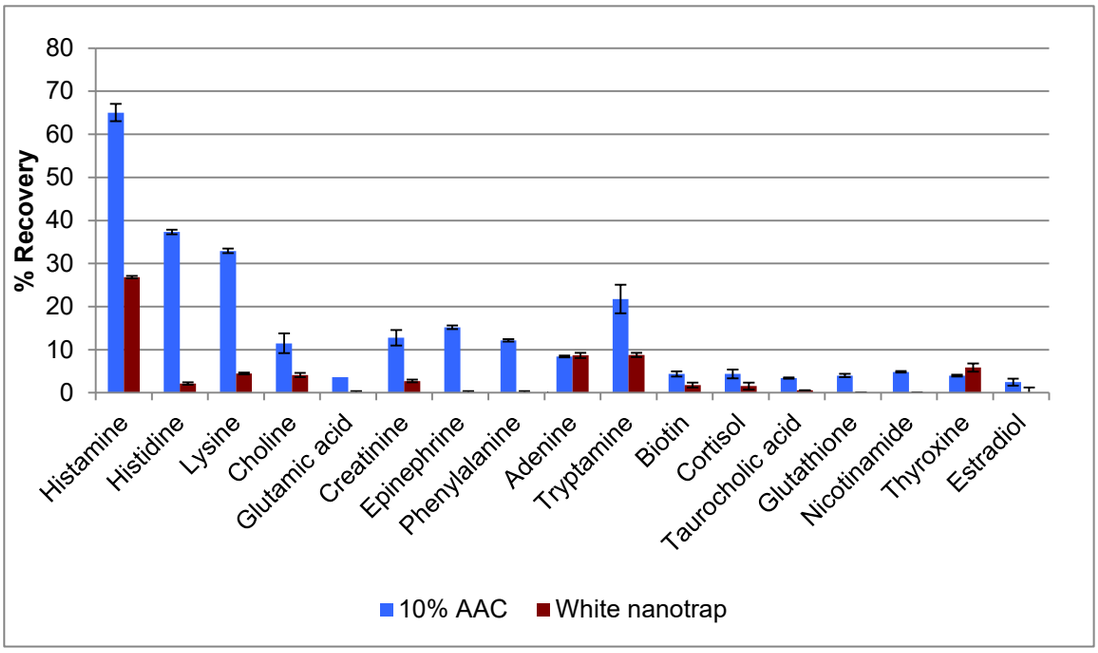

Figure 3.6 Comparison of the extraction efficiency between 10% AAC microgel and white nanotrap using metabolite standard mixture. Sample prepared as described in Section 3.2.2 and Section 2.2.3.2 and normalized the extraction phase by weights.

3.3.2 Comparison of D-SPME with ion-exchange microgel versus commercial nanotrap performance for the extraction of human plasma for known metabolites

Using reversed-phase LC-MS method, the performance of D-SPME with AAC microgel was compared to that of commercially available nanotrap in human plasma. The extraction was performed as discussed in Section 3.2.4 and 3.2.5. Example results for integrated peak areas of known metabolites are depicted in Figure 3.7 and 3.8. Similar extraction performance of AAC microgel and white nanotrap was observed for metabolites such as choline, tryptophan, biotin, cortisol and thyroxine as shown in Figure 3.7. Lysine and creatinine on the other hand showed higher peak area than AAC microgel. Figure 3.8 shows the results obtained for metabolites that can be detected in negative ESI mode. The performance of AAC microgel and white nanotrap was similar for almost all metabolites except glutamic acid which showed higher signal intensity with AAC microgel and taurocholic acid which had higher peak area in nanotraps. There are differences between plasma and standards results, which were discussed in Figure 3.5, and 3.6. This difference can be due to possible ion suppression (discussed in Section 3.3.6) or because of the reduced possibility of ionic interaction of metabolites with the extraction phase in complex biological sample such as plasma. Ions with high concentration in plasma, such as sodium, may occupy many binding sites, so there will not be enough binding sites to observe ion exchange interaction with our metabolites of interest such as amines or amino acids.

In general, white nanotrap and AAC microgel showed the same behavior in terms of extraction efficiency as expected due to the same ion exchange functionality, whereas blue nanotrap showed poorer extraction efficiency. These results agree well with the results of Table 3.1, when AAC microgel and white nanotrap had roughly the same metabolite coverage and blue nanotrap had lower number of metabolite features.

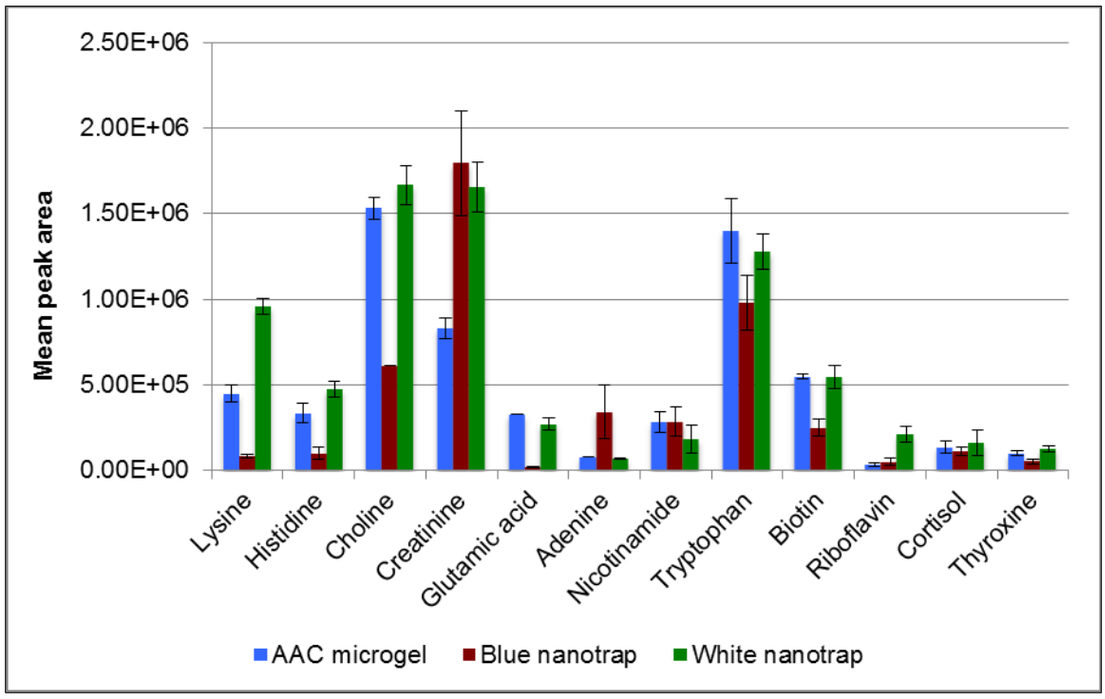

Figure 3.7 Comparison of the performance of D-SPME method with 10% AAC microgel, white and blue nanotrap for extraction of human plasma. Extraction was performed as discussed in Section 3.2.4 and 3.2.5 and the analysis was performed using positive ESI RP LC-MS method. Error bars show standard deviation from the mean.

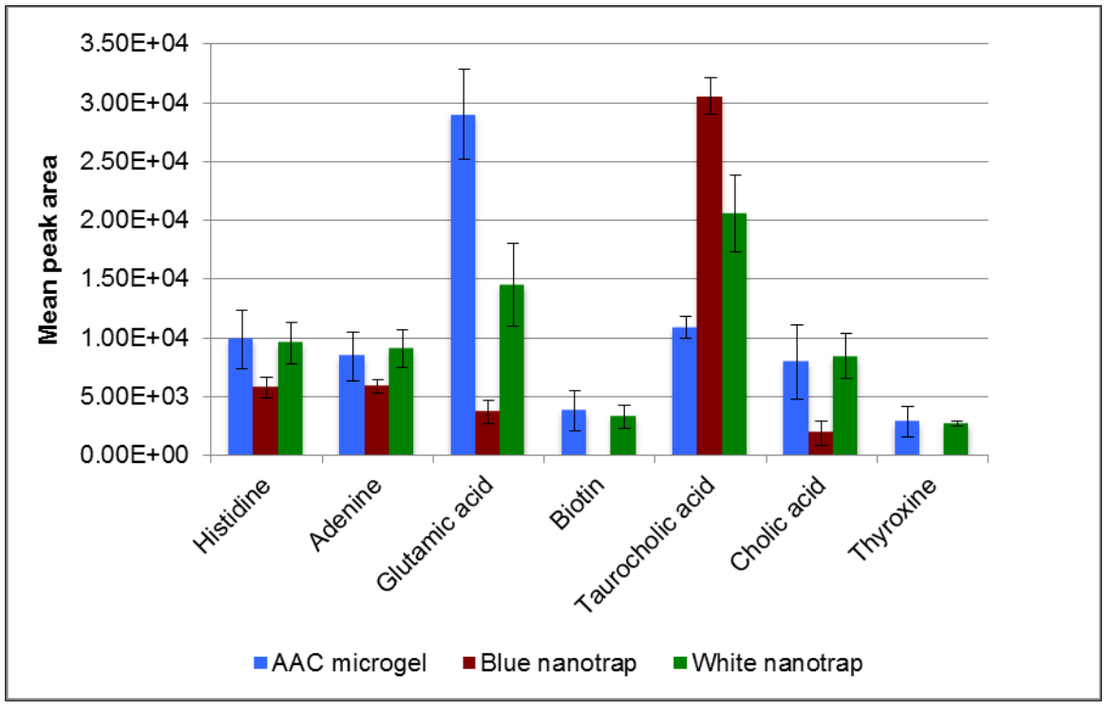

Figure 3.8 Comparison of the performance of D-SPME method with 10% AAC microgel, white and blue nanotrap for extraction of human plasma. Extraction was performed as discussed in Section 3.2.4 and 3.2.5 and the analysis was performed using negative ESI PFP RP LC-MS method.

3.3.3 Comparison of sample preparation methods in human plasma: metabolite coverage

In metabolomics, sample preparation methods are usually first compared according to the number of metabolites or metabolite features detected. MS spectra of a given compound will have more than one m/z signal as a result of isotopes; adduct formation, multiple charging and/or in-source breakdown of the compound. The data processing software used in current work is able to perform deisotoping and adduct matching in order to match all m/z values that belong to the same metabolite and assign neutral accurate mass of the metabolite. Therefore, the numbers shown in Table 3.1 represent putative number of metabolites that were detected by each sample preparation method. In older literature, the number of features reported typically represent number of distinct m/z signals observed without combining signals that belong to the same metabolite, so the number of features is generally higher than number of metabolites observed. This makes method comparisons between different studies extremely difficult due to the differences in instrument performance, acquisition parameters and data processing strategies. However, although absolute numbers of features and/or metabolites detected can vary across studies, the general conclusions about relative metabolite coverage such as the finding that methanol solvent precipitation provides better coverage than C18 SPE hold up very well across different studies.

The main results obtained for each of three methods: methanol solvent precipitation,

extraction using nanotraps and extraction using AAC microgel are summarized in Table 3.1. This table shows the metabolite coverage and median RSD of different sample preparation methods using PFP reversed-phase in both positive and negative ESI-MS methods.

Reversed-phase method with PFP column provides good separation of metabolites with intermediate polarity. In terms of metabolite coverage in positive and negative mode, methanol precipitation methods had higher metabolite coverage than D-SPME as expected with microextraction methods, which provided on the average about 50% less metabolite coverage. The main reasons behind this are: (i) small amounts of some metabolites extracted using microextraction methods may not be detectable by the instrument depending on the instrumental limit of detection for that analyte and (ii) microextraction methods will primarily extract only free metabolite, and no disruption of metabolite binding was performed prior to employing microextraction protocols. On the other hand, the coverage of white nanotrap and AAC microgel that have the same acidic functionality (acrylic acid) is almost similar in positive ESI mode and higher for white nanotrap in negative mode. Comparing AAC microgel and blue nanotrap extractions, the number of observed metabolites was higher in AAC microgel for both positive and negative ESI. The comparison of white versus blue nanotrap showed higher metabolite coverage of white nanotraps.

Table 3.1 Summary of metabolite coverage and median RSD results observed for the analysis of the same pooled human plasma sample prepared using different sample preparation methods (n=5 per method) and analyzed using PFP reversed-phase in both positive and negative LC-ESI-MS.

Methods	**Number of metabolites**		**Median RSD**	
	Positive ESI	**Negative ESI**	**Positive ESI**	**Negative ESI**
AAC microgel	1712	380	50	34
White nanotrap	1836	705	23	19
Blue nanotrap	1151	368	36	34
Methanol with evaporation (PP1)	2555	841	21	48
Methanol with dilution (PP2)	2879	916	20	13

According to the literature, the coverage of D-SPME was consistent with what was observed for fiber SPME in positive ESI (1592 features), but lower than what was observed in negative mode (2005 features). [79] Also Michopolous *et al*.[32] observed 1500 features when they used C18 SPE method, which represented 50% reduction versus methanol precipitation. A recent study compared different human plasma sample

preparation protocols such as protein precipitation with methanol; microextraction by packed solvent (MEPS) and C18 solid phase extraction with and without a previous protein precipitation step for global metabolomics. [89] The number of putative metabolites for MEPS and methanol precipitation with dilution method was 656 and 1808 respectively. In other words, the coverage of MEPS was approximately one third of the coverage observed for methanol. In our D-SPME method, the number of putative metabolites is 1712 with 2879 for methanol precipitation with dilution method. This shows an important improvement of the coverage of metabolites with D-SPME method in current study in comparison to what was seen with MEPS method. In the same study, the authors also compared the number of metabolites that could be observed using SPE after protein precipitation (1250 metabolites). [89]When this step was omitted, only 890 metabolites were observed. By using organic solvent in protein precipitation, the binding between metabolites and protein is disrupted and the total (sum of bound and unbound) metabolite concentration is accessible for extraction, which increased the metabolite coverage. This illustrates that in D-SPME, disruption of protein binding could be used in subsequent studies to further increase metabolite coverage.

PCA shown in Figure 3.9 and 3.10 shows similarity of AAC and white nanotraps as expected for extraction phases that have quite similar chemical composition. The figure also illustrates visually the considerably different selectivity of these methods versus methanol precipitation. QCs all clustered closely together that shows system was stable over the whole analysis.

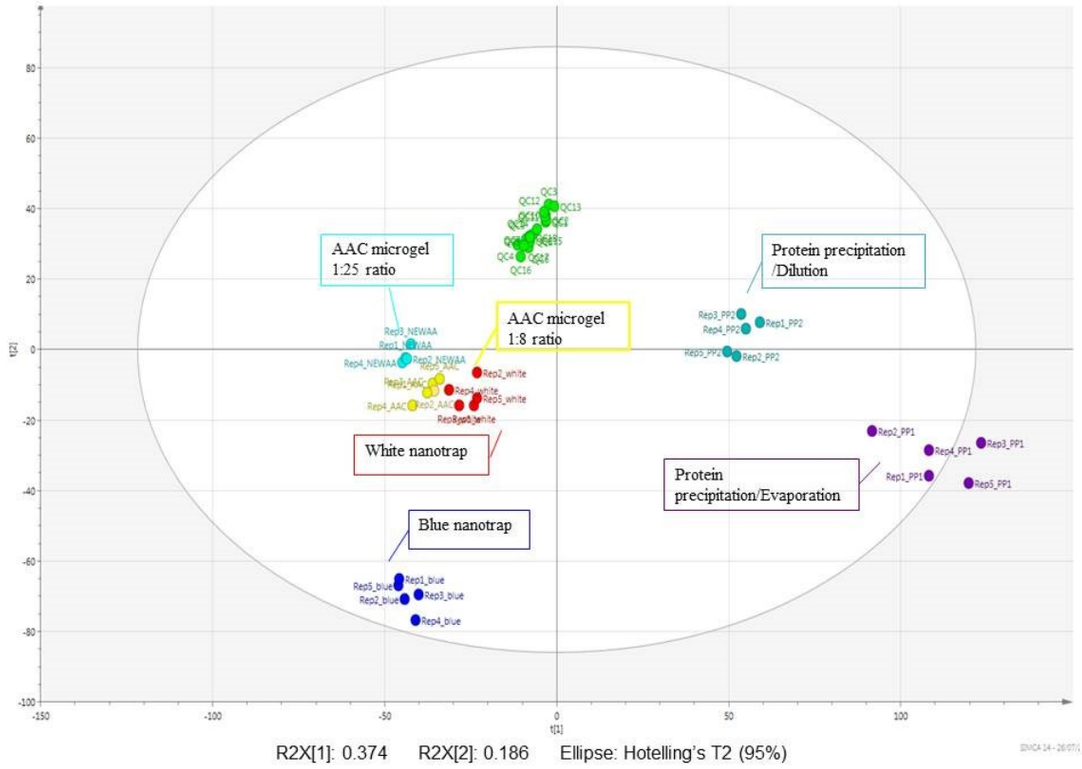

Figure 3.9 Results of PCA comparing protein precipitation method versus blue and white nanorap versus AAC microgel in different ratio (1:8 and 1:25). The samples were analyzed using PFP LC-MS method in positive ESI mode.

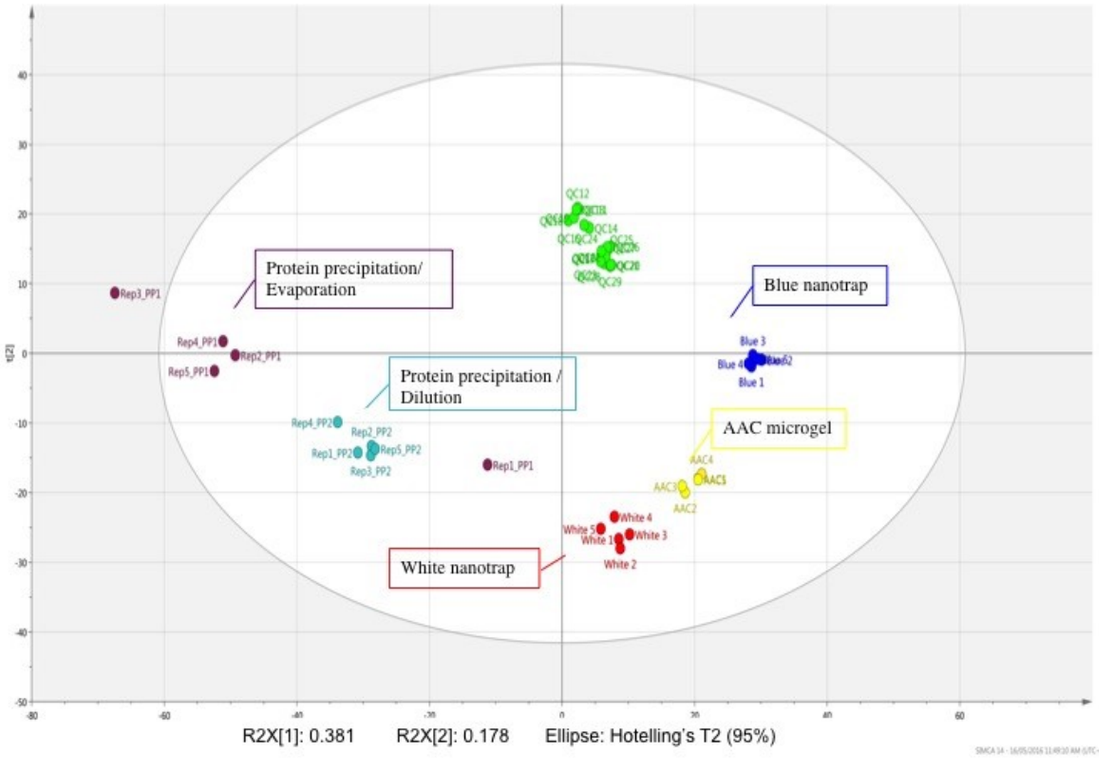

Figure 3.10 Results of PCA comparing protein precipitation method versus blue and white nanotrap versus AAC microgel. The samples were analyzed using PFP LC-MS method in negative ESI mode.

Figure 3.11 shows the pairwise orthogonality of all the methods tested using the same PFP reversed phase LC-MS analysis shown in Table 3.1. Overall metabolite coverage achieved in protein precipitation method was higher than D-SPME method however; new metabolites were detected with D-SPME (568 metabolites) that was not seen in protein precipitation method.

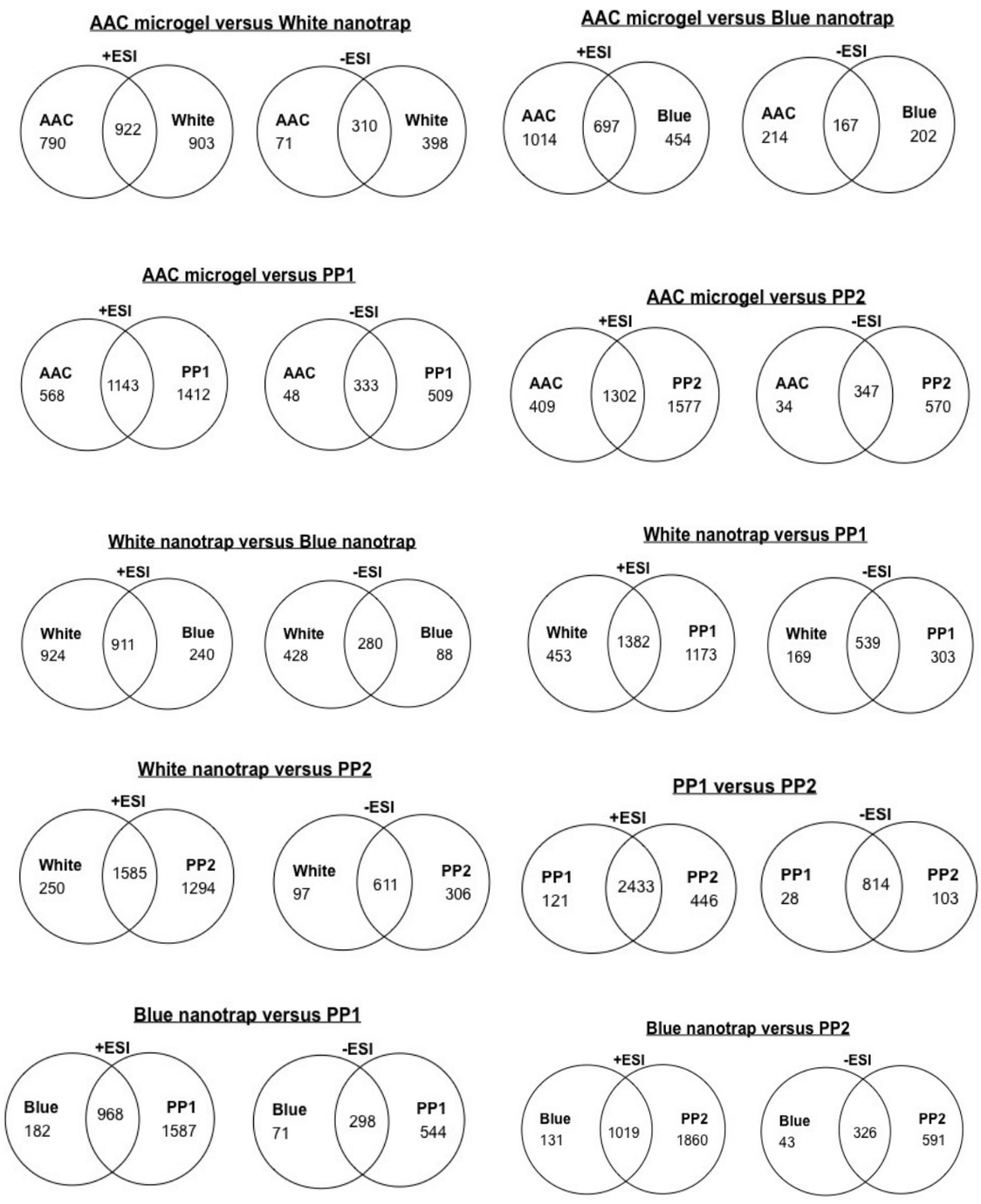

Figure 3.11 Comparison of pairwise method orthogonality using Venn diagrams for five different sample preparation methods: D-SPME with 10% acrylic acid ion exchange functionality microgel (AAC), extraction with white and blue nanotrap, methanol precipitation with evaporation and reconstitution (PP1) and methanol precipitation with dilution (PP2) after PFP LC-MS analysis in both positive and negative ESI.

Figure 3.12 shows the maps of all observed metabolites using five different extraction procedures. In all maps, there is no analytes eluting between 4-8 min, which is due to the time delay due to LC configuration used for the analysis. The standard delay volume from LC pump head to autosampler in Agilent 1100 binary pump is ~1 mL and from the injector needle to MS detector, there is ~0.5 mL delay volume (including internal volume of the column). The method flow rate in current study was 0.3 mL/min, which is optimized for 2.1 mm column diameter and MS ESI detection. Therefore, compounds that are not retained well on the column will be detected in the first 2 minutes (from the needle to MS) and the compounds that elute once the gradient starts will reach the MS with at least 4 minute delay due to the delay volumes as clearly seen in the ion maps.

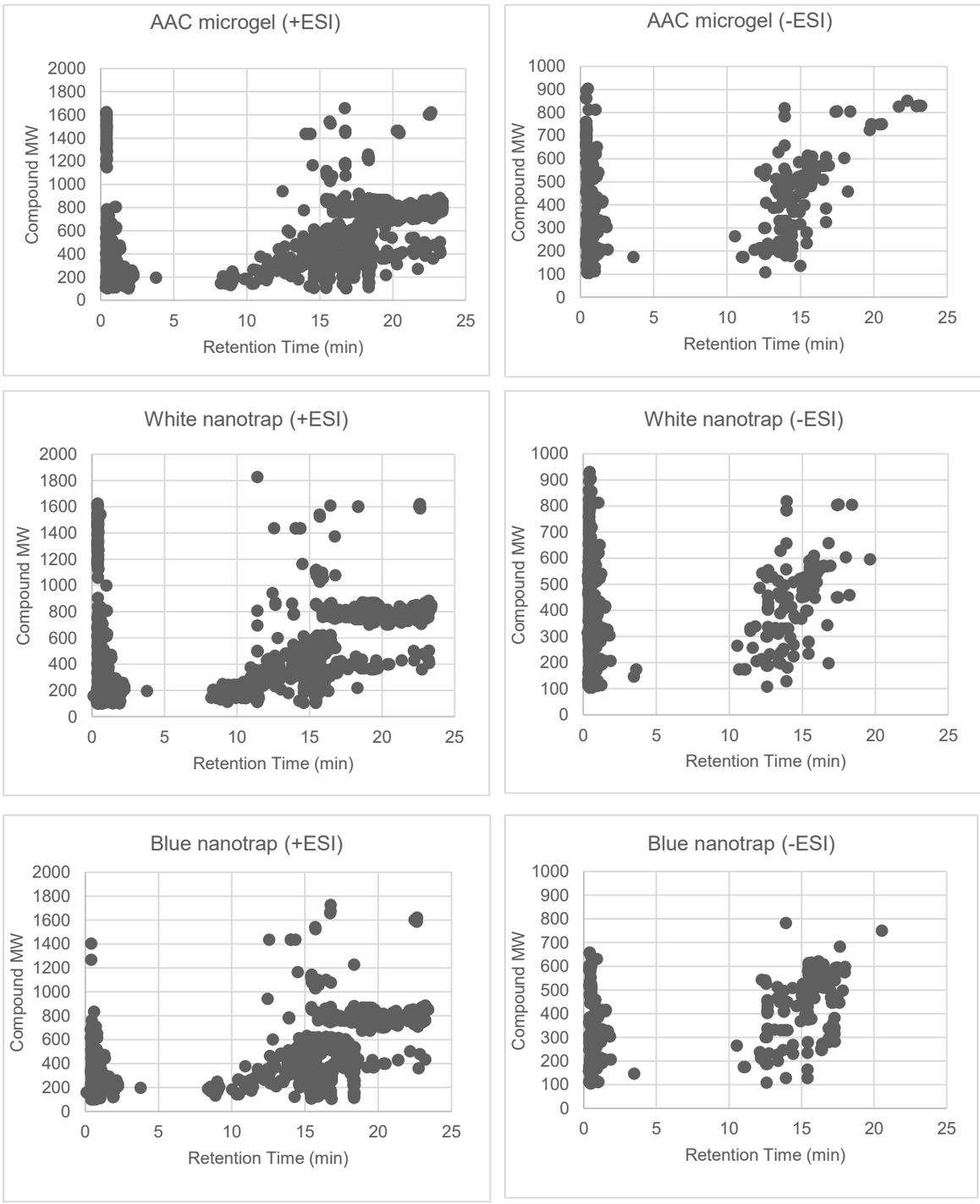

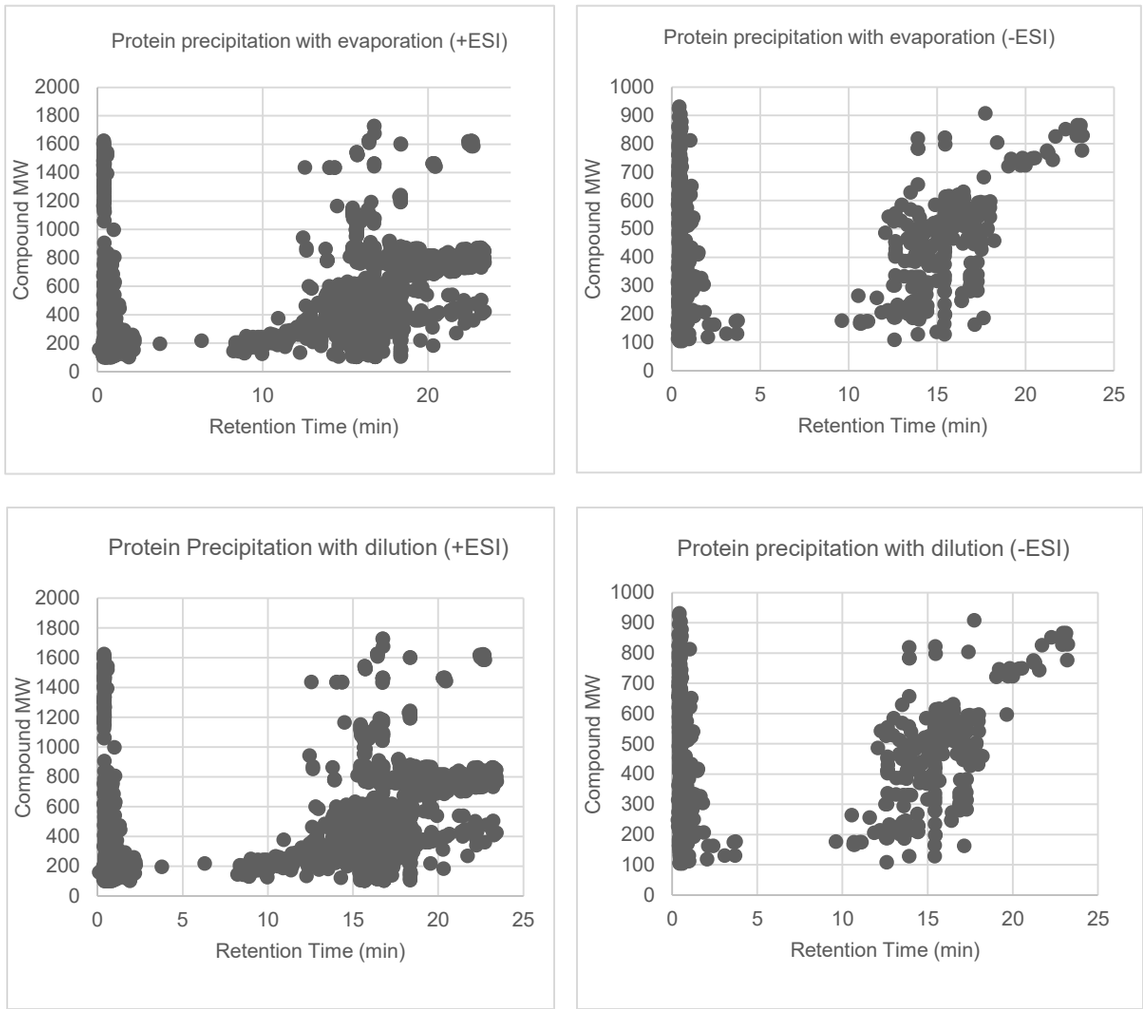

Figure 3.12 Metabolite map (compound molecular weight versus retention time) for human plasma sample prepared using D-SPME method using 10% AAC microgel, white nanotrap, blue nanotrap and methanol precipitation with evaporation/reconstitution (PP1) and dilution (PP2), analyzed using PFP reversed phase LC-MS method in positive and negative ESI.

Figure 3.13 shows unique metabolites observed only by AAC microgel or white nanotrap in both positive and negative ESI mode to illustrate their different selectivity. Overall, AAC microgel enriched hydrophobic compounds while white nanotrap covered more polar compounds, which eluted early. As shown in Table 2.11, the amount extracted for lipids in standard was high in AAC microgel in comparison to the polar compounds; this is in agreement with the results in Figure 3.13 for AAC microgel. The observed difference between AAC and white nanotrap could also be due to poor diffusion of lipids through the aqueous hydrogel network, whereas polar compounds can pass through the network. In other words, lipids may have hard time of diffusing throughout the shell to reach the core due to the difference of nanotrap geometry. In addition, VSA, which is present on the shell of the nanotrap, can change the selectivity towards lipids as well. As shown in negative mode just five hydrophobic metabolites with retention time > 10 min were observed with white nanotrap, which is less than AAC microgel. However, these results need to be interpreted with caution until HILIC and C18 CSH analyses are also performed for confirmation purposes as ion suppression can impact detection of compounds especially when they are eluting in solvent front.

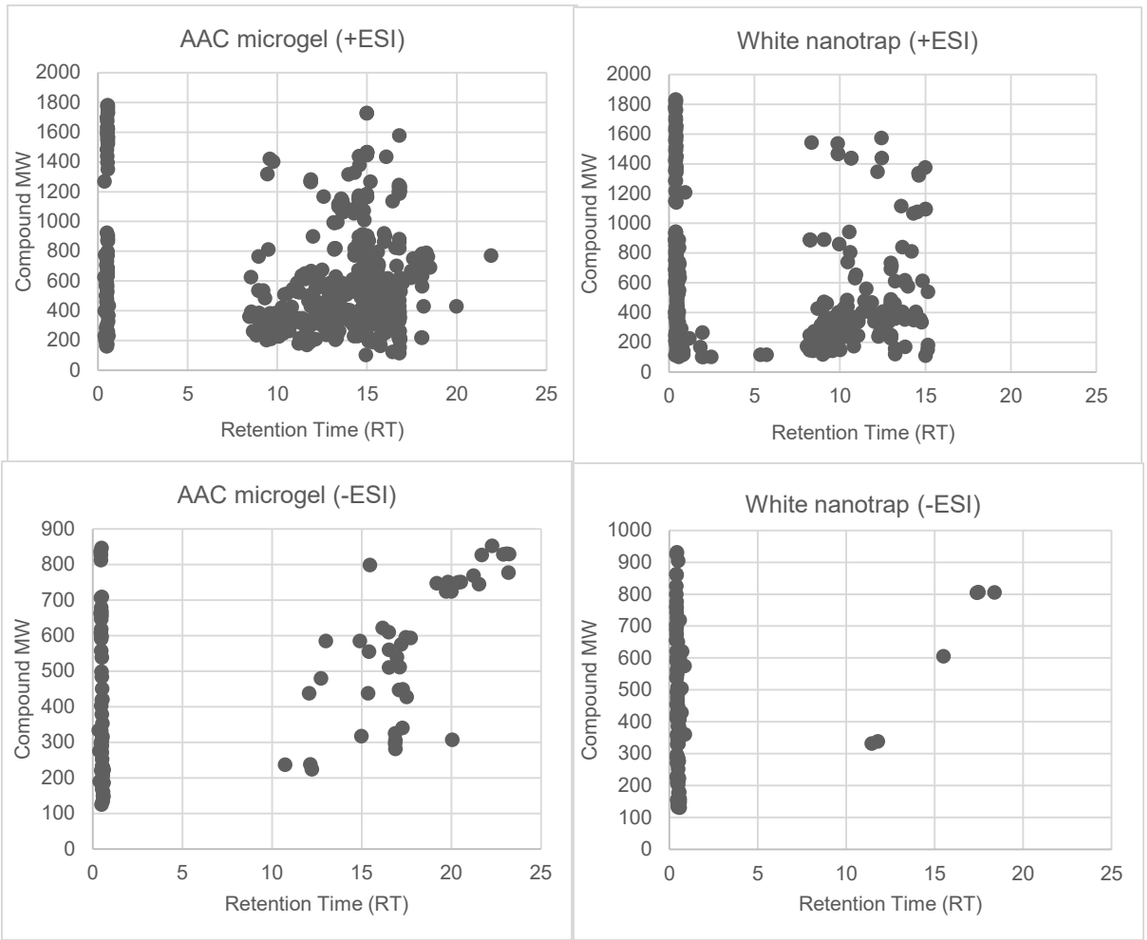

Figure 3.13 Comparison of unique ion maps using D-SPME method with 10% AAC microgel and white nanotraps analyzed in PFP LC-MS method in both positive and negative ESI mode.

Figure 3.14 shows unique metabolites observed only by AAC microgel or methanol precipitation with evaporation/ reconstitution in both positive and negative ESI mode. In general, the coverage of metabolites for methanol precipitation was higher than microgel as expected. However, the metabolites uniquely observed with AAC D-SPME in positive ESI show long retention times on RP, which means they are likely to have high log P values. The improvement in coverage of polar compounds was minor with only few new compounds detected by AAC D-SPME.

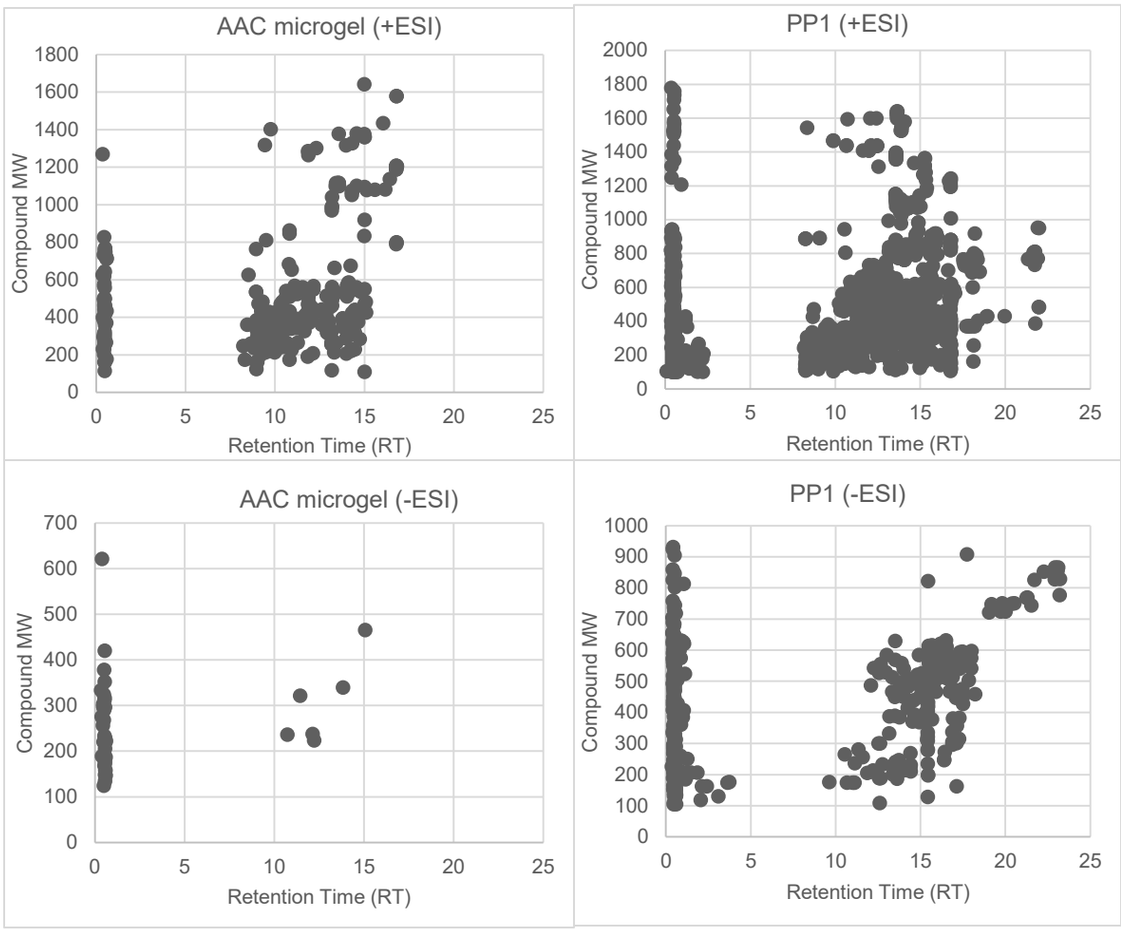

Figure 3.14 Comparison of unique ion maps using D-SPME method with 10% AAC microgel and methanol precipitation with evaporation/reconstitution analyzed in PFP LC-MS method in both positive and negative ESI mode.

3.3.4 Comparison of sample preparation methods in human plasma: precision

Method precision was evaluated both in positive and negative ESI mode. Currently there are no set requirements regarding acceptable precision in global LC-MS metabolomics analysis. By considering that RSD values of 15% are allowed for targeted quantitative analysis by LC-MS/MS, RSD values of up to 30% should be acceptable for global metabolomics considering the semi-quantitative hypothesis-generating nature of this approach. [100]

The initial batch analysis in positive ESI failed because QC pooled sample was not properly injected throughout the sequence. Therefore, the samples were reanalyzed in positive ESI mode with PFP reversed-phased method. Table 3.1 shows the median RSD of different sample preparation methods using PFP reversed-phase in both positive and negative ESI-MS methods. Median RSD is included in Table 3.1 rather than mean RSD, because median is less significantly influenced by presence of outliers.[93]

According to the results of Table 3.1, precision in positive ESI LC-MS was suitable for all methods except for D-SPME with AAC microgel and blue nanotrap. Negative ESI

LC-MS precision as reported by median RSD in Table 3.1 was suitable for all methods except precipitation with evaporation/reconstitution where high variability was observed. This can be clearly seen in PCA in Figure 3.10 where two replicates show huge variability. Considering the positive results did not show the same outliers, it appears likely that those 2 samples are LC-MS outliers. Median RSD for methanol precipitation with dilution in positive mode in current study is 20%. According to the literature, these results are consistent with median RSD for methanol precipitation of 16% [94] and 22%[89] observed in other studies. When comparing precipitation with dilution versus precipitation with evaporation/reconstitution, it is expected to have worse method repeatability when evaporation/reconstitution step is included because there is more manipulation in sample preparation and it may be difficult to fully resolubilize some of the metabolites depending on their chemical nature. However, the RSD values observed are considered too high, and may indicate an issue with resolubilization procedure that requires further investigation.

Poor method precision observed for some peaks detected in D-SPME method can possibly be attributed to low signal intensity. The effect of signal intensity on number of peaks is shown for D-SPME and PP2 method in Figure 3.15. The results show that approximately 40% of peaks had low signal < 10000-peak area in comparison to the PP2 method where only 8% of peaks had such low intensity values. Low intensity observed for D-SPME is attributed to its microextraction format so only small portion of free metabolite concentration is successfully extracted. This low intensity can then be a contributing factor to poor method precision, because low intensity signals can be inconsistently detected either by detector or by data processing software. One potential drawback of PP method is that large intensity peaks could obscure some important low intensity peaks. The effect of signal intensity on median RSD was further investigated as shown in Table 3.2. High intensity peaks, observed in methanol precipitation, had better median RSD of 30% while low intensity peaks in the same samples showed much deteriorated RSD of 60%. However, the results for SPME do not show such pronounced effect (67% RSD versus 58% RSD) indicating that method precision in plasma for D-SPME method requires further optimization and troubleshooting.

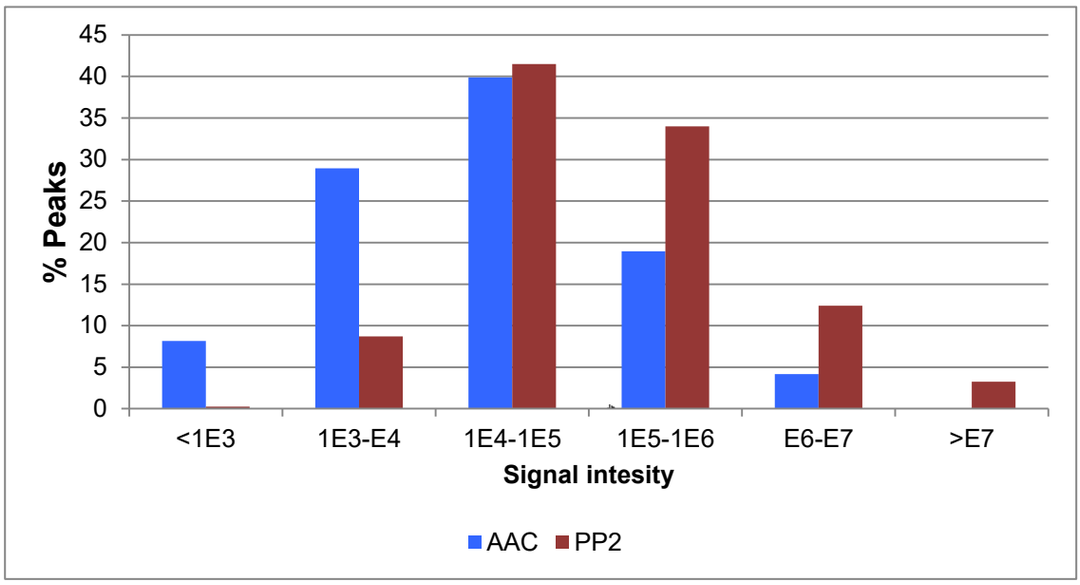

Figure 3.15 Area comparison of D-SPME to protein precipitation method with dilution (PP2)

Table 3.2 Comparison of median RSD for peaks with low and high intensity using AAC microgel and methanol precipitation with dilution in human plasma

Method	Median RSD for peaks that have intensity < E4	Median RSD for peaks that have intensity > E5
AAC microgel	67%	58%
Methanol precipitation with dilution	60%	30%

3.3.5 Comparison of 1:8 versus 1:25 ratio of microgel to sample in terms of metabolite coverage and precision

The results which are shown in Table 3.1 for AAC microgel used non-ideal ratio of microgel to sample (1:8), therefore fresh preparation of 1:25 ratio (optimum ratio of extraction phase to sample according to the Section 2.3.10) and its corresponding blanks were made and analyzed in new positive ESI batch. Table 3.3 shows the results of metabolite coverage and median RSD of D-SPME method using 1:8 and 1:25 ratio of microgel to sample in PFP RP method in positive LC-ESI-MS.

With these new results, 1712 metabolites were observed with D-SPME method for AAC microgel with 1:8 ratio and 1825 metabolites for AAC microgel with 1:25 ratio which is higher than the numbers reported in literature as discussed above. AAC microgel with the ratio of 1:25 had about 113 more metabolites than the ratio of 1:8 and the precision was

significantly improved with median RSD of 29% due to increasing the volume of microgel. Median RSD for fiber SPME was below 20% therefore further troubleshooting of precision is still required. [79]

Table 3.2 Summary of metabolite coverage and median RSD results observed for the analysis of the same pooled human plasma sample in 5 replicates prepared using D-SPME with ratio of 1:8 and 1:25 of microgel to sample and reanalyzed using PFP reversed-phase in positive LC-ESI-MS**.**

Methods	Number of metabolites	Median RSD
	Positive ESI	Positive ESI
AAC microgel Ratio 1:8	1712	50
AAC microgel Ratio 1:25	1825	29

3.3.6 Comparison of D-SPME sample preparation with ion-exchange microgel versus commercial nanotraps: ion suppression

Ion suppression or enhancement caused by co-eluting matrix components is a common problem encountered in LC-MS methods that rely on ESI. As such, it is necessary to evaluate matrix effects during validation of an LC-MS method to ensure that the analytical data will be accurate and reproducible. In metabolomics, the situation is much more complicated, as the analysis of all compounds is desired, therefore great issues with matrix effects can be expected. The degree of matrix effects encountered in a method will depend on various factors that were discussed in detail Section 1.3.1. Among these factors, the choice of sample preparation method will be one of the major contributing factors. Between traditional sample preparation techniques, protein precipitation typically provides the least amount of sample cleanup, which in turn can result in significant matrix effects. From a theoretical point of view, SPME can provide cleaner sample extracts due to the smaller amount of extraction phase employed. In this section, the performance of D-SPME and nanotrap extraction in terms of ion suppression was evaluated. In this experiment, unspiked plasma samples were extracted using commercially available hydrogel (white and blue nanotrap) and microgel with 10% AAC according to methods described in Section 3.2.4 and 3.2.5, which were prepared in 5 replicates. The resulting extracts were spiked with known concentration (200 ng/mL) of the metabolites after extraction. The % of signal was evaluated by the comparison of the signal obtained for this post-extraction spike versus the signal for neat standard prepared directly in the desorption solvent at the same concentration after considering any endogenous compounds as shown in Equation 3.1. If no significant matrix effect is observed, the signal should be between 80-120%. Percent signal >120% represents ion

enhancement for a given metabolite and % signal <80% represents ion suppression for a given metabolite. Thus, if the analyte signal in the matrix is low compared to the signal in desorption solvent or even undetectable, this indicates that the presence of interfering agents is causing the ion suppression.

Equation 3.1

$$\textbf{\textit{\% Signal}} = \frac{(signal\ of\ postextraction\ spike - signal\ of\ unspiked\ \ extraction)}{signal\ in\ desorption\ solvent} \times 100\%$$

The results obtained from this experiment are shown in Figure 3.16. The majority of metabolites showed no ion suppression or enhancement using AAC microgel except for lysine and histidine as expected. These species are polar metabolites, which eluted early in reversed phase chromatography and were not retained well on PFP column. These two compounds were not even detected with white nanotrap due to the severe ion suppression. For example, in thyroxine, which was retained in PFP column, there was no ion suppression for AAC microgel while there is ion suppression for white and blue nanotrap. The normal level of thyroxine is 15.53 ng/mL in plasma according HMDB[119] and 100 ng/mL standard was spiked for ion suppression evaluation. It means that even 6-fold increase in thyroxine could not be observed for nanotraps for this compound. 6-fold increases in concentration are not very common in plasma, and even 50% change in metabolite concentration can have significant clinical effect(s) depending on the metabolite in question and its biological role. This example illustrates an important shortcoming of current metabolomics studies and that more attention should be paid to minimizing ion suppression. In negative mode, for some compounds such as riboflavin, adenine and biotin ion enhancement was observed as it is shown in Figure 3.17. This could possibly be a solubility effect; whereby extracted plasma is better able to solubilize these compounds than desorption solvent. This may also arise due to the difference in droplet formation during electrospray process due to the different surface tension. As it was shown in Figure 3.16 and 3.17 there is also discrepancy in results between positive and negative ESI for adenine because of the ion suppression and co-eluting interferences that can be ionized in positive ESI better than negative mode. Overall it indicates that D-SPME method using 10% AAC performed well in terms of ion suppression and outperformed extraction using both white and blue nanotraps. Methanol precipitation was not compared in this experiment as other group members have performed this experiment and observed even more severe suppression than what is seen for nanotraps here [Sitnikov *et al*., manuscript submitted].

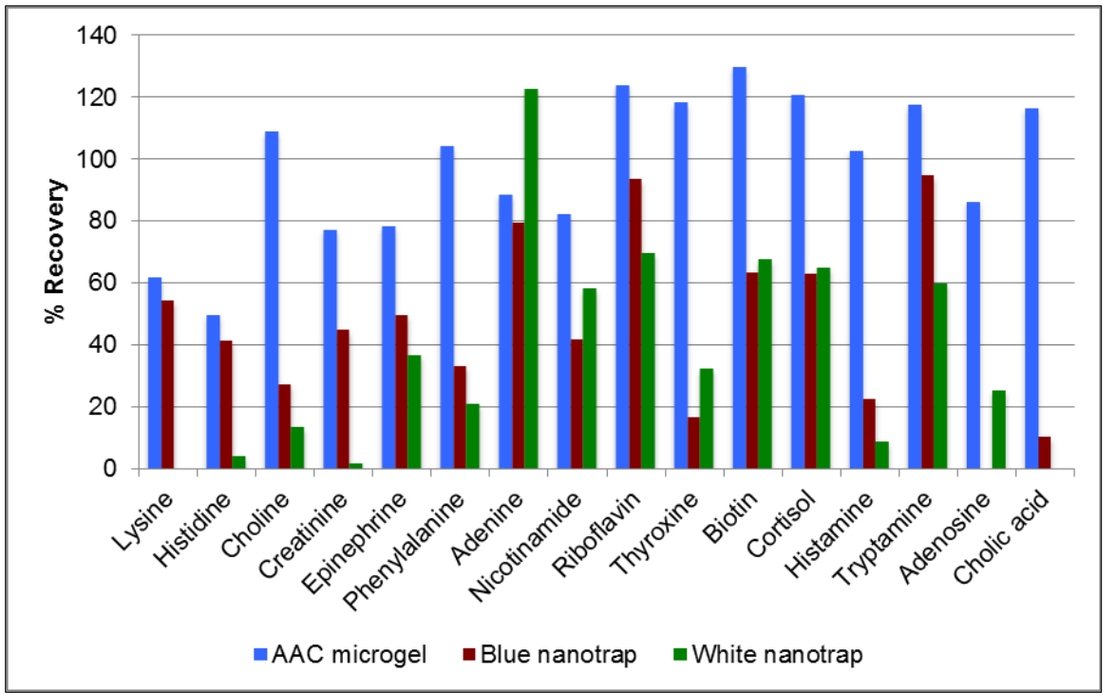

Figure 3.16 Evaluation of ion suppression comparing D-SPME using blue nanotrap versus white nanotrap versus AAC microgel. The samples were spiked with known concentration (200 ng/mL) of the metabolites after extraction and analyzed using reversed phase PFP LC-MS analysis in positive ESI with Orbitrap mass spectrometry.

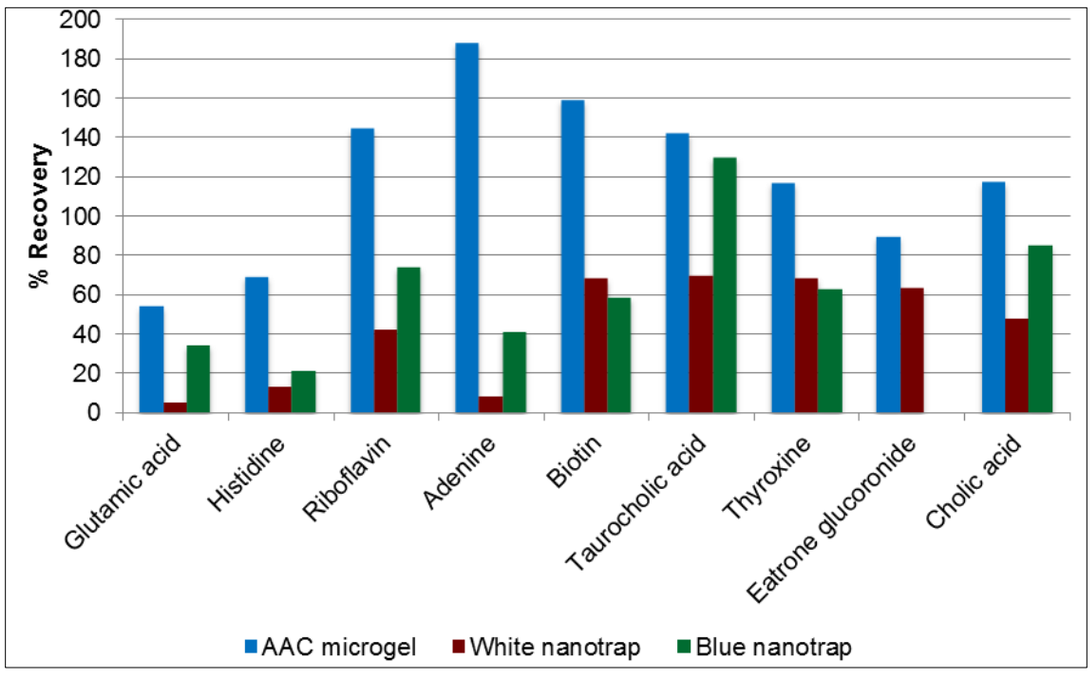

Figure 3.17 Evaluation of ion suppression with D-SPME of different hydrogels; commercial nanotrap and ion-exchange microgel. The samples were spiked with known concentration (200 ng/mL) of the metabolites after extraction and analyzed using reversed phase PFP LC-MS analysis in negative ESI with Orbitrap mass spectrometry.

3.4 Conclusions

Overall, the results are promising in comparison to the literature as discussed in this Chapter. In terms of metabolite coverage in plasma, AAC microgel performed as well as white nanotrap and better than blue nanotrap. Overall metabolite coverage achieved in protein precipitation method was higher than D-SPME method; new metabolites were detected with D-SPME (568 metabolites) that was not observed in protein precipitation method.

In terms of precision, microextraction with both AAC microgel with the ratio of 1:8 and nanotraps had worse precision than methanol however; the precision was significantly improved with fresh preparation of AAC microgel with the ratio of 1:25 with median RSD of 29%. On the other hand, precision of precipitation with evaporation/reconstitution in negative mode had high variability due to the instrumental error, as the precision of this method was reasonable in positive mode. In terms of ion suppression, AAC microgel performed well and better than nanotraps and methanol precipitation in human plasma.

The results from plasma were different than standards and it could be due to limited number of ion-exchange binding sites to interact with analytes, which would cause a drop in ion-exchange contribution. For example, Na^{+}, Ca^{2+} and Mg^{2+} are positive ions that are present in plasma with high concentration of 142600, 2420 and 833 μM respectively. HCO_3^{-} and Cl^{-} are major negative ions, which are present in plasma with high concentration of 24900 and 103700 μM respectively. The concentration of creatinine in plasma is 82.6 μM, which is much smaller in comparison to positive ions in plasma. Similarly, the concentration of taurocholic acid in plasma is 0.38 μM which again is much lower than the concentration of smaller anions in plasma, therefore these compounds will have slight chance to have ion-exchange interaction in presence of high concentration of ions in plasma.[119] There are some strategies that can be used to evaluate the contribution of ion-exchange capacity. By using particular ions that bind strongly to the extraction phase, total ion exchange capacity can be evaluated.

In future, the same samples must be analyzed with HILIC and CSH C18 RP methods to further evaluate polar and lipid coverage of these new extraction materials and better characterize their selectivity in plasma.

Chapter 4

Conclusions and future work

4.1 Conclusions

In this work, for the first time, systematic optimization across metabolite classes with D-SPME sample preparation for hydrogel materials was investigated. Solid phase microextraction with fiber format was previously investigated in global metabolomics, however for the first time dispersive format of solid phase microextraction was used in this study. This kind of format is expected to provide higher surface area to increase the extraction efficiency and reduce equilibration time due to the increased contact of analytes and the support. It is also a single use format therefore there is no carry over issue to consider. A general problem with the applications of SPME in metabolomics is the unavailability of commercial SPME coatings for polar and ionic analytes so that this study attempted to improve the detection of polar and ionic analytes with using functionalized hydrogel materials.

Hydrogel with ion exchange functionality (AAC, VAC, APMAH microgel) has not been previously used in global metabolomics. There is one study that used poly (N-isopropylacrylamide-acrylic acid) hydrogel particles for removal of abundant plasma proteins, prior to proteome analysis.[77] In another study, pNIPAm-based thermo-responsive hydrogel with different co-monomer was used as the stationary phase for SPE for drug analysis. They concluded that the separation of acidic and basic drugs can be performed due to the electrostatic interaction.[120] In another study, pNIPAm-based hydrogel with ion-exchange groups could separate organic acids and amino acids via hydrophobic interaction and electrostatic interaction by controlling the temperature and pH.[121] NIPAAm, hydrogel cross-linked with 3,4-Ethylenedioxy-N-methylamphetamine (EDMA) was investigated for in-tube solid phase microextraction. Extraction efficiency increased with wide range of pH and through hydrophobic interaction. [124]The effect of cross-linked poly (N-isopropylacrylamide) hydrogel on steroid extraction was also investigated. The results showed that changing temperature affects the separation of steroids with different hydrophobicity. For instance, the separation of hydrophobic steroids was achieved at lower temperature.[122] In the other study, the extraction of fluvoxamine using thermo sensitive poly [N-isopropylacrylamide] (pIPAAm)-based nano-particles was evaluated in terms of temperature, pH, and contact time. It was found that at a temperature higher than the lower critical solution temperature of the polymer, more fluvoxamine would be released.[123] The adsorption of amino acids on pNIPA microgels was also studied at different temperature (25 °C and 37 °C). The binding for all

amino acids was improved by increasing temperature to 37 °C. The binding of hydrophobic amino acids was controlled via hydrophobic interactions and hydrogen bonding dominated the binding of the hydrophilic amino acids.[125] Therefore the effect of temperature should be investigated in current study in order to improve the binding.

The optimized D-SPME was found to perform well for acidic and basic metabolites and for lipid metabolites across all lipid classes. Acidic metabolites (such as organic acids) are extracted well using N-3-aminopropyl methacrylamide hydrochloride (APMAH) functionalized microgel, while basic metabolites (such as amines) are extracted better using vinyl acetate (VAC) and acrylic acid (AAC) functionalized microgels.

Sequential extraction of metabolites using solvents with different polarity provides the benefit of desorbing polar metabolites while most phospholipids remain in the sorbent. This may increase the metabolite coverage and decrease potential for ion suppression. The obtained D-SPME extract was compatible for direct injection using both HILIC and RP methods. The step of evaporation/reconstitution is completely avoided in the current workflow in order to avoid possible issues with metabolite solubility in a given reconstitution solvent.

Commercial core-shell nanoparticles (CERES Nanotrap) functionalized with acrylic acid (white nanotrap) or Cibachron blue cores (blue nanotrap) were also compared with microgel because AAC microgel and white nanotrap had the same acrylic acid functionality. These commercially available nanotraps are expensive and overall time of the final D-SPME sample preparation approach using nanotrap was 21 hours (including overnight incubation) whereas using ion-exchange microgel the experimental time was 4 hours. Therefore, developed D-SPME protocol using microgels can be an inexpensive alternative to expensive and time consuming nanotrap protocol for global metabolomics with plasma.

Ion suppression is a common phenomenon in LC-MS analysis of complex samples and can be effectively eliminated/minimized by an appropriate sample preparation method. Because of simplicity of protein precipitation, this method remains a popular technique in plasma analysis but is highly susceptible to severe matrix effects. In this thesis, it was clearly shown that D-SPME sample preparation could minimize ion suppression issues, even from samples in complex matrix and thus improve data quality of resulting metabolomics studies. In comparison to the traditional methods, SPME had lower MS signal intensities due to the non-exhaustive nature. This helped to reduce ion suppression and improved quantitation and data quality. Overall AAC microgel performed better than nanotrap and methanol precipitation in terms of ion suppression

In terms of metabolite coverage, hydrogel microparticles performed as well as white nanotrap and better than blue nanotraps. Metabolite coverage achieved in D-SPME method was lower than protein precipitation method as expected, whereas new metabolites (568 metabolites) were detected with D-SPME that were not observed in methanol precipitation method. One important aspect of SPME is that the amount extracted is proportional to free concentration under conditions employed for typical plasma extraction, where only small amount of free analyte concentration is extracted Consequently, D-SPME method could be potentially useful in biomarker discovery due to providing a useful readout of biologically active concentration of metabolites, which would be highly complementary information to total metabolite concentration obtained by solvent precipitation methods. In addition, as shown in this thesis, D-SPME considerably reduces matrix effects so it can provide much better quality of data in metabolomics studies.

.

4.2 Future work

For future plan, one aspect is to investigate the identification of new metabolites whose detection was improved by D-SPME and not by other methods. A second important aspect to address is to further improve method precision for D-SPME. There are some parameters that need to be investigated. First, internal standard mixtures that covers all different kinds of metabolite such as cholic acid-2, 2,4,4-d_4, histamine d_4, phenylalanine-d_5, L-thyroxine-^{13}C6, cortisol-d_4 should be added at the beginning of the extraction to correct for slight differences in the amount of extraction phase and human error. Second, in the optimized protocol 20% methanol was used for the wash step. It is required to use the solvent that is strong enough to remove impurities, but weak enough to leave the compounds of interest bound. It was observed that 20% methanol is not weak enough to leave polar compounds behind but it is good for lipids therefore, decreasing the amount of organic solvent could help for polar compounds. Furthermore, increasing the amount injected for LC-MS analysis even further either by increasing the amount of hydrogel during extraction or more simply by increasing injection volume or decreasing further the volume of desorption solvent could also help further improve the precision. Testing the effect of temperature and tighter control of temperature throughout all steps should also be investigated. Additionally, a detailed investigation of evaporation and reconstitution conditions can also help to improve precision for all the methods that use this step.

UPLC is a useful tool for LC-MS-based metabolomics since more features will be detected due to significant improvements in detection limits, reduction in total analysis time, and increased resolution. Therefore, for future applications using UPLC instead of HPLC would be beneficial and could improve precision and metabolite coverage without increasing the concentration of SPME extracts.[56] It is also important to remember that electrospray LC-MS is simply one suitable ionization platform for global metabolomics; other platforms and ionization methods can be added to achieve comprehensive metabolite coverage.

In this thesis D-SPME was optimized for different kinds of ion-exchange functionalized hydrogels (AAC, VAC and APMAH) with metabolite standard mixtures however in Chapter 3 D-SPME only AAC microgel was compared to methanol precipitation in a complex sample such as plasma to keep batch size to ~100 samples, which is preferred length for metabolomics batches. Hence, for the future plan APMAH and VAC microgel performance also needs to be evaluated against methanol precipitation in plasma in terms of metabolite coverage, ion suppression, precision and recovery. Another interesting aspect for future studies is to test other nanoparticles such as carbon nanotubes (single-wall, multi-wall and functionalized carbon nanotubes), polystyrene-divinyl benzene

nanoparticles and titanium dioxide nanocomposite to investigate if they can increase the numbers of metabolites.

The use of complementary HILIC and reverse phase methods, as well as positive and negative ionization modes will increase metabolite coverage. In this study, with reversed-phase with PFP column 568 new metabolites were detected versus methanol precipitation for intermediate polarity metabolome, which is promising. On the other hand, reversed-phase with CSH-C18 column and HILIC method as optimized in Section 2.2.4.2 and 2.2.4.4 still need to be evaluated to investigate the performance for polar and lipid metabolites.

The results of this thesis clearly showed that dispersive solid phase microextraction using hydrogels with ion exchange functionality can be a very useful sample preparation method for global metabolomic studies in order to decrease ion suppression and to improve quantitative information of the collected metabolomics data but, further studies are required to characterize unique metabolites detected by D-SPME.

.

References

1. Goodacre, R., Vaidyanathan, S., Dunn, W. B., Harrigan, G. G. & Kell, D. B. Metabolomics by numbers: acquiring and understanding global metabolite data. *Trends Biotechnol.* **22,** 245–252 (2004).

2. Jewison, T., Knox, C., Neveu, V., Djoumbou, Y. YMDB: The yeast metabolome database. *Nucleic Acids Res.* **40,** 815–820 (2012).

3. Wishart, D. S., Jewison, T., Guo, A.C., Wilson, M., Knox, C. HMDB: The human metabolome database in 2013. *Nucleic Acids Res.* **41,** 801–807 (2013).

4. Theodoridis, G.A., Gika, H. G., Want, E. J. & Wilson, I. D. Liquid chromatography–mass spectrometry based global metabolite profiling: A review. *Anal. Chim. Acta.* **711,** 7–16 (2012).

5. Fiehn, O. Metabolomics - The link between genotypes and phenotypes. *Plant Mol. Biol.* **48,** 155–171 (2002).

6. Dodson, R.M. Separation of steroid by gas chromatography. *Ghromatography, G.A.S.* 5–6 (1960).

7. Pauling, L., Robinson, a B., Teranishi, R. & Cary, P. Quantitative analysis of urine vapor and breath by gas-liquid partition chromatography. *Proc. Natl. Acad. Sci. U. S. A.* **68,** 2374–2376 (1971).

8. Dunn, W. B., Bailey, N. J. C. & Johnson, H. E. Measuring the metabolome: current analytical technologies. *Analyst.* **130,** 606–625 (2005).

9. Büscher, J. M., Czernik, D., Ewald, J. C., Sauer, U. & Zamboni, N. Cross-Platform comparison of methods for quantitative metabolomics of primary metabolism. *Anal Chem.* **81,** 2135–43 (2009).

10. Nicholson, J. K.; Wilson, I. D. Understanding 'global' systems biology: metabonomics and the continuum of metabolism. *Nat. Rev. Drug Discov.* **2,** 668–676 (2003).

11. Nicholson, J. K., Lindon, J. C. & Holmes, E. Understanding the metabolic responses of living systems to pathophysiological stimuli via multivariate statistical analysis of biological NMR spectroscopic data. *Xenobiotica.* **29,** 1181–1189 (1999).

12. Theodoridis, G., Gika, H. G. & Wilson, I. D. LC-MS-based methodology for global

metabolite profiling in metabonomics/metabolomics. *TrAC Trends Anal. Chem.* **27,** 251–260 (2008).

13. Allwood, J. W., Ellis, D. I. & Goodacre, R. Metabolomic technologies and their application to the study of plants and plant–host interactions. *Physiol. Plant.***132,** 117-135 (2008).

14. Fernie, A. R. & Schauer, N. Metabolomics-assisted breeding: a viable option for crop improvement. *Trends Genet.* **25,** 39–48 (2009).

15. Bundy, J. G., Davey, M. P. & Viant, M. R. A critical review and future perspectives. *Metabolomics.* **5,** 3–21 (2009).

16. Lin, C. Y., Viant, M. R. & Tjeerdema, R. S. Methodologies and applications in the environmental sciences. *J. Pestic. Sci.* **31,** 245–251 (2006).

17. Ryan, D. & Robards, K. The greatest omics of them all *Anal. Chem.* **78,** 7954–7958 (2006).

18. Monteiro, M. S., Carvalho, M., Bastos, M. L. & Guedes de Pinho, P. Metabolomics analysis for biomarker discovery: advances and challenges. *Curr. Med. Chem.* **20,** 257–71 (2013).

19. Sang, H. L. Woo, H. M., Jung, B. H., Lee, J.. Metabolomic approach to evaluate the toxicological effects of nonylphenol with rat urine. *Anal. Chem.* **79,** 6102–6110 (2007).

20. Orešič, M. Metabolomics, a novel tool for studies of nutrition, metabolism and lipid dysfunction. *Nutr. Metab. Cardiovasc. Dis.* **19,** 816–824 (2009).

21. Rezzi, S., Ramadan, Z., Fay, L. B. & Kochhar, S. Applications and perspectives. *J. Proteome Res.* **6,** 513–525 (2007).

22. Robertson, D. G. Metabonomics in toxicology. *Toxicol. Sci.* **85,** 809–822 (2005).

23. de Gouw, J. & Warneke, C. Measurements of volatile organic compounds in the earth's atmosphere using proton-transfer-reaction mass spectrometry. *Mass Spectrom. Rev.* **26,** 223–257 (2007).

24. Zhou, B., Xiao, J. F., Tuli, L. & Ressom, H. W. LC-MS-based metabolomics. *Mol. BioSyst.* **8,** 470–481 (2012).

25. Zivkovic, A. M., Michelle, M., Nguyen. U.T., Davis, R.. Effects of sample

handling and storage on quantitative lipid analysis in human serum. *Metabolomics.* **5,** 507–516 (2009).

26. Bruce, S. J., Tavazzi, I., Rezzi, S., Kochhar, S. & Guy, P. a. Investigation of Human Blood Plasma Sample Preparation for Performing Metabolomics Using Ultrahigh Performance Liquid Chromatography / Mass Spectrometry. *Anal. Chem.* **81,** 3285–3296 (2009).

27. Zelena, E. *et al.* Development of a robust and repeatable UPLC-MS method for the long-term metabolomic study of human serum. *Anal. Chem.* **81,** 1357–1364 (2009).

28. Pham-Tuan, H., Kaskavelis, L., Daykin, C. A. & Janssen, H.-G. Method development in high-performance liquid chromatography for high-throughput profiling and metabonomic studies of biofluid samples. *J. Chromatogr. B.* **789,** 283–301 (2003).

29. Want, E. J., Maille, G., Smith, C. A., Brandon, T. R., Uritboonathai, W. Solvent-dependent metabolite distribution, clustering, and protein extraction for serum profiling with mass spectrometry. *Anal. Chem.* **78,** 743–752 (2006).

30. Idborg-Björkman, H., Edlund, P. O., Kvalheim, O. M., Schuppe-Koistinen, I. & Jacobsson, S. P. Screening of biomarkers in rat urine using LC/electrospray ionization-MS and two-way data analysis. *Anal. Chem.* **75,** 4784–4792 (2003).

31. Huck, C. W. & Bonn, G. K. Recent developments in polymer-based sorbents for solid-phase extraction. *J. Chromatogr. A.* **885,** 51–72 (2000).

32. Michopoulos, F., Lai, L., Gika, H., Theodoridis, G. & Wilson, I. UPLC MS based analysis of human plasma for metabonomics using solvent precipitation or solid phase extraction. *J. Proteome Res.* **8,** 2114–2121 (2009).

33. Calderón-Santiago, M., Priego-Capote, F. & de Castro, M. D. L. Enhancing detection coverage in untargeted metabolomics analysis by solid-phase extraction on-line coupled to LC-MS/MS. *Electrophoresis.* **36,** 2179–2187 (2015).

34. Gika, H. G., Theodoridis, G. a. & Wilson, I. D. Hydrophilic interaction and reversed-phase ultra-performance liquid chromatography TOF-MS for metabonomic analysis of Zucker rat urine. *J. Sep. Sci.* **31,** 1598–1608 (2008).

35. Griffiths, W. J. & Wang, Y. Mass spectrometry: from proteomics to metabolomics and lipidomics. *Chem. Soc. Rev.* **38,** 1882 (2009).

36. Souverain, S., Rudaz, S. & Veuthey, J.-L. Matrix effect in LC-ESI-MS and LC-APCI-MS with off-line and on-line extraction procedures. *J. Chromatogr. A.* **1058,** 61–66 (2004).

37. Bowen, B. P. & Northen, T. R. Metabolomics and Metabolite Atlases. *J. Am. Soc. Mass Spectrom.* **21,** 1471–1476 (2010).

38. Jede, R., Peters, H. Quantitative depth profile and bulk analysis with high dynamic range by electron gas sputtered neutral mass spectrometry. J. Vac. Sci. Technol. **6**, 2271-2276 (1988)

39. Fardet, A., Liorach, R., Martin, J., Besson., C., Lyan, B. A Liquid Chromatography Quadrupole Time-of-Flight (LC Q-TOF) based Metabolomic Approach Reveals New Metabolic Effects of Catechin in Rats Fed High-Fat Diets. *J. Proteome Res.* **7,** 2388–2398 (2008).

40. Zubarev, R. a. & Makarov, A. Orbitrap mass spectrometry. *Anal. Chem.* **85,** 5288–5296 (2013).

41. Hu, Q. Noll, R. J., Li, H., Markarov, A., Hardman, M., Cooks, R. G.. The Orbitrap: A new mass spectrometer. *J. Mass Spectrom.* **40,** 430–443 (2005).

42. Schwudke, D., Schuhmann, K., Herzog, R., Bornstein, S. R. & Shevchenko, A. Shotgun lipidomics on high resolution mass spectrometers. *Cold Spring Harb. Perspect. Biol.* **3,** 1–13 (2011).

43. Alonso, A., Marsal, S. & Julià, A. Analytical methods in untargeted metabolomics: state of the art in 2015. *Front. Bioeng. Biotechnol.* **3,** 23 (2015).

44. King, R., Bonfiglio, R., Fernandez-Metzler, C., Miller-Stein, C. & Olah, T. Mechanistic investigation of ionization suppression in electrospray ionization. *J. Am. Soc. Mass Spectrom.* **11,** 942–950 (2000).

45. Ikonomou, M. G., Blades, A. T. & Kebarle, P. Investigations of the Electrospray Interface for Liquid ChromatographyIMass Spectrometry. *Anal. Chem.* **62,** 957–967 (1990).

46. Kebarle, P. & Tang, L. From ions in solution to ions in the gas phase. *Society.* **65,** 972-986 (1993).

47. Annesley, T. M. Ion suppression in mass spectrometry. *Clin. Chem.* **49,** 1041–1044 (2003).

48. Antignac, J. P., Wasch, K., Monteau, F., Brabander, H. D., Andre, F., Bizec, B. L. The ion suppression phenomenon in liquid chromatography-mass spectrometry and its consequences in the field of residue analysis. *Anal. Chim. Acta* .**529,** 129–136 (2005).

49. Holčapek, M., Volna, K., Kolarova, J. L., Lemer, K., Exner. Effects of ion-pairing reagents on the electrospray signal suppression of sulphonated dyes and intermediates. *J. Mass Spectrom.* **39,** 43–50 (2004).

50. Nelson, M. D. & Dolan, J. W. Ion Suppression in LC–MS–MS — A Case Study. *Lcgc North Am.* **20,** 25–32 (2002).

51. Souverain, S., Rudaz, S. & Veuthey, J.-L. Protein precipitation for the analysis of a drug cocktail in plasma by LC–ESI–MS. *J. Pharm. Biomed. Anal.* **35,** 913–920 (2004).

52. Matuszewski, B. K., Constanzer, M. L. & Chavez-Eng, C. M. Matrix effect in quantitative LC/MS/MS analyses of biological fluids: a method for determination of finasteride in human plasma at picogram per milliliter concentrations. *Anal. Chem.* **70,** 882–9 (1998).

53. Yang, Y., Cruickshank, C., Armstong, M., Mahaffey, S., Reisdorph, R., Resdrorph, N. New sample preparation approach for mass spectrometry-based profiling of plasma results in improved coverage of metabolome. *J. Chromatogr. A.* **1300,** 217–226 (2013).

54. Fauland, A., Trotzmuller, m., Ebret, A., Kofeler, H., Guo, X., Lankmayr, e. An improved SPE method for fractionation and identification of phospholipids. *J. Sep. Sci.* **36,** 744–751 (2013).

55. Mostovenko, E., Hassan, C., Rattke, J., Deeider, A. M., Palmblad, M. Comparison of peptide and protein fractionation methods in proteomics. *EuPA Open Proteomics.* **1,** 30–37 (2013).

56. Churchwell, M. I., Twaddle, N. C., Meeker, L. R. & Doerge, D. R. Improving LC-MS sensitivity through increases in chromatographic performance: Comparisons of UPLC-ES/MS/MS to HPLC-ES/MS/MS. *J. Chromatogr. B Anal. Technol. Biomed. Life Sci.* **825,** 134–143 (2005).

57. Want, E. J., Nordstrm, A., Morita, H., Siuzdak, G. & Nordstro, A. From Exogenous to Endogenous : The Inevitable Imprint of Mass Spectrometry in Metabolomics. J. Proteome Res. **6**, 459–468 (2007).

58. Grebe, S. K. G. & Singh, R. J. LC-MS / MS in the Clinical Laboratory – Where to From Here. *Clin. Biochem. Rev.* **32,** 5–31 (2011).

59. Vuckovic, D. Current trends and challenges in sample preparation for global metabolomics using liquid chromatography–mass spectrometry. *Anal. Bioanal. Chem.* **403,** 1523–1548 (2012).

60. Arthur, C. L. & Pawliszyn, J. Solid phase microextraction with thermal desorption using fused silica optical fibers. *Anal. Chem.* **62,** 2145–2148 (1990).

61. Pawliszyn, J. *Theory of Solid-Phase Microextraction*. *Handbook of Solid Phase Microextraction.* **38,** (Elsevier Inc., 2012).

62. Yang, X. & Peppard, T. Solid-Phase Microextraction for Flavor Analysis. *J. Agric. Food Chem.* **42,** 1925–1930 (1994).

63. Kumar, S., Jain, S., Kumar, S. & Jain, S. History, Introduction, and Kinetics of Ion Exchange Materials, History, Introduction, and Kinetics of Ion Exchange Materials. *J. Chem.* **56**, 1289-1294 (2013).

64. Holms, B. A. A. and E. L.Sodium -aluminosilicate cation exchanger in water. *Soc. Chon* **54,** 34-42 (1935).

65. Simon, G. P. *Ion Exchange Training Manual*. (1991).

66. Hamidi, M., Azadi, A. & Rafiei, P. Hydrogel nanoparticles in drug delivery. *Adv. Drug Deliv. Rev.* **60,** 1638–1649 (2008).

67. Hu, L. & Serpe, M. J. The influence of deposition solution pH and ionic strength on the quality of poly(N-isopropylacrylamide) microgel-based thin films and etalons. *ACS Appl. Mater. Interfaces.* **5,** 11977–83 (2013).

68. Peppas, N. A. & Khare, A. R. Preparation, structure and diffusional behavior of hydrogels in controlled release. *Adv. Drug Deliv. Rev.* **11,** 1–35 (1993).

69. Smith, M. H., South, A. B. & Lyon, L. A. Microgels and Biological Interactions. *Hydrogel Micro and Nanoparticles.* **50**, 209–235 (2012).

70. Peppas, N. A., Hilt, J. Z., Khademhosseini, A. & Langer, R. Hydrogels in biology and medicine: From molecular principles to bionanotechnology. *Adv. Mater.* **18,** 1345–1360 (2006).

71. Vinogradov, S. V. Colloidal microgels in drug delivery applications. *Curr. Pharm.*

Des. **12,** 4703–12 (2006).

72. De, K. S., Aluru., N. R., Jonhson, W. C., Beebe, D. J. Equilibrium swelling and kinetics of pH-responsive hydrogels: Models, experiments, and simulations. *J. Microelectromech.* **11,** 544–555 (2002).

73. Korrekturen, D. *Physical Properties of Microgel Particles*. Chapter 2. WILEY-VCH Verlag GmbH & Co, (2011)

74. Shibayama, M. & Tanaka, T. Volume phase transtition and related phenomena of polymer gels. *Adv. Polym. Sci.* **109,** 1–62 (1993).

75. Zagorodni, A. A. *Ion Exchange Materials: Properties and Applications.* Chapter 2. Springer Science Business Media New York, (2011)

76. Tamburro, D., Fredolini, C., Espina, V., Douglas, T. A., Ranganathan, A. Multifunctional core-shell nanoparticles: discovery of previously invisible biomarkers. *J. Am. Chem. Soc.* **133,** 19178–88 (2011).

77. Such-Sanmartín, G., Ventura-Espejo, E. & Jensen, O. N. Depletion of abundant plasma proteins by poly(N-isopropylacrylamide-acrylic acid) hydrogel particles. *Anal. Chem.* **86,** 1543–1550 (2014).

78. Gao, Y., Zago, G. P., Jia, Z. & Serpe, M. J. Controlled and Triggered Small Molecule Release from a Con fi ned Polymer Film. *Appl. Mater. Interfaces.* **5**, 9803−9808 (2013).

79. Vuckovic, D. & Pawliszyn, J. Systematic evaluation of solid-phase microextraction coatings for untargeted metabolomic profiling of biological fluids by liquid chromatography-mass spectrometry. *Anal. Chem.* **83,** 1944–1954 (2011).

80. Bird, S. S., Marur, V. R., Stavrovskaya, I. G. & Kristal, B. S. Separation of cis-trans phospholipid isomers using reversed phase LC with high resolution MS detection. *Anal. Chem.* **84,** 5509–5517 (2012).

81. Uhl, O., Glaser, C., Demmelmair, H. & Koletzko, B. Reversed phase LC/MS/MS method for targeted quantification of glycerophospholipid molecular species in plasma. *J. Chromatogr. B.* **879,** 3556–3564 (2011).

82. Bojko, B., Bessonneau, V., Gorynski, K., Mousavi, F., Silva, E. A. S., Pawliszyn, J. Solid-phase microextraction in metabolomics. *TrAC Trends Anal. Chem.* **61,** 168–180 (2014).

83. Moein, M. M., Said, R., Bassyouni, F. & Abdel-Rehim, M. Solid Phase Microextraction and Related Techniques for Drugs in Biological Samples. *J Anal Methods Chem.* **2014,** 921350 (2014).

84. Chambers, E., Wagrowski-Diehl, D. M., Lu, Z. & Mazzeo, J. R. Systematic and comprehensive strategy for reducing matrix effects in LC/MS/MS analyses. *J. Chromatogr. B Anal. Technol. Biomed. Life Sci.* **852,** 22–34 (2007).

85. Gokmen, M. T. & Du Prez, F. E. Porous polymer particles - A comprehensive guide to synthesis, characterization, functionalization and applications. *Prog. Polym. Sci.* **37,** 365–405 (2012).

86. Yagi, K. Assay for blood plasma or serum. *Methods Enzymol.* **105,** 328-331 (1984).

87. Activity at 37 ° C for Restriction Enzymes with Alternate Incubation Tempreture. *New england biolab.* **2**, 36–37 (2012).

88. Polson, C., Sarkar, P., Incledon, B., Raguvaran, V. & Grant, R. Optimization of protein precipitation based upon effectiveness of protein removal and ionization effect in liquid chromatography-tandem mass spectrometry. *J. Chromatogr. B Anal. Technol. Biomed. Life Sci.* **785,** 263–275 (2003).

89. Rico, E., González, O., Blanco, M. E. & Alonso, R. M. Evaluation of human plasma sample preparation protocols for untargeted metabolic profiles analyzed by UHPLC-ESI-TOF-MS. *Anal. Bioanal. Chem.* **406,** 7641–7652 (2014).

90. Gika, H. &Theodoridis G. Sample preparation prior to the LC–MS-based metabolomics/metabonomics of blood-derived samples. *Bioanalysis.* **3,** 1647–1661 (2011).

91. Bruce, S. J., Jonsson, P., Antti, H., Cloarec, O., Trygg, J. Evaluation of a protocol for metabolic profiling studies on human blood plasma by combined ultra-performance liquid chromatography/mass spectrometry: From extraction to data analysis. *Anal. Biochem.* **372,** 237–249 (2008).

92. Dunn, W., Broadhurst, D., Begley, P., Zelena, E., Francis-McIntyre, S. Procedures for large-scale metabolic profiling of serum and plasma using gas chromatography and liquid chromatography coupled to mass spectrometry. *Nat. Protoc.* **6,** 1060–83 (2011).

93. Smilde, A. K., van der Werf, M. J., Schaller, J.-P. & Kistemaker, C. Characterizing

the precision of mass-spectrometry-based metabolic profiling platforms. *Analyst.* **134,** 2281–5 (2009).

94. Crews, B., Wikoff, W. R., Gary, J., Kalisiak, E., Hedeker, J., Siuzdak, G. Variability analysis of human plasma and cerebral spinal fluid reveals statistical significance of changes in mass spectrometry-based metabolomics data. *Anal Chem.* **81,** 8538–8544 (2009).

95. Wei, C., Grace, J. E., Zvyaga, T., Drexler, D.M. Utility of high-resolution accurate MS to eliminate interferences in the bioanalysis of ribavirin and its phosphate metabolites. *Bioanalysis.* **4,** 1895–1905 (2012).

96. Fernandez, A. R., Lacorte, S. Time of flight mass spectrometry applied to the liquid chromatographic analysis of pesticides in water and food. *Mass Spectrum.Rev.* **25,** 866-880 (2006).

97. Qizhi, H., Noll, R. The Orbitrap: a new mass spectrometer. *J.Mass Spectrom.* **40**, 430–443 (2005)

98. Kawaguchi, H. Thermoresponsive microhydrogels: preparation, properties and applications. *SCI.* **63,** 925-932 (2014).

99. Flory, P.J. Principles of Polymer Chemistry, Chapter 1, Cornell University Press: Ithaca, (1953)

100. Koulman, A.; Cao, M.; Faville, M.; Lane, G.; Mace, W.; Rasmussen, S. Rapid common mass spectrum. **23**, 2253-2263 (2009).

101. Kratz, K.; Hellweg, T.; Eimer, W. Influence of charge density on the swelling of colloidal poly(*N*-isopropylacrylamide-co-acrylic acid) microgels. *Colloids and Surfaces A*: *Physicochem*. *Eng*. *Aspects.* **170**, 137–149 (2000)

102. Perrin, D.D., Dempsey, B., Serjeant, E. P. pK_a prediction for organic acids and bases. Chapter 1, (1981)

103. Cesh, N. B., Enke, C. G. Practical implications of some recent studies in electrospray ionization fundamentals. *Mass Spectrum.Rev.* **20**, 362-387 (2001)

104. Boyd, K., Basic, C., Bethe, R.A. Trace Quantitative Analysis by Mass Spectrometry. Chapter 2, Wiely, (2010)

105. Igor, V., Bruce, A. An introduction to quadrupole–time-of-flight mass spectrometry. *J.Mass Spectrom.* ***36****, 849-865 (2001)*

106. Fernandez, H., Wyss, M., Mattsson, J. Microgel Suspensions: Fundamentals and Applications. Chapter 2, WILEY-VCH Verlag GmbH & Co.

107. Lars, B. The bioanalytical challenge of determining unbound concentration and protein binding for drugs. *Bioanalysis*. **5**, 3033-3050 (2013)

108. https://www.agilent.com/cs/library/technicaloverviews. 2016/08/10

109. Minder, E., Schibli, A., Mahrer, D. Effects of different centrifugation conditions on clinical chemistry and Immunology test results. *BMC Clinical Pathology.* **11**, 1472-1476 (2011)

110.http://www.fda.gov/downloads/drugs/guidancecomplianceregulatoryinformation/guidances/ucm368107.pdf. 2016/08/10

111. Tianbao, S., Yuxia, W., Piping, L., Guanghui, M., Zhiguo, S. Effect of acrylic acid weight percentage on the pore size in poly (N-Isopropyl acrylamide-co-acrylic acid) microspheres. *React. Funct. Polym.* **71**, 728–735 (2011)

112. McMillan, G. K. Essentials of modern measurements and final elements in the process industry . Page 296. International society of automation.

113. Olsen, V., Schwartz, J. C., Griep-Raming, J., Nielsen, M. L., Damoc, E., Denisov, E., Lange, O., Remes, P., Taylor, D., Splendore, M., Wouters, E. R., Senko, M., Makarov, A., Mann, M., Horning, S. A dual pressure linear Ion Trap Orbitrap instrument with very high sequencing speed. *Mol. Cell. Proteomics.* **18,** 2759-2769 (2009)

114. Downard, k. Mass Spectrometry: A Foundation Course, Chapter 4, 67-83 (2006)

115. Downard, k. Mass Spectrometry: A Foundation Course, Chapter 3, 23-25 (2006)

116. Westman, A., Brinkmalm, G. Mass Spectrometry: Instrumentation, Interpretation, and Applications. Chapter 3, 93-95 (2008)

117. Dass, C. Fundamentals of contemporary mass spectrometry. Chapter 3. 67-92 (2007).

118. Subirats, X., Rose´s, M., Bosch, E. On the effect of organic solvent composition on the pH of buffered HPLC mobile phases and the pK_a of analyte. *Sep purif rev*. **36**, 231–255 (2007)

119. www.hmdb.ca, 2016/08/17

120. Akimaru, M., Okubo, K., Hiruta, Y., Kanazawa, H. Temperature-responsive solid-phase extraction column for biological sample pretreatment. *Analyt. Sci.* **31**, 881-886 (2015)

121. Sakamoto, c., Okada, Y., Kanazawa, H. Temperature- and pH-responsive aminopropyl-silica ion-exchange columns grafted with copolymers of N-isopropylacrylam. *J. Chromatogr. A.* **1030**, 247–253 (2004)

122. Yakushiji, T., Sakai, K. Effects of Cross-Linked Structure on Temperature-Responsive Hydrophobic Interaction of Poly (N-isopropylacrylamide) Hydrogel-Modified Surfaces with Steroids. *Anal. Chem.* **71**, 1125-1130 (1999)

123. Panahi, H. A., Tavanaei, Y., Moniri, E., Keshmirizadeh, E. Synthesis and characterization of poly[N-isopropylacrylamide-co-1-(N,N-bis-carboxymethyl) amino-3-allylglycerol] grafted to magneticnano-particles for the extraction and determination of fluvoxamine in biological and pharmaceutical samples. *J. Chromatogr. A*. **1345**, 37–42 (2014)

124. Ma, Q., Chen, M., Shi, Z., Feng, Y. Preparation of a poly(N-isopropylacrylamide-coethylene dimethacrylate) monolithic capillary and its application for in-tube solid-phase microextraction coupled to high-performance liquid chromatography. *J. Sep. Sci.* **32**, 2592 – 2600 (2009)

125. Rahman, M., Elaissari, A. Temperature and magnetic dual responsive microparticles for DNA separation. *Sep. Purif. Technol*. **81**, 286–294 (2011)

126. Berezhkovskiy, L, M. Some features of the kinetics and equilibrium of drug binding to plasma proteins. *Expert Opin. Drug Metab. Toxicol.* **4**, 1479-1498 (2008)

127. Jiang, R., Xu, J., Zhu, F., Luan, T., Zeng, F., Shen, Y., Ouyang, G. Study of

complex matrix effect on solid phase microextraction for biological sample analysis. *J. Chromatogr. A*. **1411**, 34–40 (2015)

128. Musteata, F, M., Pawliszyn, A., Qian, M, J., Wu, J, T. Determination of drug plasma protein binding by solid phase microextraction. *J. Pharm. Sci*. **95**, 1712-1722 (2006)

129. Rehim, M. A., Carlsson, G., Bielenstein, M. Arvidsson, T., Blomberg, L. G. Evaluation of solid-phase microextraction for the Study of protein binding in human plasma samples. *J. Chromatogr. Sci.* **38**, 458-464 (2000)

130. Perogamvros, I., Ray, D, W., Trainer, P, G. Regulation of cortisol bioavailability—effects on hormone measurement and action. *Nat. Rev. Endocrinol.* **8**, 717–727 (2012);

131. Kwon, Y. Handbook of Essential Pharmacokinetics, Pharmacodynamics and Drug Metabolism for Industrial Scientists. Chapter 7, 105-119. Kluwer Academic Publishers,